19941228 050

CHARACTERIZATION AND REDESIGN OF
THE AFIT MULTIELECTRODE ARRAY

THESIS

Richard G. Darenberg, Captain, USAF
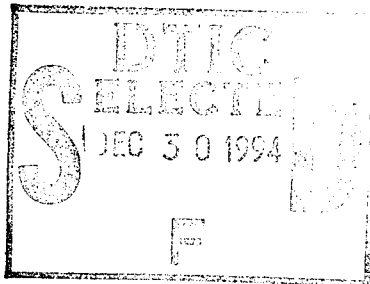
AFIT/GE/ENG/94D-03

DEPARTMENT OF THE AIR FORCE
AIR UNIVERSITY
AIR FORCE INSTITUTE OF TECHNOLOGY

Wright-Patterson Air Force Base, Ohio

AFIT/GE/ENG/94D-03

CHARACTERIZATION AND REDESIGN OF
THE AFIT MULTIELECTRODE ARRAY

THESIS

Richard G. Darenberg, Captain, USAF

AFIT/GE/ENG/94D-03

DTIC QUALITY INSPECTED 2

Approved for public release; distribution unlimited

AFIT/GE/ENG/94D-03

CHARACTERIZATION AND REDESIGN OF THE AFIT
MULTIELECTRODE ARRAY

THESIS

Presented to the Faculty of the Graduate School of Engineering

of the Air Force Institute of Technology

Air University

In Partial Fulfillment of the

Requirements for the Degree of

Master of Science in Electrical Engineering

Richard G. Darenberg Jr., B.S.E.E.
Captain, USAF

December 1994

Acknowledgment

I would like to thank my committee members, Dr. Victor M. Bright, Dr. Steven K. Rogers, Dr. Matthew Kabrisky, for their help and support in this research. Without their assistance and encouragement, this thesis would never have been accomplished.

I would like to thank Maj. Mark Mehalic for his unselfish, tireless, and patient assistance during the last year. He was always there to help and always seemed to have the correct solution. Thanks also to Russ Milliron and Greg Richardson for their help in keeping that voodoo beast out of the VLSI UNIX machines.

Thanks to Charlie Powers for helping me wade through the contracting paperwork. Without his dogged efforts and many trips to the contracting office, my circuits would still be waiting to get mailed out to vendors.

Thanks to Chris O'Brien and Bill Trop for their help in the AFIT Cooperative Electronics, Materials, and Processes Laboratory. I want to apologize to them for single-handedly using about a year's supply of masking plates. I never thought developing masks and my golf swing had anything in common, but I kept finding myself saying "I think I've finally figured this out!"

Thanks to Tray Read and Joel Junker of the "VLSI guys". Your help getting through this year is greatly appreciated and the spirited conversations will be missed.

I would like to thank Carol Naylor of Dupont Electronics Materials and Joe Raffa of Phillips Technologies for providing some of the material used for this research.

Thanks to Mitch Wentzel of Frame Technologies for providing Framemaker®4, the document processor and to the superb technical support offered by Frame Technology

ii

Corp. There is no better program, on any platform, that does document processing as well as Framemaker.

Finally, I'd like to thank my wife, Sally and son, Ryan for allowing me to drop into and out of their lives, at my convenience, without making me feel anything but wanted. Sally, you are the main reason I got through this and Ryan, you are the main reason I can still smile about it.

Richard G. Darenberg Jr.

Table of Contents

List of Figures

List of Tables

AFIT/GE/ENG/94D-03

Abstract

Since 1978, faculty and graduate students from the Air Force Institute of Technology (AFIT) have been working on an implantable circuit array that can record visual signals from the brain or stimulate the brain. In the current design the circuit is a 16 x 16 array of pads, each pad being 160 x 160 μm with 250 μm spacing with an "L" shaped reference pad used as a ground reference. The array is multiplexed so that only one I/O line is required to access all 256 pads.

This research was twofold: first to analyze the existing circuit and identify sources for noise and then to redesign the circuit with the intent of reducing noise and power consumption.

As a result of the research, a new 16 x 17 array has been developed. The new design incorporates new demultiplexing and synchronizing circuitry. The new circuitry exhibits lower noise and consumes much less power. The "L" shaped reference pad has been removed—instead each pad and the pad to its right are sampled concurrently—one as the sample and one as a reference.

CHARACTERIZATION AND REDESIGN OF THE AFIT

MULTIELECTRODE ARRAY

1. Introduction

The brain is a fascinating machine, especially in the area of pattern recognition. The healthy human brain has no trouble distinguishing a pen from a pencil or even a specific pen as being either "mine" or "yours". This recognition is virtually independent of position, distance, angle, or available lighting (within broad constraints). Despite the advances in computer technology, the seemingly simple task of identifying objects with any degree of certainty has not been demonstrated.

Since 1978, faculty and graduate students from the Air Force Institute of Technology (AFIT) have been working on an implantable circuit array that can record or stimulate the brain [1–12]. This circuit array will be referred to in this thesis as the "brain chip" or simply the "circuit". In the current design the circuit is a 16 x 16 array of pads, each pad being 160 x 160 μm with 250 μm spacing, with an "L" shaped reference pad used as a ground reference for the brain (Figure 1-1, [12]). The array is multiplexed so that only one I/O line is required to access all 256 pads. The goal of this research has been to try to unlock the mystery of how the brain recognizes objects.
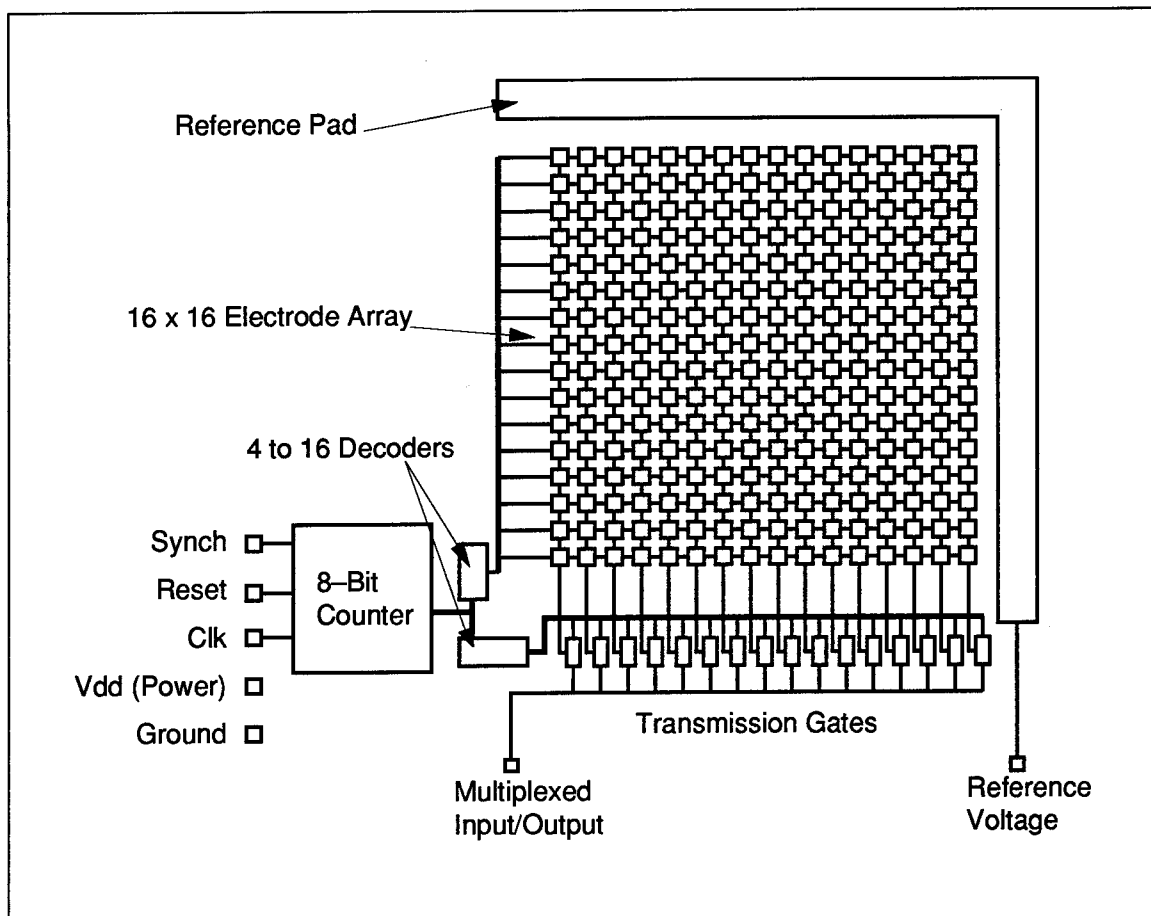
Figure 1-1. Multielectrode array (current design) [12].

1.1. Background

1.1.1. Early Research.

In 1934, Lorente de Nó described the basic anatomy of the cerebral cortex. He proposed that the cortex is actually a cortical sheet, approximately 2-3 millimeters thick composed of cortical neurons arranged in a columnar structure, called cortical columns [13]. In 1957, Mountcastle accomplished an *in vivo*[1] experiment showing these columns behaved as a functional unit [13]. These columns are thought to have a diameter as small as 50 microns in the human primary visual cortex to as large as 500

---

1. In the living body of an animal or plant [20].

microns in the visual cortex of a cat [13]. The cortical columns are believed to be the smallest functional elements in the cortex. Although interconnected, these columns are thought to have little interaction with their nearest neighbors, instead being accessed through the input/output axons running through the cerebral alba and between the cortex and the brain stem [13].

Although the exact makeup of the brain is well known, how these individual columns behave as a functional unit has remained a mystery [13]. Kabrisky has stated that "the most important unsolved brain problem is deducing the organization of the cortico-cortical conductivity matrix and its relation to the function of the cortical column system" [13].

In the visual cortex, there is a direct one-to-one mapping of information received from the eye and transferred to the primary visual cortex, also known as V1 [14]. From there the information is processed to other areas of the cortical sheet to discern form, color and motion. These other areas are referred to as the association areas. How this information is processed and "integrated" to the point that recognition takes place is unknown [14].

In 1966, Kabrisky suggested that there may be a transfer function between areas of the brain [13]. Although the interconnections between cortical columns are well documented, there is no simple one-to-one relationship—one column in V1 is tied to many other columns in different areas of the visual cortex. Kabrisky proposed placing electrodes on different areas of the visual cortex, stimulating one area and then recording the response in the other areas [13].

1.1.2. AFIT Research - Circuit Design. In 1979, AFIT students began research to investigate the visual cortex based on Kabrisky's model. The first phase of this research culminated in 1982 and resulted in a successful implantation of a 4 x 4 electrode array coated with polyimide (PI-2555[1]) and implanted on the visual cortex of a laboratory beagle (*Canis familiaris*) named Rickie [4]. The circuit successfully recorded electroencephalographic (EEG) and visual evoked response (VER) data. The circuit was removed 19 days after implantation due to the threat of infection. On examination of the device, some corrosion had taken place but it was not clear whether this was due to the removal procedure or contamination from cerebral spinal fluid (CSF). Rickie lived until the summer of 1994 and died at the age of 20.

The second phase of this research started in 1983, when Ballantine designed two circuits, each with a 16 x 16 electrode array for one of his VLSI (very large scale integration) design sequence courses [7]. The first design incorporated a 4-bit counter and one 4 x 16 demultiplexer[2] so only 16 output lines and 4 control lines were required. Ballantine's demultiplexer was designed using NMOS (n–channel metal oxide semiconductor) circuits instead of JFETs (junction field effect transistors). Ballantine sent this design to MOSIS® (Metal Oxide Semiconductor Implementation System[3]) for fabrication. His second design incorporated a second demultiplexer and an 8-bit counter.

---

1. Brand of polyimide from Dupont Electronic Materials.
2. Ballantine called this circuit a selector because it selects a single row from the 16 available. Strictly speaking, however, the circuit is a demultiplexer.
3. MOSIS® provides fabrication services to government contractors, agencies, and universities under the sponsorship of the Advanced Research Projects Agency (ARPA) with assistance from the National Science Foundation (NSF).

For his thesis, Ballantine designed and fabricated a JFET array using the AFIT Cooperative Electronic Materials and Processes Laboratory. His intent was to use the JFET array with the counter and demultiplexing circuitry from the designs sent to MOSIS® [7]. Unfortunately, the JFET array did not function properly, apparently due to errors or problems in fabrication rather than design [5].

Sopko, in 1984, used Ballantine's JFET array design but revised his fabrication techniques to successfully fabricate a working array. Sopko did not have time to mate Ballantine's NMOS demultiplexer to his array or work on passivating the array.

In 1989, Szczublewski, also modeling Ballantine's design, switched from a JFET array to CMOS (complementary metal oxide semiconductor) technology utilizing transmission gates (t-gates) as switching devices. The advantage of CMOS technology is it's low power consumption, which is critical for implanted devices. Another advantage in using t-gates is that t-gates are bi-directional. This design was intended to allow the brain chip to either read or write data. Rather than use the AFIT Cooperative Electronic Materials and Processes Laboratory, Szczublewski had the circuit fabricated through MOSIS®. Unfortunately, due to wiring errors to the row selector, his circuit did not function properly [10].

LeFevre, in 1990, used Szczublewski's basic design and attempted to reduce the I/O lines from 32 to 2 by adding a on-chip clock, 8 bit counter, and column demultiplexer [11]. In testing his design, LeFevre also found some wiring errors. The clock behaved as a voltage controlled oscillator and the new counter "behaved erratically" [11]. LeFevre also

reported that although the bond wires could withstand at least 0.7 A of continuous current flow, he had problems with bond wires melting, especially the V_{dd} bond wire [11].

Finally in 1993, Reid modified and fabricated a completely functional circuit. He removed the internal clock and replaced the counter LeFevre had designed, corrected several minor wiring errors and tested the output function of the design using VLSI CAD tools (ESIM[1]). He also investigated a new procedure for surgical implantation based on the work of Turner [12]. From this he designed and fabricated an implantable package. Finally, he switched the electrode metallization layer from gold/nickel and platinum to titanium/iridium because tests done at the University of Michigan indicated that titanium/iridium has a lower impedance [12].

1.1.3. AFIT Research - Passivation. In 1980, Fitzgerald learned that his design needed passivation before it could be implanted [1]. Cerebral Spinal Fluid (CSF) is an ion-rich fluid containing sodium and potassium ions. Of these elements, sodium is the most destructive to silicon devices. Sodium ions pass quickly through silicon dioxide (Figure 1-2). Fitzgerald tested and verified the functionality of his circuit in ambient air. However, when he tested the circuit in the simulated CSF environment his circuit failed in a matter of seconds due to a lack of adequate passivation [1].

German's 1981 thesis concentrated on finding suitable passivation material that could be applied using AFIT and Wright Avionics Laboratory facilities [2]. He tested silicon dioxide, silicon nitride, aluminum oxide, phosphosilicate glass (PSG) and poly-

---

1. ESIM is a switch level simulator. It will identify wiring errors, but cannot give timing information or verify that a circuit is functional.
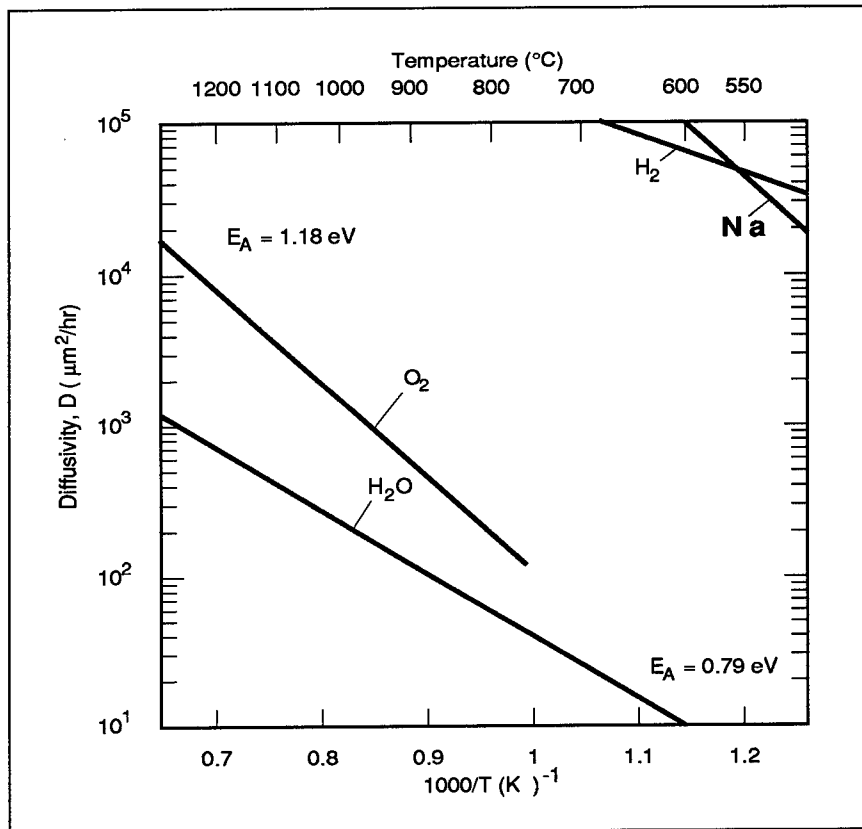
Figure 1-2. Diffusivity of sodium (Na) in silicon dioxide [15].

imide (Dupont brand PI-2545) using various application processes [2]. He concluded that

two materials—Phosphosilicate glass (PSG) or a double layer of silicon dioxide and poly-

imide—provided the best protection [2].

In 1983, LaVoie's research concentrated on fully characterizing polyimide

(Dupont brand PI-2555) [6]. His research was sponsored by the Wright Avionics Labora-

tory to help them find a suitable passivation material for GaAs circuits. Due to funding

constraints, LaVoie was limited to coating blank silicon wafers rather than GaAs wafers

with polyimide and testing it for pin holes. From this research he developed a 4 step

curing process and determined that polyimide coatings needed to be at least 2 μm thick in

order to effectively eliminate pin holes and the tendency of the polyimide to "pull up" around the edges [6].

Turner's 1984 thesis again researched the passivation issue [8]. He used Ballantine's designs and had them fabricated through MOSIS®. He found that a circuit coated with eight microns of polyimide could survive in a simulated CSF environment for at least three weeks. The switch to MOSIS® fabrication created another problem, however. MOSIS® uses aluminum for its metal layers. This created another problem because sodium ions quickly corrode aluminum. Turner reported the aluminum electrodes lasted three weeks with little signal loss, but as the electrodes deteriorated further, the signal loss became noticeable [8]. When there was no current passing through the electrodes, little deterioration was noticed. Turner attempted to coat the aluminum pads with silver but did not have time to test the coated chips [8].

In 1986, Ernst investigated four different polymers in an attempt to find a passivation material that would last for at least 30 days [9]. He researched four compounds—polyimide PI-2555, Accuglass -07, U-series glass, and Parylene C. The first three materials were solvent based polymers. They are applied to the chip, the chip is spun to spread the solvent evenly, and then the chip is heated to evaporate the solvent and initiate the polymerization process. Parylene C is a product of Union Carbide Chemicals and Plastics Company, Inc. It is applied to the circuit using a vacuum thermal evaporation deposition method. Parylene is only sold to companies that are licensed by Union Carbide. Because of the strict licencing requirements, Ernst decided not to test Parylene and only tested the

solvent based polymers. Ernst found that the two glass polymers, Accuglass and U-series glass were ineffective at stopping ion contamination of the circuit [9].

1.2. Problem Statement

Although the current design of the AFIT multielectrode array has been updated many times over the past 11 years, many of the components still reflect old technologies. From testing the current design, many questions arose as to the specific functionality of individual components on the chip and the source(s) of noise recorded on the output of the circuit.

1.3. Goals

The goals for this research were to fully characterize each component of the current design as well as the full switching and signal paths. Based on this characterization, components were replaced and the entire layout redesigned. The redesign focused on the following areas:

1.3.1. Power Consumption. The AFIT multielectrode array is intended to be implanted on the surface of an animal's brain–therefore the heat generated or power consumed by the device should be kept as small as possible. Others have set a limit on the amount of power consumed by their devices to 5 mW or less [16]. The current design of the AFIT array uses NMOS row and column selectors. NMOS circuits usually draw more current than CMOS equivalent circuits [17] so a CMOS replacement was fabricated and compared with the old design.

4-Oct-94
17:15:46

1 μs
100 mV

1 μs
2.00 V

pkpk(2)   3.38 V
mean(2)   ∿   1.4026 V
sdev(2)   ∿   1.5327 V
rms(2)   ∿   2.0774 V
1 μs RIS   ampl(2)   3.06 V

1 20 mV 50Ω
2 2 V   50Ω
3 10 mV 50Ω   2 DC 0.00 V
4 10 mV 50Ω

400 Ms/s

□ AUTO
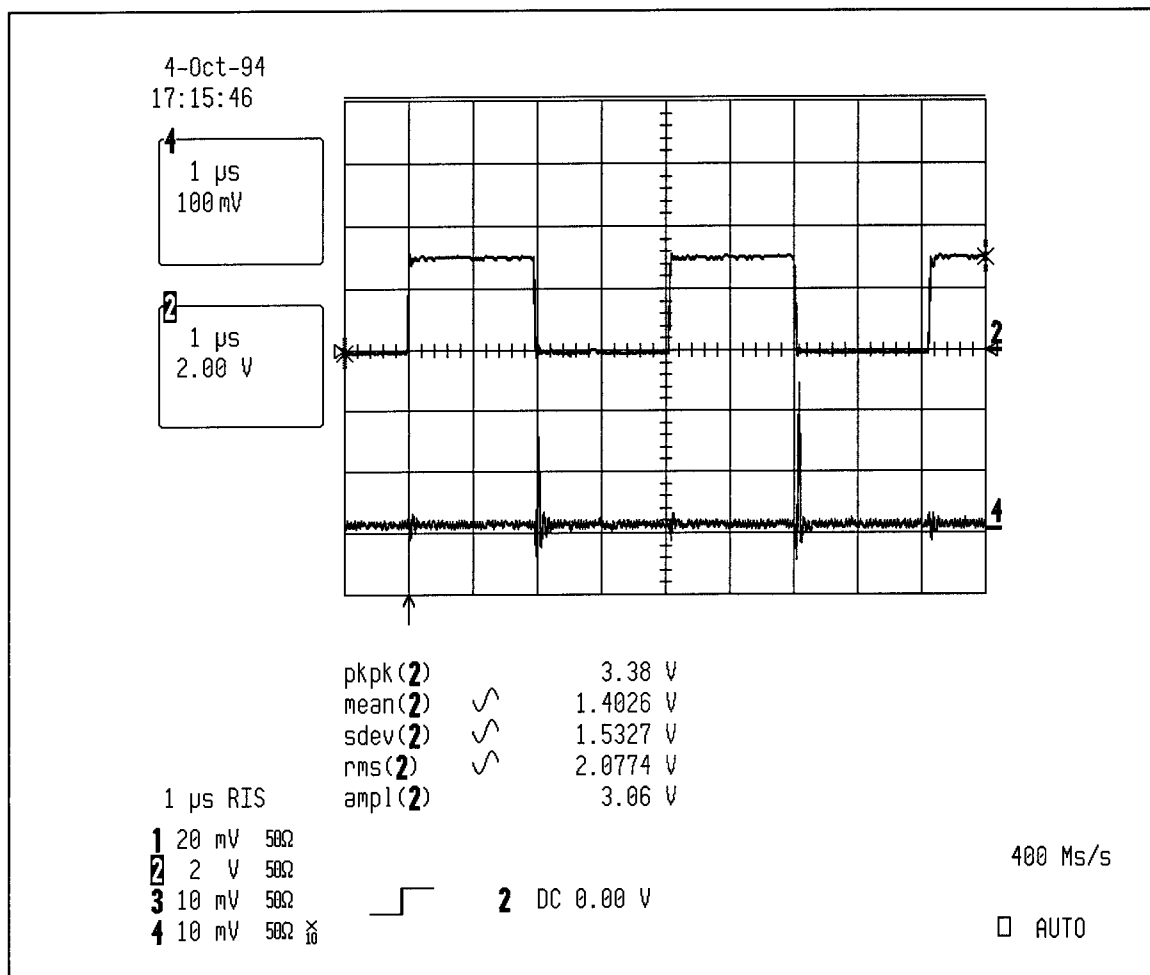
Figure 1-3. Oscilloscope output of current design.
Trace #2 is from the external clock and trace #4 is the output signal.
Note: trace #4 has been offset to show the spiking.

1.3.2. Noise. The amplitude of the signals this device will need to detect and record have been reported to be as low as 20 μV. Therefore, reducing any internal noise in the circuit is very important. In testing this circuit, a voltage spike of approximately 300 mV was discovered (Figure 1-3). Although the amplitude of the spike varied, it always occurred on each downward pulse of the clock signal. One of the primary goals of this research was to find the source of this noise and, if possible, reduce or eliminate it.

1.4. Scope

This research was limited to the characterization and redesign of the AFIT array. This new circuit was sent out for fabrication, but there was no time to test the actual circuit. Two differential operational amplifiers (opamps), one non-inverting and the other inverting, were designed, sent in for fabrication and tested. The "L" shaped reference pad was used as a ground source for the opamp. Unfortunately, the "L" shaped pad proved to be an inadequate ground reference for the differential opamp. These devices did not function properly.

1.5. Assumptions

This research assumes that SPICE[1] is an accurate circuit level modelling tool. The model card used in the analysis of the current design and the new design is based on the device models provided by MOSIS® for the Orbit Technologies 2 µm p-well process[2].

1.6. Approach

1.6.1. Characterization of Old Chip.
The current design was built modularly, in that an electrode, counter, selector, rowdriver etc. was designed separately. Each piece was then moved to the overall layout. The advantage of this design methodology is that the

---

1. SPICE is a component level circuit simulator.
2. SPICE uses model cards to calculate capacitances, resistance, etc. of of the various layers of material used to fabricate devices. The most accurate of these model cards are the models based on actual devices. These parameters are provided by MOSIS® for each of their fabrication processes. The 2 µm p-well process is a manufacturing process that starts with an n-doped silicon substrate. In this substrate p-doped "wells" are diffused where NMOS circuits are needed. For this process, 2 µm is the minimum feature size of the CMOS gates.

analysis can be concentrated on smaller parts. Each of the components mentioned above was simulated using SPICE. The first tests simply determine the functionality of the circuit. Other tests included current draw, noise and speed analysis.
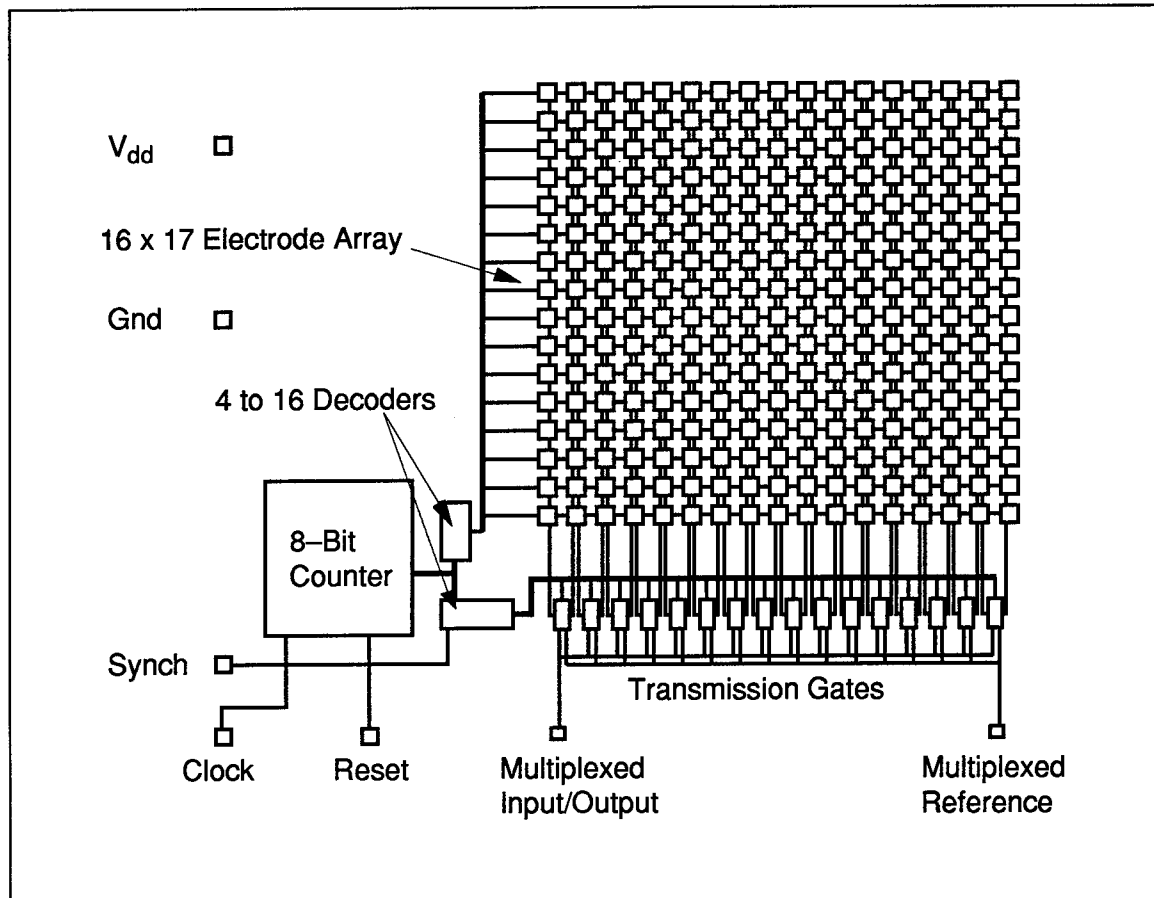
Figure 1-4. New design of the AFIT array.
The "L" shaped reference pad has been removed, and the input/output pads are spread out to aid in bonding.

1.6.2. Design of New Chip. After fully characterizing the old design, a completely new array was designed. Figure 1-4 shows the new chip design. The design changes were meant to address some of the weaknesses of the current design—noise and current draw. Other changes were made so the chip is more compatible with the header package used to

mount the device. The "L" shaped reference pad was removed because it proved to be a poor ground reference. In its place a second sample from the electrode immediately to the right of the primary electrode is output to a pad labelled "multiplexed reference". The outputs from the two adjacent electrodes can then be hooked up to a differential amplifier to record the signal coming directly off the primary electrode.

1.7. Sequence of Presentation

Chapter 2 describes some of the work others have done regarding exploration of the human visual system. Their research and findings have been the basis for the current and future design of the AFIT array. Chapter 3 describes the functionality of the current design and characterizes each component as well as the full switching circuitry and signal paths. Chapter 4 describes changes in the current design and the design considerations for the new circuit. Chapter 5 summarizes the results of this thesis research and provides recommendations for future efforts.

2. Literature Review

2.1. Review of Work In Brain Area

2.1.1. DeMott 1966. DeMott used an array of 400 electrodes to investigate the brain activity of six cats, three raccoons, nine squirrel monkeys and one tupaia[1] (glis) [18]. While his experiment recorded visual, aural and tactile stimulation, only the visual portion of his data is presented. Although DeMott and others performed similar experiments in the past, this experiment used a more closely spaced array (0.25 mm versus 1.5 mm electrode spacing). DeMott referred to this field of study as *cortical micro–toposcopy* and he did not expect to see any significant changes or finer data from this tighter array. During the implantation of the array, the scalp, skull, and dura were removed. Testing was accomplished with the brain exposed and the animal under light anesthesia. To prevent drying, the area was irrigated with Ringer's solution[2].

2.1.1.1. Apparatus. DeMott's array consisted of 400 plastic insulated, 0.15 mm stainless–steel wires bundled together as tightly as possible. The 0.25 spacing was the thickness of the plastic insulation. The bundle was made into a flat surface and then was embedded in a smoothly filed thermo–setting plastic. The array measured 7 by 4 mm.

---

1. The principle genus of the family of Tupaiidae - commonly called the squirrel shrew. The squirrel shrew is an insect eating, tree dwelling creature, that, except for a long, narrow, head, closely resembles a common squirrel [19].
2. Named after an English physician, Sidney Ringer - it is a balanced aqueous solution that contains chloride, sodium, potassium, calcium, bicarbonate, and phosphate ions. The solution closely matches the cerebrospinal fluid [20].

Each probe on the array was amplified and the output fed into an array of neon tubes. The brightness of the neon tube varied linearly with the amount of current being fed into it. This gave the researchers a visual pattern of the electric activity in the cortex. This neon array was photographed with a high–speed movie camera for later analysis. The amplifiers had a frequency response from 10 to 1000 Hz. Total noise was reported to be about 20 μV. Amplifier gain was fixed to give "a usable range of input signals from 50 to 500 μV," while interchannel variations in gain were held to ±1.5 dB [18].

2.1.1.2. Experiment. The visual stimuli presented to the subject were discrete, one–second flashes of light from a flashlight bulb about 10 cm from the subject's eye. The movie camera frame rate was about 300 frames per second (fps). Most of this data was analyzed with the motion picture film and the playback at real time was said to be quite striking. Some frames were digitized and a voltage contour map was made from the digitized data (Figure 2-1) [18]. DeMott noted that little background noise was observed due to the isolation of individual probes. When no stimulus was presented to the subject, the neon array showed a "steady, uniform brightness" [18]. Also, recordings made outside the areas being stimulated showed no activity.

2.1.1.3. Results. Responses to the flash varied with the location of the electrodes and the type of animal being tested. The only variation noted regarding different animals was the time delay in which reactions were recorded. For this reason, all times mentioned will be those of the raccoons.
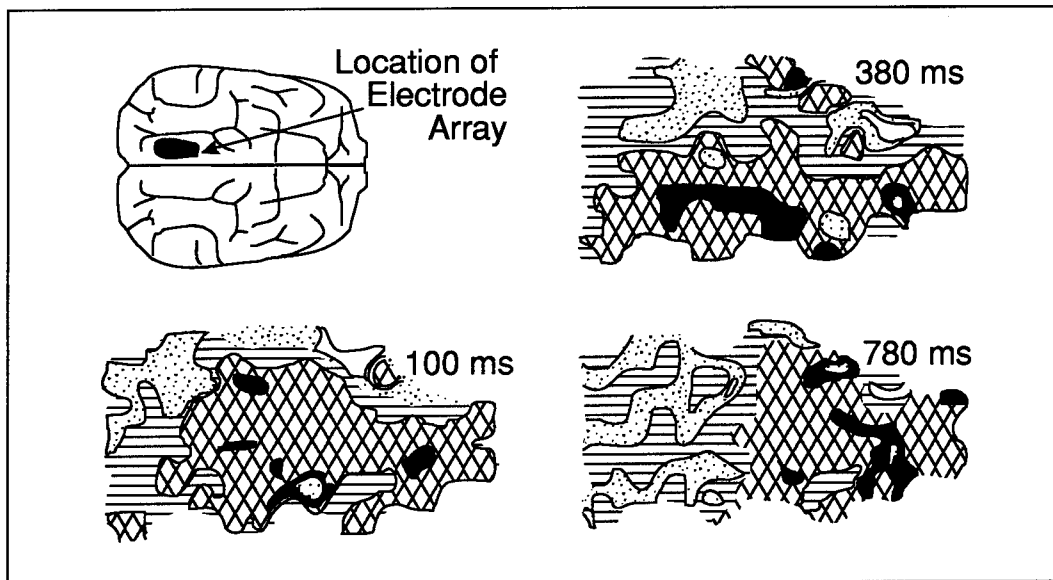
Figure 2-1.   Sample recording of a raccoon response to a narrow (3
               degree) beam of white light approximately 20 degrees
               to the right of the fixation point.
               The time since onset of the flash is shown in the upper
               right corner of each frame. Flash duration was greater
               than the period of response shown. [18]
               Voltage codes:
               Horizontal lines– ±75 µV of the average potential
               across the recording area.
               Stippled pattern– +75 to +200 µV
               White– more than +200 µV
               Crosshatched– –75 to –200 µV
               Black– more than –200 µV

In the posterior portion of the lateral gyrus[1], responses varied with the position of

the flash of light and the intensity of the response diminished rapidly with repeated

flashes. For a one-second flash, the first response was observed about 80 msec after the

onset of the flash and either lasted the entire duration of the flash or started to fade out at

about 200 to 300 msec. If the same stimulus was repeated a second time the response

began to fade after about 100 msec. Subsequent stimuli resulted in little or no recorded

response.

---

1. The brain is mapped by its contours and grooves. Gyrus means convoluted ridge between ana-
   tomical ridges [20].

To see how the intensity of the light affected the observed responses, DeMott decreased the intensity of the light by 3 log units. This resulted in the first response lasting about 170 msec as opposed to 70 msec.

In the anterior portion of the lateral gyrus, the response was independent of the location of the stimulus and did not vary with repetition. Times were similar in the anterior region—"fast" patterns started after about 80 msecs and had a duration of only 20 msec. After a period of inactivity, "slow" patterns began to develop and continued for 200 msec to 1 second.

Voltage levels varied from more than −200 to more than +200 μV with levels as low as ±75μV recorded (Fig. 2-1) [18].

2.1.2. Brindley and Lewin 1968.

Brindley and Lewin implanted an array of 80 electrodes into a 52 year–old blind patient [21]. Instead of recording information from the brain, they input signals to the array which caused the patient to "experience sensations of light" called phosphenes[1]. The array consisted of an extracranial cap of radio receivers and intracranial probes which were implanted on the occipital pole of the right cerebral hemisphere.

2.1.2.1. Initial Investigation.

Brindley and Lewin conjectured from previous work that their electrodes would become insulated from the brain by a continuous sheet of fibrous tissue. This tissue develops as a natural reaction to foreign substances in the brain.

---

1. Interestingly, Webster's Collegiate Dictionary (10th edition) defines phosphenes as "a luminous impression due to excitation of the *retina*" [20]. Apparently Brindley and Lewin have expanded the definition.

To test their hypothesis, they implanted sample electrodes in the brains of 18 baboons and left them in place anywhere from 3 weeks to 2 years. A fibrous membrane was found covering the inner surface of every implant that had been in place for at least 6 weeks. This tissue varied in thickness from 0.08 mm (in an animal that had the electrodes implanted for 18 months) to 0.5 mm (in an animal that had the electrodes implanted only 6 weeks). The membrane tightly adhered to the array and separated from the brain upon removal of the implant. Resistivity measurements were taken of the membranes and were found to range from 390 to 560 Ω-cm. (at 100 Hz and 37°C) [21]. The team concluded that this membrane would have little effect on the voltage threshold of the implant or it's resolving power. Their studies confirmed this analysis—the voltage and power required to stimulate the implants varied only slightly during the studies which lasted as long as 2 years.

2.1.2.2. *Apparatus.* Brindley and Lewin's experiment was modeled after an earlier device constructed by Brindley in 1964. A cap consisting of an array of 80 radio receivers insulated in silicone rubber was attached to the actual implant by means of a cable. The receivers formed a rectangular grid and were alternately tuned to 6 and 9.5 MHz. Stimulating an individual electrode was accomplished by pressing a transmitting coil of an oscillator, tuned to the appropriate frequency, against the scalp immediately over the desired radio receiver. As such, selection was primarily based on location and secondly on frequency.

The implant consisted of 80 platinum electrodes with a square working surface 0.8 mm in length. Each of the electrodes was attached to a radio receiver. For shorter

pulses lasting less than 400 μsec, the electrodes behaved as simple 3000 Ω resistors. During longer pulses, the capacitive behavior of the metal–Cerebrospinal Fluid (CSF) junction had be taken into account.

Electrode stimulation was accomplished with pulsed radio signals. Although, many variations were evaluated, the most successful pulse train was found to be 100 pulses/sec—each pulse lasting 200 μsec. Brindley and Lewin reported that the oscillator needed the capability to deliver a mean power of 90 mW and a peak power of 900 mW [21].

2.1.2.3. Experiment. The patient was a 52 year old woman who developed glaucoma 6 years prior to the experiment. Her vision progressively worsened, and at the time of the experiment, she could see only "a flash of light in a narrow strip of the temporal field of the right eye, and hand movements in a small part of the peripheral lower temporal field in the left eye" [21]. Neither of these areas were within 15° of the fovea.

The platinum electrodes were implanted in the right cerebral hemisphere between the medial[1] surface of the occipital pole and the falx cerebri, nearly centered on the calcarine fissure[2] [21]. Electrode spacing varied from 2.4 mm toward the center of the implant, to 3.4 mm around the outer edges (Figure 2-2) [21]. The extracranial cap was mounted beneath the pericranium[3] and secured with screws.

---

1. Inner surface facing the left hemisphere.
2. One of the grooves on the medial (inner) side of the occipital lobe—typically used as a marker for the primary visual cortex. See Appendix A, Figure A-2.
3. The external membrane of connective tissue surrounding the skull [20].

```
                              □30 □39      □53      □63      □74
              ■14      ■21      ■31 ■40 □49      □58      ■69
          ■11      ■18      ■25 □32 □41      ■54      □64      □75
   □3      □8      □15      ■22 ■26 □33 ■42 ■50      ■59      □70      □80
  ■1      □6      □12      ■19      ■27 ■34 ■43      □55      ■65      □76      ■47
   □4      ■9      ■16      □23 □28 ■35 □44 □51      □60      ■71
  ■2      ■7      ■13      ■20      □29 ■36 ■45      ■56      ■66      □77      □81
  ■5      ■10      □17      ■24      □37 ■46 □52      □61      ■72
                        □38         □57      □67      ■78

        Frontal      Occipital
                                       □62      □73
                                          □68      □79
```
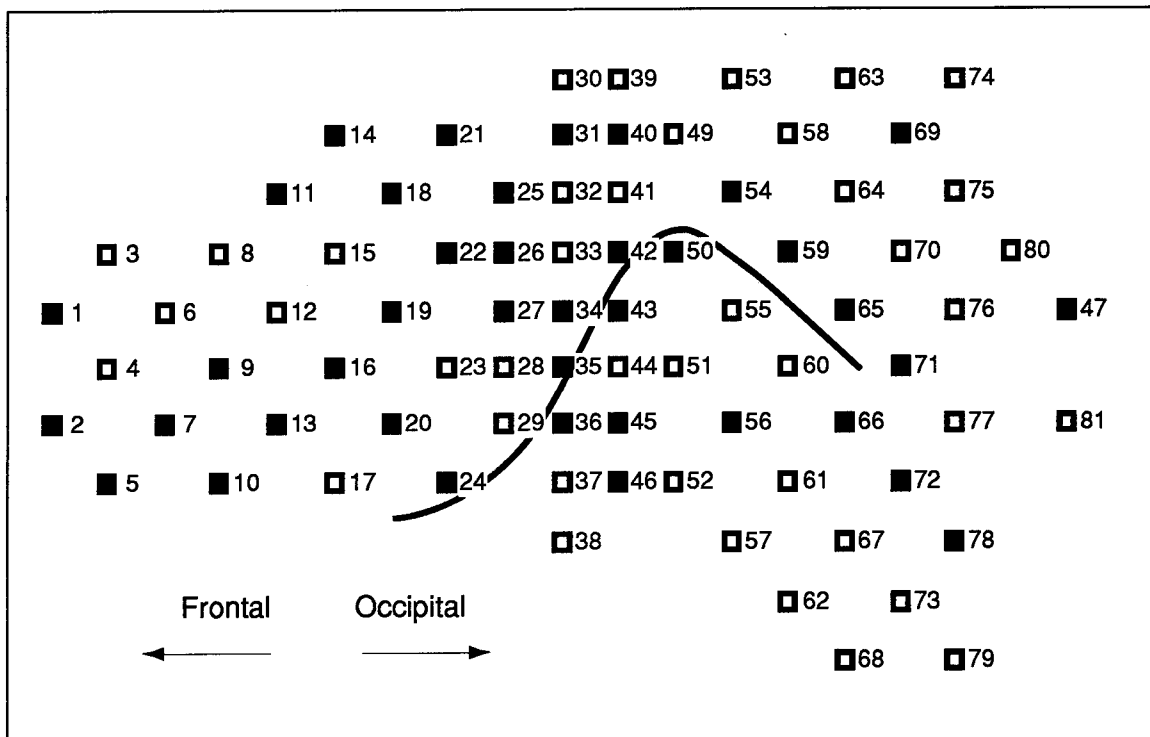
Figure 2-2.   The arrangement of probes in Brindley's patient and their estimated relation to the calcarine fissure (represented by the heavy line).
The thirty-nine filled squares represent electrodes that have produced phosphenes. No explanation was given for electrode #47 being out of place or the missing electrode #48 [21].

2.1.2.4. Results. Brindley and Lewin successfully produced phosphenes from roughly half of the electrodes (Figure 2-2) [21]. In an effort to provide a point of reference for their patient, they had her sit near a translucent dome and point to the areas on the dome where she saw points of light. Etched in the dome was a circular grid to allow for accurately mapping the points of light. Brindley and Lewin noted that all stimulation produced light spots—no dark spots were produced and unless the stimulation was very strong, the sensation of light went away as soon as the stimulus was removed [21].

As a point of reference, points numbered 16, 18, 19, 24 and 27 in Figure 2-3(a), were described as "a grain of rice at arms length" [21]. All the points within 10° of the
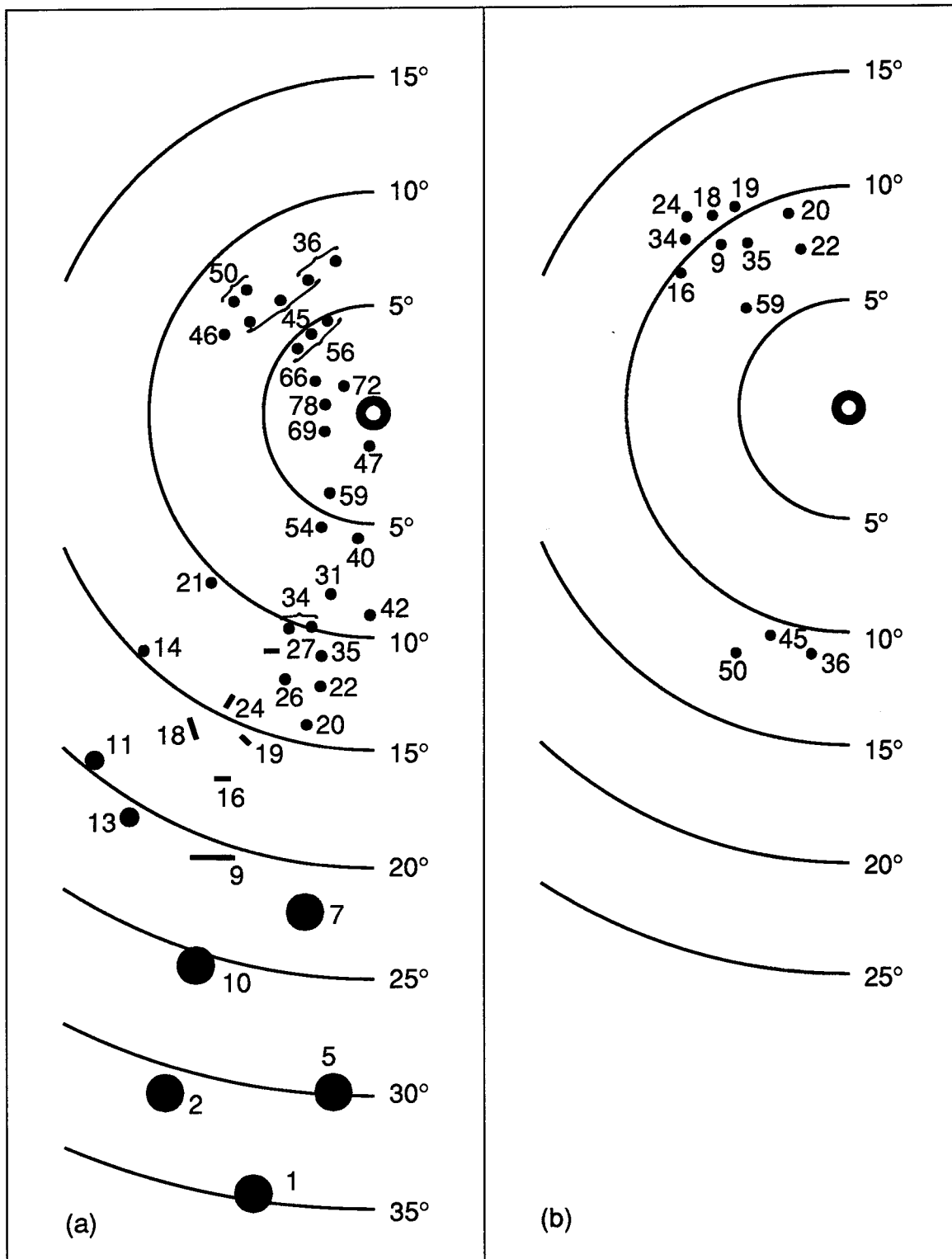
Figure 2-3. (a) The positions of low-threshold phosphenes in the visual field.
(b) The positions of high-threshold phosphenes.
The sizes and shapes of the symbols roughly match those described by the patient [21].

point of regard were single points of light. The larger points, 1, 2, 5, 7, 10 were described as clouds of light rather than point sources. Some of the electrodes produced multiple points of light (34, 36, 45, 50, 56). Lowering the threshold voltage of the oscillator had no effect on being able to produce only single individual phosphenes. Finally, some electrodes, if stimulated at a high voltage produced different phosphenes than they would if stimulated at a lower voltage. These are referred to as the high-threshold phosphenes (Figure 2-3 (b)) [21].

There were ten pairs of electrodes, spaced at 2.4 mm that produced phosphenes. For each of these 10 pairs of electrodes, the patient was able to distinguish between the phosphene produced by stimulation of one electrode from the phosphene produced by stimulation of the other electrode if they were fired in quick succession (anywhere from 0.1 sec to 2 sec). Delays beyond 2 seconds were distinguished in only a few pairs of electrodes and then only because they differed, not only spatially, but by some other qualities [21].

Table 2-1

The Relation Between Pulse Duration and Threshold Voltage for Electrode #19, Measured at 30 pulses/sec [21].

Duration (μsec)	Threshold Voltage (V)	Duration (μsec)	Threshold Voltage (V)
1000	8	60	19
600	9	40	25
400	9	30	28
300	10	20	36
200	13	10	56
100	16		

When two electrodes were stimulated simultaneously, Brindley and Lewin noted the following: if the pairs of electrodes to be stimulated were not in close proximity to each other, no interaction took place. Although, some of the 2.4 mm spaced electrode pairs also showed no interaction, others caused the neighboring phosphene to diffuse and the combined result was a diffuse strip of light rather than two distinct points.

By stimulating several electrodes at once, Brindley and Lewin were able to create simple patterns, however there were not enough electrodes to permit the patient to discern even one character of text [21].

Table 2-2

The Relation Between Frequency and Threshold Voltage for Electrode #19,
Keeping Pulse Duration Constant at 30 μsec [21].

Frequency (pulses/sec)	Threshold Voltage (V)	Frequency (pulses/sec)	Threshold Voltage (V)
25	29	400	35
50	27	630	37
100	21	1000	39
160	21	1600	35
250	25	4000	29

Finally, the effects of pulse duration and frequency of pulses were plotted versus the threshold voltage required to produce a phosphene. In the first case, a constant 30 pulses/sec was applied to the electrode (data given is for electrode #19, see Table 2-1). For a given pulse duration, the voltage applied to the electrode was varied until the patient reported seeing a phosphene. The actual reported potentials were measured from a duplicate of one of the receivers used in the implant, connected to a dummy load of 3000 Ω in

series with a 1.0 μF capacitor [21]. When frequency and strength of radio pulses were held constant, the effect of increasing the pulse duration made the phosphene seem brighter. Further increase in the duration of pulse had little effect, but it was surmised that this may be caused by the increased blocking capacitance of the probe, rather than a physiological constraint.

Little change in voltage potential was recorded when pulse duration was held constant and the frequency was varied from 25 to 4000 pulses/sec (Table 2-2). Interestingly, the patient noted that all phosphenes seemed to flicker, regardless of the stimulating frequency—the phosphenes produced by a 20 pulse/sec input varied only slightly with those produced at 200 or 2000 pulses/sec [21]. Brindley and Lewin discounted mechanical vibration, low-frequency modulation of the transmitter, and the patient's heartbeat as the source of the vibration.

2.1.2.5. Side effects. The transmitters caused two unwanted side-effects: tingling and deep pain in the head. The tingling usually came about whenever five or more transmitters were strongly activated and the pulses in all of them were synchronous [21]. The cure for the problem was simply to place slight delays in the pulses so they wouldn't be synchronous.

The second problem was more serious. When receivers 14, 19, 31, or 40 were stimulated, the patient reported a sharp, deep pain. All of these receivers produced phosphenes. When receiver 31 was stimulated the pain was felt in the right side of the head. All other pain was felt mid line. Receiver number 14 was the only receiver that had an equal pain and phosphene threshold. The other receiver's required about twice the voltage

potential of phosphene generation to produce a sensation of pain. The pain started with the onset of stimulation and usually went away as soon as the stimulation ceased. This pain was believed to have occurred due to stimulation of the meningeal[1] pain fibers [21].

2.1.3. Dobelle, 1974. In follow-on work, Dobelle et al [22], implanted platinum electrode arrays in two blind patients—one blind for 7 years (referred to as patient 7) and the other for 28 years (referred to as patient 28). Although, their results were similar to Brindley and Lewin, some of their discoveries are significant.

2.1.3.1. Apparatus. Dobelle used 64 platinum disk electrodes, each with an area of 1 mm^2 and 3 mm center to center spacing. The 64 electrodes were arranged to form an 8 by 8 hexagonal array. These arrays were mounted in contact with the mesial surface of the right occipital lobe of each patient [22].

The devices were designed for easy removal, which caused numerous problems. The device implanted in patient 28 did not make good contact with the surface of the brain. As a result, consistently higher amplitude thresholds were required to generate phosphenes in this patient. Also, the implant shifted on the surface of the patient's brain which made it impossible for Dobelle to accurately map the phosphenes.

The implant installed in patient 7 made better contact with the surface of the brain, which generated much better results. On the third day however, the implant shifted slightly, which resulted in a dramatically different detail map.

---

1. Three membranes (meninx) that envelop the brain and spinal cord.

2.1.3.2. Experiment. Dobelle examined the effects of pulse amplitude, duration, frequency and train length with both patients. He also did simple pattern recognition testing with patient 7. An absolute map of the phosphenes was accomplished with patient 7. He was instructed to place his right thumb on a fixation spot, focus on that spot, and use his left finger to point to the phosphene positions relative to that fixation point. A researcher would then mark down these positions on a map. This map was transferred to a computer screen to aid researchers in pattern recognition tests.

2.1.3.3. Results. At some point in the experiment, 4 of the electrodes developed broken wires. The remaining 60 all produced phosphenes, although 21 of them were difficult to distinguish from other phosphenes.

Patient 7 reported similar findings regarding phosphene size to those reported by Brindley's patient—ranging in size from a "grain of rice at arm's length" to a "coin at arm's length" in the peripheral portions of the visual field [22]. All phosphenes in this region were colorless and were believed to be generated from the striate cortex[1]. Unlike, Brindley's patient, patient 7 reported that only some of the phosphenes flickered, while others did not. A second group of phosphenes was reported by patient 7—these characterized by an orange hue, consistent size ("coin at arm's length") and all flickered. These were thought to be generated by the surrounding association areas [22].

Dobelle was able to vary the brightness of the phosphenes by changing the amplitude of the pulse, although this change was non-linear or consistent from phosphene to

---

1. The Striate Cortex is located in the back of the brain (occipital lobe). It is directly connected to the retina via the optic nerve and lateral geniculate nucleus and effectively contains a map of the entire retinal field [14]. Also called the primary visual cortex, area 17, and V1.

phosphene. Also, both patients reported the brightness level diminish if pulse trains lasted longer than 10 to 15 seconds [22].

Current amplitude measurements were conducted on both patients. Stimulation was typically accomplished using symmetric biphasic (+/-, 0.5 msec duration for each phase, 1 msec total pulse, 50 Hz) pulses coupled through a 1 μF series capacitor. For 46 tested electrodes, patient 7 had thresholds ranging from 1.2 to 2.8 mA (peak to peak) with an average of 2.6 mA. In testing 32 electrodes in patient 28, thresholds varied from 4.2 to 16.1 mA (peak to peak) with an average of 9.0 mA. Again, this higher threshold current for patient 28 was mostly attributed to poor contact of the electrodes [22].

For the most part, pattern recognition tests were successful. Up to seven electrodes were used to generate patterns. The researchers used pulse trains of 0.5 to 3.0 seconds and interlaced the pulses to each electrode so that no two electrodes were activated at the same time. Changing the interlace pattern seemed to have no effect on the appearance of any phosphene nor on the success of the pattern being recognized [22].

Although most attempts at pattern recognition were successful, failures seemed to fall into two distinct categories: spurious phosphenes and varying phosphene brightness. In the first case, certain patterns of phosphene stimulation caused other phosphenes to be generated. These spurious phosphenes were dimmer than the intended phosphenes and it was felt that, with practice, they could be ignored [22]. In the second case, some intended phosphenes were not seen because other, brighter phosphenes made them difficult to distinguish. Dobelle thought this could be fixed by custom tailoring each individual electrode to make all electrodes have the same brightness level.

2.1.4. Dobelle 1974. Dobelle and Mladejovsky performed more extensive research using fifteen sighted volunteers and a smaller array (12 electrodes versus 64) [23]. All patients in this study were undergoing neurosurgery to remove tumors or other lesions on or near the striate cortex. Dobelle conceded this was a less than ideal arrangement because of the limited amount of time that could be spent with each patient, the fact that all patients were under anesthesia during the experiment and because the area of interest (striate cortex and association areas) was traumatized by tumors or lesions [23]. Dobelle also questioned the validity of extrapolating the data gathered from sighted patients as compared to blind patients [23]. Nevertheless their research led to many more important discoveries in the effort to build a visual prosthesis. Pertinent findings in their research follow and will be examined in detail: changes in stimulus parameters and factors depending on thresholds, and variations in the size and spacing of electrodes.

2.1.4.1. Apparatus. Dobelle's electrode array was a configurable 3 by 4 electrode array. Initially (in 13 out of 16 reported experiments) ball electrodes made from platinum iridium (90-10%) were used, but these proved unsuitable for stimulation on the mesial surface and were replaced with pure platinum, ribbon cable electrodes, embedded in a Teflon matrix. Both types of electrode arrays could be modified to change the electrode size and spacing. The impedance of the 1 mm^2 electrodes averaged 3 kΩ. Changing the size of the electrodes made no drastic change in the input impedance of the implant [23].

2.1.4.2. Changing stimulus parameters: Monophasic(+ and -) and biphasic(+/- and -/+) wave forms were evaluated, with and without a 1 μF capacitive coupler. In all

waveform tests a constant current of 5 mA was maintained for consistency. The

monophasic train duration was 1 msec with a pulse repetition rate of 50 Hz. This was

broken into two pulse durations of 0.5 msec for biphasic stimulation. Subjectively, no

patients reported any significant variations in phosphenes when different waveforms were
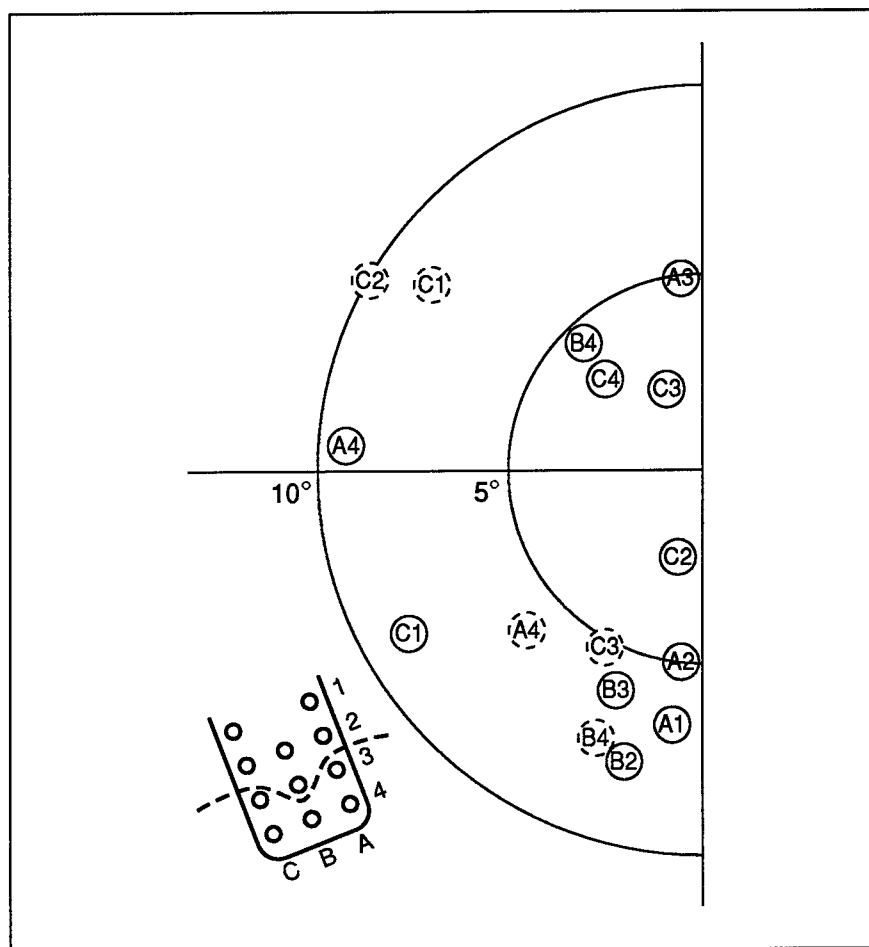
used [23].

Figure 2-4.   Phosphene map of the visual field for one of
Dobelle's patients.
Phosphenes indicated by dashed circles are
high amplitude phosphenes. The electrode
array and numbering scheme is also shown.
The dashed line across the array is the esti-
mated location of the calcarine sulcus [23].

When amplitude variations were tested, constant currents thresholds of between 1 and 5 mA, with a 3 mA average were reported. Changes in pulse amplitude above the threshold produced brighter phosphenes, as had been reported earlier [21, 22]. When amplitude pulses exceeded threshold many electrodes produced a second conjugate phosphene (Figure 2-4). Dobelle's preliminary results suggested that biphasic stimulation seemed to elicit these multiple phosphenes more frequently than monophasic pulses, but thought additional experimentation was needed to confirm this [23].

Table 2-3

Relationship Between Pulse Duration and Threshold Amplitude [23].

Pulse duration for each phase (msec)	Electrode (See Figure 2-4 for electrode layout)									
	B4 (mA)	C4 (mA)	A3 (mA)	B3 (mA)	C3 (mA)	A2 (mA)	B2 (mA)	B2 (mA)	A1 (mA)	C (mA)
1.000	5	4	5	3	3	3	2	2	3	3
0.500	—	5	5	4	4	4	3	3	4	3
0.250	—	—	—	—	—	—	5	5	—	5
0.125	—	6	—	—	—	—	8	7	—	6
0.062	—	—	—	—	—	—	—	12	—	—

All stimulations were biphasic (-/+), and currents given are zero to peak values. Pulse rate was 50 Hz, with a 1 sec train duration and a 1.0 µF series capacitor. Electrodes B1 and A4 did not respond to stimulation. Due to time constraints, currents higher than 5, 8 and 12 mA were not tested at 0.25, 0.125 and 0.062 seconds respectively [23].

Changing the pulse duration seemed to have little effect on the subjective perception of the phosphenes, although at pulses less than 100 msec, brightness modulation could be achieved. Unfortunately these short pulses required currents in excess of 20 mA

to be perceived. Table 2-3 shows the relationship between pulse duration and threshold amplitude and is based on one patient's response [23].

Dobelle reported that changing the pulse repetition rate from 30 to 200 pulses/sec had little effect on the subjective sensation. At frequencies below 30 pulses/sec, flickering became more pronounced [23]. There were conflicting reports as to whether or not this increased flickering was caused by the speed of the flickering or the intensity levels of the phosphenes changing. Table 2-4 is a compilation of the tests done on one of Dobelle's

Table 2-4

Relationship Between Frequency and Threshold Amplitude [23].

Pulse repetition rate (Hz)	**Electrode** (See Figure 2-4 for electrode layout)										
	A4 (mA)	B4 (mA)	C4 (mA)	A3 (mA)	B3 (mA)	C3 (mA)	A2 (mA)	B2 (mA)	B2 (mA)	A1 (mA)	C (mA)
200	5	5	3	2	2	2	2	2	2	2	2
50	—	5	4	4	4	4	4	2	2	4	2
25	—	—	4	—	4	—	—	—	3	—	—
12	—	—	8	—	—	—	—	8	7	—	6

All stimulations were biphasic (-/+), and currents given are zero to peak values. Pulse duration for the positive and negative pulses was 0.5 msec each with a 1 sec train duration. Electrode B1 did not respond to stimulation. Due to time constraints, currents higher than 5, and 8 mA were not tested for frequencies 25 and 12 Hz respectively [23].

patients, showing the relationship between frequency and threshold amplitude [23].

Finally, the relationship between threshold amplitude and train duration was investigated (Table 2-5). Dobelle reported that under their testing conditions, between five and

fifteen pulses per pulse train were required to elicit a response. He viewed this as the most critical parameter of the test because the minimum pulse width would directly determine the minimum frame rate that information could be presented.

Table 2-5

Relationship Between Amplitude and Threshold Train Duration [23].

Pulse current (zero to peak)	Electrode (See Figure 2-4 for electrode layout)										
	A4 (sec)	B4 (sec)	C4 (sec)	A3 (sec)	B3 (sec)	C3 (sec)	A2 (sec)	B2 (sec)	B2 (sec)	A1 (sec)	C (sec)
4 mA	—	—	0.125	0.5	0.25	0.5	0.25	0.25	0.125	0.5	0.25
8 mA	0.25	0.25	0.06	0.125	0.125	0.125	0.125	0.125	0.125	0.125	0.125

All stimulations were biphasic (-/+), and currents given are zero to peak values. Pulse duration for the positive and negative pulses was 0.5 msec each. Electrode B1 did not respond to stimulation [23].

Dobelle concluded that changing the frequency of pulses was more effective than increasing the threshold. This is good news for two reasons: using a higher frequency would allow information to be transferred at a higher rate and keeping the voltage/current amplitude down would make building a permanent prosthesis easier and more reliable.

In most experiments, the electrode pads were 1 mm² with 3 mm center spacing (Figure 2-4). Ball electrode diameters of between 0.5 and 2.0 mm were also evaluated. In one experiment, using the ribbon cable electrodes, electrode disks of 1 mm², 3 mm², and 9 mm² were evaluated. Dobelle found that the patient's ability to discriminate between two distinct phosphenes broke down somewhere between 2 to 3 mm center to center spacing. Also, varying the size of the electrodes had little or no effect on the size of the

phosphenes produced. Dobelle suggested that bigger pads may be better for chronic implants because current densities through the pads would be decreased if larger pads were used [23].

While DeMott, Dobelle and others have concentrated their research on surface mounted electrodes, others have begun research using insertable probes. While one might question the need for using insertable probes, these devices must meet similar design criteria: surviving in an ion-contaminated environment, creating electrodes capable of reading signals in the micro-volt range and choosing an optimum geometry of electrode size and spacing to accurately record signals from the brain.

2.1.5. BeMent et al, 1986. BeMent, Wise et al, from the University of Michigan were working on single and multi-probe, multi-electrode, insertable devices with the goal of creating multichannel recording arrays for studying the nervous system [16]. BeMent reported on two versions of their probes: the first being a passive device and the second incorporating on-chip amplification. This discussion will primarily focus on the latter device.

BeMent's design is built on a silicon substrate that supports a thin film electrode array (Figure 2-5) [16]. The entire structure is formed using photolithography techniques and all dimensions are reproducible to 1 μm [16]. The design in Figure 2-5 has 4 gold plated electrodes which are spaced at 50 μm intervals. Although the current design only uses four probes, contained on the probe are all the electronics for multiplexing 11 electrodes, a synch signal, on-chip preamplification, and buffer/driver circuitry. The only outputs from the probe are power (5 V), ground, and multiplexed output. To minimize heat
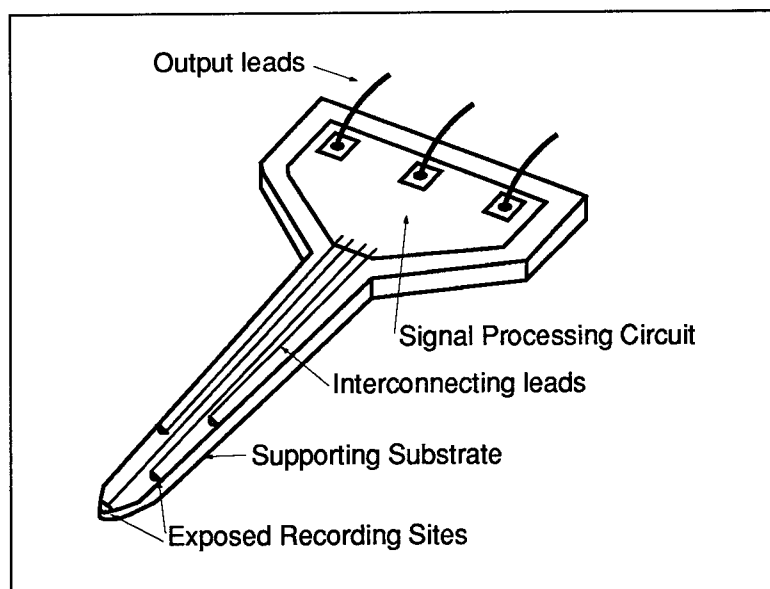
Figure 2-5. BeMent's multichannel, multiplexed
intracortical array [16].

build up in the neuronal environment, BeMent set a design limit on the power consumption of his device to 5 mW or less [16].

Figure 2-6 is a block diagram of the electronics used in BeMent's design. Although not shown in the block diagram, an on–chip clock and shift register are also included. The input signal is first amplified, then multiplexed and then a broad band output buffer passes the multiplexed signal to external circuitry. The external circuitry strips the synch signal and uses it to demultiplex the data stream before it is passed to the test equipment.

Since metal electrodes, on-chip amplification, and multiplexed circuitry are critical to the design of the AFIT array, BeMent's work in these areas will be discussed in detail.

2.1.5.1. Electrodes. BeMent states that in order to sense extracellular currents adequately, an electrode needs to have a surface area of between 20 to 80 μm. He further states that since an electrode is primarily capacitive, an impedance of between 1 to 20 MΩ

2–21

at 1 KHz is required for good recording [16]. BeMent's group uses gold over chromium

(200 nm and 20 nm in thickness, respectively) as the recording surface. Tantalum[1] was

also used in earlier designs but discarded when it was found to have an ac impedance at

least an order of magnitude greater than that of gold [16].

2.1.5.2. On-chip Amplification. With the expected signal from the brain being

about 20 μV, on-chip amplification was seen as the only solution to obtaining a clean

signal. BeMent uses per-channel preamplifiers in his design. This has two advantages:

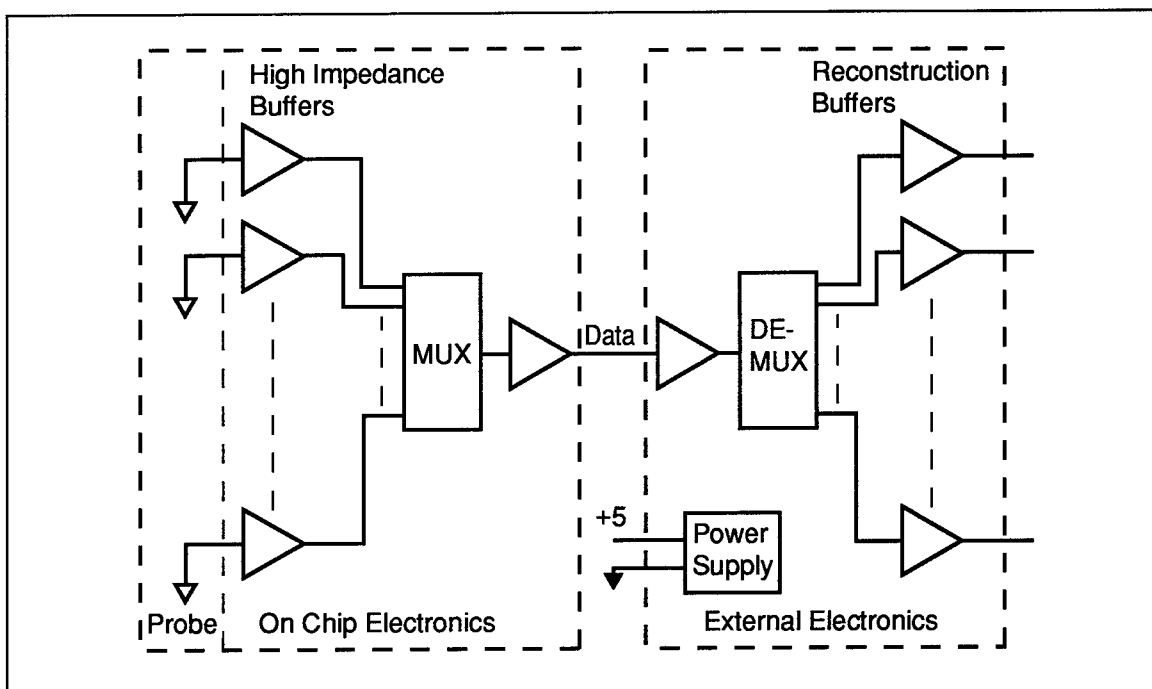lower bandwidth requirements and a cleaner signal. BeMent states that the required band-

Figure 2-6.   Block diagram of the electronics used in BeMent's design [16].

width to record neural data is from 100 Hz to 6 KHz. The cleaner signal is due to the fact

---

1. A hard ductile gray-white, acid resistant metallic element of the vanadium family [20].

that he is amplifying the signal immediately. If he were to use a single amplifier, any noise picked up by the multiplexing circuitry and clock would also be amplified. The trade off for this cleaner signal is that it requires much greater chip area. To provide 12 preamplifiers, BeMent's design uses an area of 1.75 mm^2 using 6 µm technology [16]. His goal for amplification is a gain of 100 over the bandwidth of 100 Hz to 6 KHz. He also states that:

> The amplifier should be insensitive to dc variations from random wandering of the voltage associated with the metal-electrolyte electro-chemical cell. While the remote reference electrolyte can perhaps be taken as constant in potential (and can reference the electronics as well as the recording sites), noble metal recording sites can wander ± 50 mV about their normal level. This is 100–1000 times the ac signal levels to be recorded.

> The amplifier input impedance should be high enough that it won't significantly load the recording channels. Amplification also reduces the output impedance of the probe, which reduces the sensitivity to electrical leakage on the output probes [16].

2.1.6. Multiplexing-Demultiplexing Circuitry. The multiplexing circuitry consists of an on-chip clock, shift register, and analog multiplexer. The clock is two-phase, non-overlapping type and operates at a frequency of 200 KHz. Each channel has a 6 µsec sampling time over an 80 µsec frame. The clock output drives the shift register which sequentially cycles the multiplexer through all twelve channels.

Demultiplexing is accomplished off chip. First the synchronization pulses are fed into a phase-locked loop which reconstructs the clock signal. The regenerated clock is

used to demultiplex the recorded signals. Output amplifiers and active low-pass filters are used to reconstruct and filter the signals (Figure 2-6) [16].

2.1.6.1. On-chip testing/calibration.

BeMent's second design adds on–chip testing of electrode impedance. This allows the research team to closely monitor any changes in electrode performance due to electrode deterioration or surrounding tissue damage, and to evaluate passivation materials *in vivo*.

A test waveform generator and test enable circuitry was added to the existing design. To initial a test, the power supply is pulsed from 5 to 7 volts. In the test mode, a 1 KHz square wave is generated and coupled to all recording sites simultaneously. The estimated induced voltage applied to each electrode is about 250 μV. This voltage is transmitted through the preamplifiers and multiplexer in the usual manner. The output voltage is then a measure of the recording site impedance [16].

Recording site impedance measurements were measured at several frequencies before and after in vivo studies for three reasons: to prescreen probe sites for individual recording capabilities, determine changes in the electrical properties of recording sites, and investigate possible correlations between electrical characteristics of the probes and their ability to successfully record neural data. Passivation studies in long and short term saline baths have also been planned [16].

2.1.6.2. Results.

Using the on-chip test circuitry, BeMent's team has obtained "general correlation between impedance properties of recording sites and their ability to

record neural activity." [16] In sites with 1 KHz impedances greater than 25 MΩ or less than 1-2 MΩ, good neural activity could not be recorded [16].

In animal study testing, probes were used multiple times in different animals. Although scanning electron microscope (SEM) showed no signs of chipping, dulling or fracturing, probes used more than once seemed to have greater difficulty penetrating the pia-arachnoid layers. During probe advancement, BeMent's team seldom noticed the high frequency transient "buzz" associated with neural destruction. External signs of hemorrhaging were also infrequent [16].

2.1.7. Edell, et al, 1992. Edell's team studied the effects of neuron destruction when probes were inserted into the brain. They evaluated various probe and tip geometries, insertion angles, insertion speed, and cleanliness of probe in an attempt to find the probes that caused the least amount of damage to brain. Edell used an array of insertable probes, 100 μm in length, but of varying geometries to try and determine the optimal shape for an insertable probe.

In all tests, probes were inserted in the brains of rabbits and following a six-month survival, neuron densities were evaluated in order to find the "kill zone", a term Edell and his team have defined as an area where the neuron density is lower than the expected neuron density by a 90% confidence interval [24].

When a probe is inserted into the brain, four things can happen to the surrounding tissue—it can be torn, cut, stretched or compressed by the probe structure. Of these, tearing causes the most damage. Tearing the neural tissue causes temporary loss of action potential capability and possibly cell death due to the influx of calcium [24]. Tearing of the

surrounding capillaries and larger vessels may result in a ragged rupture of the vessel wall which will cause microhemorrhages that could displace the neural tissue from the surface of the structure. Compression and stretching of neural tissue can distort cell membranes leading to leakage of ions and loss of cellular homeostasis. If ion leakage is large enough, the affected cells may die. Cutting tissue is the least damaging result of probe insertion. An ideally designed probe will only pierce, nick or sever blood vessels, without stretching or tearing the walls [24].
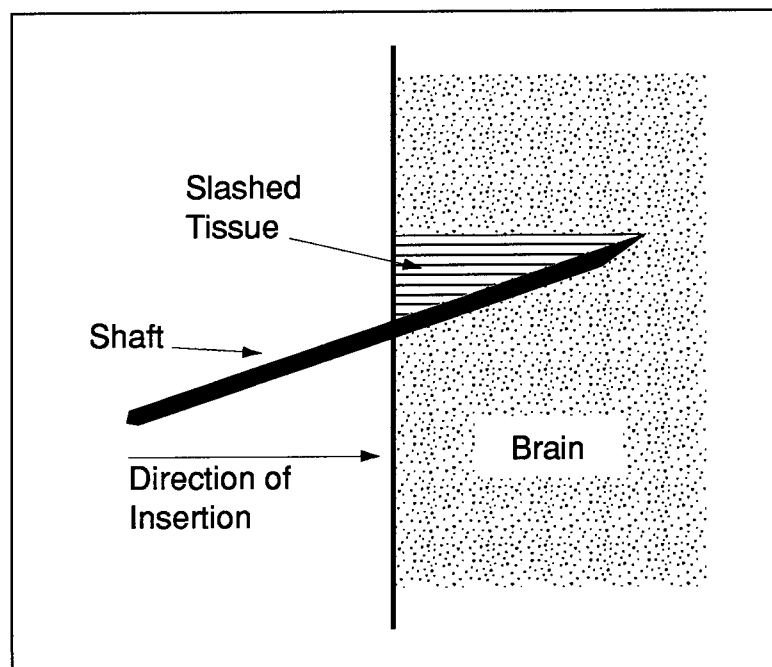
Figure 2-7.   Diagram showing how axial misalign-
                ment causes a swath of damaged brain
                tissue during insertion [24].

Besides shaft design, other critical factors needed to insure minimal damage to the surrounding tissue are insertion angle, probe cleanliness, and insertion speed. According to Edell, the "importance of axial alignment of the shafts with the axis of the insertion device cannot be overstated" [24]. As an example of damage that can be caused by

misalignment (Figure 2-7), a 1 mm shaft misaligned only 1° could cause a 17 µm slash in the surrounding tissue [24].

Thoroughly cleaning implants is critical for two reasons: biocompatibility and roughness. Edell found that leaving only a monolayer or less of sharpening agent residue on the shafts could trigger an inflammatory response from the surrounding tissue [24]. Their research found a combination of deionized water adjusted to a pH of 11 and NH_4OH functioned as an adequate polishing agent that left no residue. A highly concentrated solution of cesium hydroxide was used during the final etching process to insure a very clean surface.

Inserting unclean probes into the brain tissue caused excessive dimpling and compression of the surrounding tissue. Frequent cleanings with a 2:1 mix of H_2SO_4:H_2O_2 maintained the clean surface of the probe [24].

Although not studied quantitatively, probe insertion speed was found to have an enormous effect on the amount of tissue damage that can occur. Edell's research team found that even a blunt tip probe, inserted rapidly would transect tissue in shear— minimizing the extent of tissue damage [24].

Even with perfectly clean, sharp, probes, inserted properly, damage to the surrounding brain tissue can occur as the brain volume changes due to hydration, blood pressure and other factors. This volume change tends to concentrate pressure changes on the tips of the arrays. For a volume change of only 1%, tissue movement on the tip of a 3 mm shaft can be as much as 30 µm. As this tissue expands and contracts, cells are

destroyed and replaced by gliosis[1]. Normal brain tissue will be pushed further away from the electrode tips [24].

Quantitative studies from Edell's research show that for a clean, smooth-sided, chisel-point shaft that is inserted properly, the kill zone can be minimized to an area extending less than 10 μm from the side of the shafts and long term biocompatibility has been exhibited [24].

2.2. Conclusions

DeMott showed that it is possible to record visual evoked response (VER) data using surface mounted electrodes. His work also suggests the level of signals coming off the surface of the brain. Any device used to pick up VER data must be able to properly record voltage potentials as low as ±75μV [18]. DeMott also proved that a device with electrode spacing of 0.25 mm is capable of discerning individual signals.

Brindley and Lewin showed that it was possible to input signals into the visual system while bypassing the eye and optic nerve. The minimum electrode separation on their device was 2.4 mm and their patient was able to distinguish separate phosphenes at this distance [21].

Dobelle's research helps to refine information regarding the current needed to produce phosphene's from a surface mounted electrode array, and to confirm Brindley's research. Dobelle also experimented with various input pulses, waveforms and pulse trains to determine the optimum input signal to produce phosphenes. He concluded that

---

1. Excessive development of a fibrous support tissue called neuroglia. See glossary for more information [19].

using larger electrodes made no difference in the resolution his patients' could perceive, but reduced the current densities through the electrodes. His experiments showed that the resolution at which his patients could distinguish separate electrodes broke down somewhere between 2 to 3 mm [23]. This contradicts the research done by DeMott, but may have something to do with the fact that Dobelle was inputting signals onto the brain while DeMott was recording signal s off the brain.

Although BeMent's research involves using an insertable probe, his discussion on it's design was helpful in designing a new AFIT surface array. BeMent's goal was to produce an implantable array that had was capable of receiving a signal off the brain as low as 20 µV, had high signal to noise ratio, on-chip amplification, and only consumed 5 mW or less of power.

Finally, Edell's research showed that insertable probes are difficult to fabricate and use without destroying the tissue of the brain. Since, DeMott, Brindley and Dobelle proved that surface mounted electrodes are capable of recording from and inputting signals onto the brain, there is little engineering justification for switching to an insertable probe design.

3.1. Overview

The current design of the AFIT multielectrode array originated from one of Robert

Ballantine's VLSI classes [10]. Others [2, 7, 10–12], have updated the design. Figure 3-1

is a diagram of the current design. All location references mentioned will be based on the

orientation shown. Not shown in this diagram are test pads to verify the counter and multi-
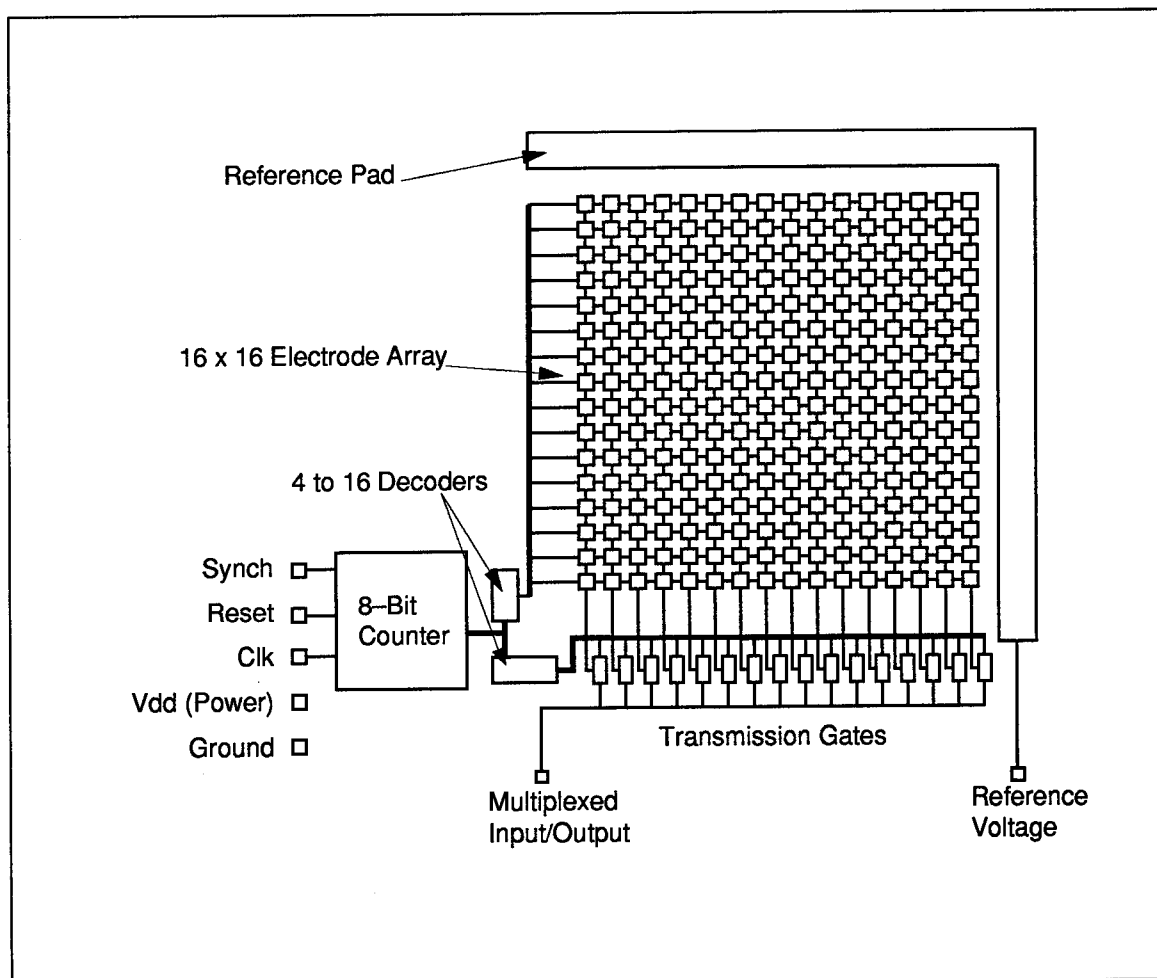

Figure 3-1.   Current design of the AFIT multielectrode array.

plexers, and column output pads (See Appendix B, Figure B-1 for Magic layout of the current circuit design). The column output pads were left over from an old design that only had a single demultiplexer. When the new counter and column demultiplexer were added, these pads were used to verify the output of the fully multiplexed signal. The design incorporates a resetable counter, 4 to 16 row and column decoders, 256 metal electrodes arranged in a 16 by 16 square array, row drivers, a "L" shaped reference pad, and switching gates. Inputs required for the chip are $+3.5 - 5^1$ V power, ground, a single, square-wave clock signal, and a reset signal. The 256 electrodes are multiplexed to a single output pad. The design has the capability of placing a signal on the surface of the brain by inputting a signal onto the multiplexed output line but, as yet, this capability has not been tested.

The general flow of the AFIT array is as follows: A square-wave clock signal is generated off chip and input to the 8 bit-counter. The counter operates at half the clock signal. The lower four bits of the counter are fed to a 4 to 16 demultiplexer (called the selector) while the upper four bits from the counter feed another 4 to 16 demultiplexer. The first demultiplexer acts as a column selector, while the other acts as a row selector. In the orientation shown in Figure 3-1, the top row and left column are selected first. The electrodes are selected left to right, down one row, then left to right again. This sequence is

---

1. Originally a 5 V power supply was used to test the circuit in Reid's thesis and current testing [12]. During testing, bond wires (especially power and ground wires) melted and it was thought to be caused by high currents through the bond wires. (LeFevre also reported problems with melting bond wires [11]). When the supply voltage was lowered to 3.5 V, problems with the bond wires melting disappeared. During SPICE tests, the current used at 5 V was nearly double that from the current used at 3.5 V (4.7 mA vs. 2.4 mA). Therefore, unless specifically mentioned otherwise, all test data shown will be based on using a 3.5 V power supply.

repeated until all electrodes are selected. Every time the top-left electrode is selected, a synch signal is generated (negative pulse).

The output of the demultiplexers/selectors does not go directly to the electrodes. The output of the row selector feeds rowdrivers, while the output of the column selector feeds the gating circuits. At any given time, the entire row of electrodes is passing signals through the circuit. The column selectors determine which of these signals is passed to the output pad.

Transmission gates (t-gates) are used to switch the electrodes on and off. Figures 3-2 a) and b) are schematic diagrams of transmission gates. Although t-gates use both NMOS and PMOS devices they are not a CMOS design, in that both devices are on or off simultaneously. Some important characteristics of t-gates are: they require both logic high and logic low signals to function, they are bi-directional, and they have no drive capability.
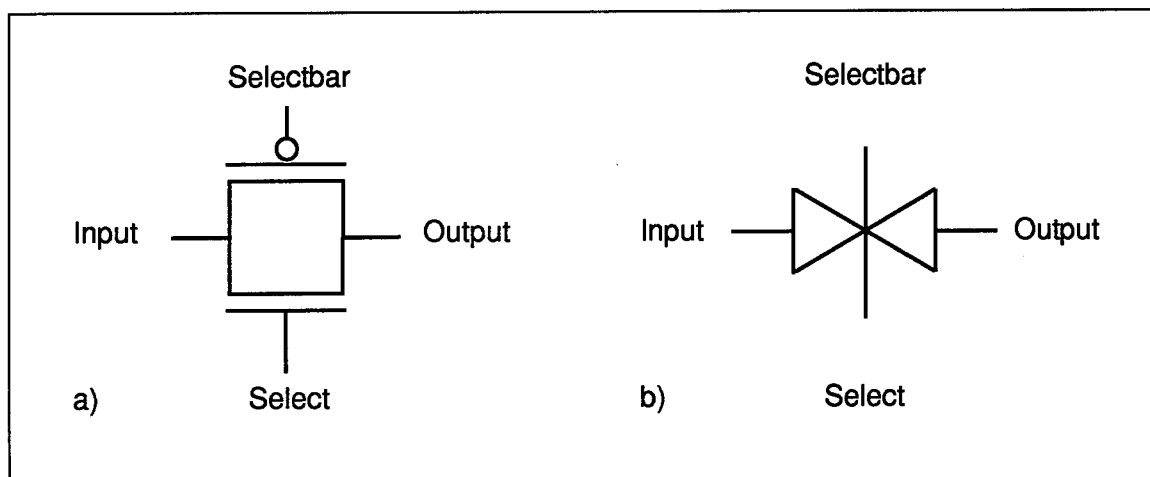
Figure 3-2.   a) Diagram of transmission gate (t-gate) showing NMOS
and PMOS transistors.
b) Schematic diagram of t-gate.

The following is a detailed description and circuit analysis of the AFIT multielectrode array. The counter, demultiplexers, rowdrivers, gating signals, and signal path are analyzed in detail. In most cases, this analysis discusses how the device operates with a supply voltage of 3.5 V and a clock signal of 50 KHz (as used in actual testing [27]).

3.2. Counter

The counter is an 8 bit binary counter with a reset line. It requires a square-wave clock signal input (generated off-chip), reset signal, power and ground lines. Output is an 8 bit binary signal labelled from low bit to high bit in Magic[1] "cstate[0]" to "cstate[7]". The counter is incremented on the negative edge of the clock pulse. The lower four bits (cstate[0] – cstate[3]) are routed to the column decoder while the upper four bits (cstate[4] – cstate[7]) are routed to the row decoder. The counter is resetable from off chip. A logic high signal on the reset pad, causes the counter to go to a '00000000' state, which selects the top–left electrode, while a logic low signal is required for the counter to increment.

The counter was designed using behavioral synthesis and standard-cell design. Behavioral synthesis allows the designer to describe *how* a circuit is to function behaviorally and the software generates a mask level design. The AFIT VLSI lab uses the VLSIC Hardware Description Language (VHDL[2]) to create the behavioral description and generate the cell layout. An example of the VHDL language that might be used to describe the low–order bit of the counter follows:

---

1. Magic is an interactive system for creating and modifying VLSI circuit layouts.
2. VHDL is an offshoot of the very high speed integrated circuit (VHSIC) program funded by the Department of Defense in the late 1970's. A new version of the language was proposed in 1981 and called VHDL. In 1987 it was adopted as the IEEE 1076 standard [25].

```
ARCHITECTURE behave OF counter IS
BEGIN
--Comment - this process only activates when a clk
--event takes place
PROCESS (clk)
BEGIN
    IF (clk = `0') AND (clk'event) THEN
        IF (Cstate[0] = `1')
            Cstate[0] <= `0';
        ELSE
            Cstate[0] <= `1';
        END IF;
    END IF;
END PROCESS;
END behave;
```

This code activates on changes in the clock signal and is further defined to trigger

on the negative edge of the clock signal. From this behavioral description the VHDL tools

generate a logic layout and finally a Magic file using standard cell design.

Standard-cell design is characterized by identical or nearly identical rows of alter-

nating power and ground lines [26]. Standard sized logic gates are placed between alter-

nate rows—signal lines are routed in the adjacent rows. Figure 3-3 is the Magic layout of

the the counter. Power and ground lines run horizontally through the circuit, with input

lines on the left and output lines on the right. These logic gates can be thought of as

building blocks. Libraries of these logic gates are available—some are optimized for

speed and some for density [26]. The library used for the counter was optimized for speed

rather than density.

The counter was tested from 10 Hz to 1 GHz using SPICE simulation. In these

tests, the focus was on the least significant bit's waveform (Cstate0), and the current

through the circuit. Figure 3-13 is a chart showing the clock signal, Cstate0, clock current,

and supply current at a clock input frequency of 50 KHz. As can be seen from this figure,
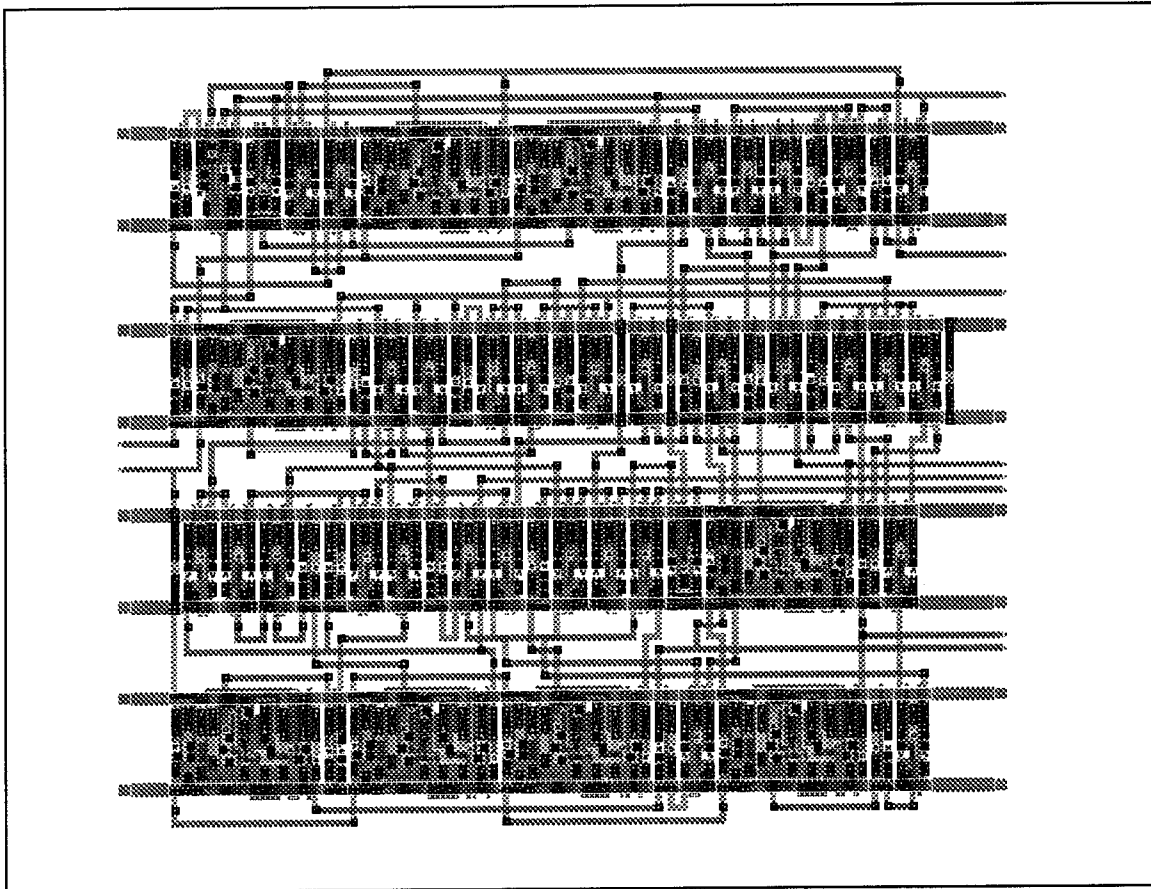
Figure 3-3.   Magic layout of the 8-bit counter.

the counter is triggered on the negative edge of the clock pulse. The frequency of Cstate0

is half that of the clock. The counter functioned properly up to 100 MHz—after that the

Cstate0 waveform was no longer a square wave (See Appendix B, Figure B-4).

3.3. Selectors

The output of the 8-bit counter is routed to two 4 to 16 bit demultiplexers which

are referred to as *selectors* in this thesis because they select specific rows or columns.

Figure 3-4 shows the Magic layout of the selector. The two selectors are the only compo-

nents of the current design that are still an NMOS design. The four input lines are located
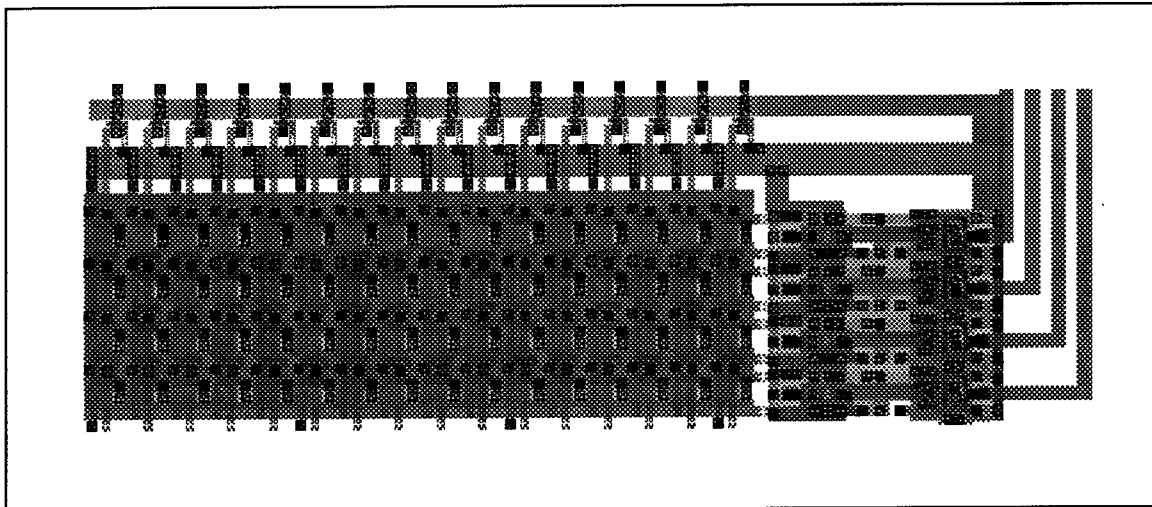
Figure 3-4.   Row and column selectors.
Input lines are in the upper right corner (4 inputs) and out-
put lines (16) are along the bottom left.

in the upper right corner of the circuit and the 16 output lines are evenly spaced along the

bottom.

Figure 3-14 is the output of the selector using a 50 KHz clock signal. For clarity

only output 0, 2, 7, and 15 are shown. Although not shown in this chart, the SPICE

charting tools showed considerable spiking (peaks of 3 mV) on the falling transition of all

outputs (See Appendix B for SPICE generated charts). The spiking occurs at the exact

clock frequency—not the counter frequency. This is significant because it is exactly what

is seen when testing the actual circuit (see Figure 1-3). The counter was tested at 50 KHz

and 250 KHz.   Based on MOSIS® supplied parameters for gate length and the area of the

NMOS and PMOS gates, a calculated load capacitance of 153 fF was placed between each

output and ground to simulate the gate capacitance of the rowdrivers and gate circuits.

Figure 3-15 is a chart of the current used by the selector when a 3.5 V supply

voltage and 50 KHz clock are applied. The disadvantages of using NMOS technology are

clearly apparent here. Each selector draws a constant 2.4 mA, or over 35 times more
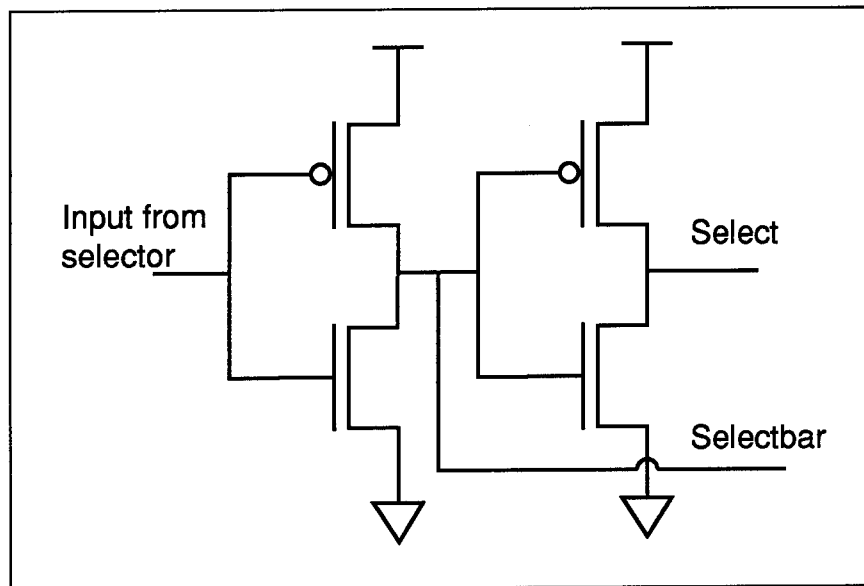
Figure 3-5.   Schematic diagram of the rowdriver circuit.

current than the counter. If a 5 volt supply voltage is used, the current draw jumps to

4.7 mA (See Appendix B, Figure B-2). Heat generated from the counter using a 3.5 V

supply voltage is 115 KW/m². If a 5 V supply is used, the heat generated is 317 KW/m².

3.4. Rowdriver/Gate circuits

The output of the selector is fed into either the rowdriver or the gate circuit. There

are 16 rowdrivers and 16 gate circuits on the array, each associated with a single row or

column.

3.4.1. Rowdrivers. The rowdriver is simply two inverters tied together as shown in

Figure 3-5. The outputs (select and selectbar—both required to operate t-gates) of each

rowdriver run horizontally along the entire length of the array between the rows of elec-

trodes (see Figure 3-10). When the chip is operating, an entire row of electrodes is being

sampled at a given time. The 16 rowdrivers are aligned vertically on the left side of the

array. Figure 3-6 shows the Magic layout of the rowdriver. The rowdriver was tested at
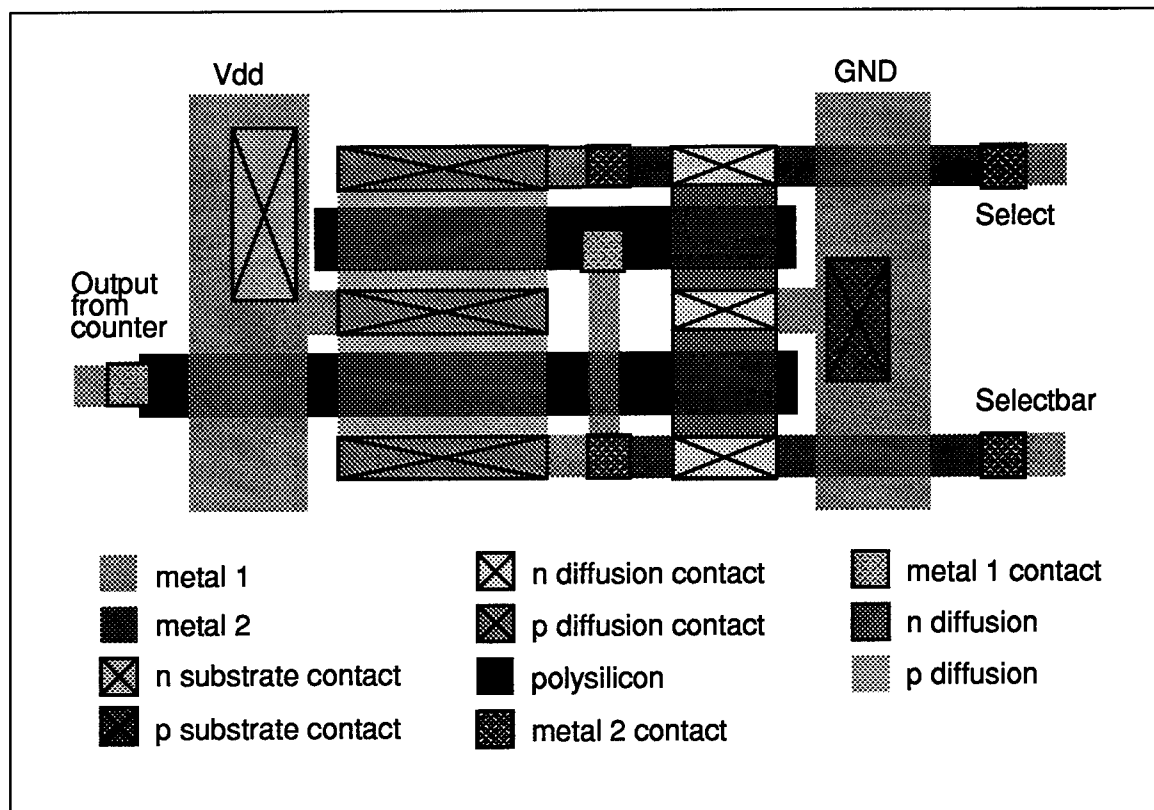
Figure 3-6.   Magic layout of the rowdriver circuit.
Sixteen of these located on the left side of the array.

50 KHz and 250 KHz. Figure 3-16 is a chart showing the current waveforms of the

rowdriver at 50 KHz. A load capacitance of 220 fF and 440 fF was used to simulate the

gate capacitance of the NMOS and PMOS transistors used for the t-gates. No major prob-

lems were noted with the rowdriver, however, the gate length for all the transistors on the

current version is 6 μm, which was apparently the minimum feature size when this circuit

was designed.

3.5. Gate circuits

Figure 3-7 is a schematic diagram of the gate circuit. The gate circuits run along
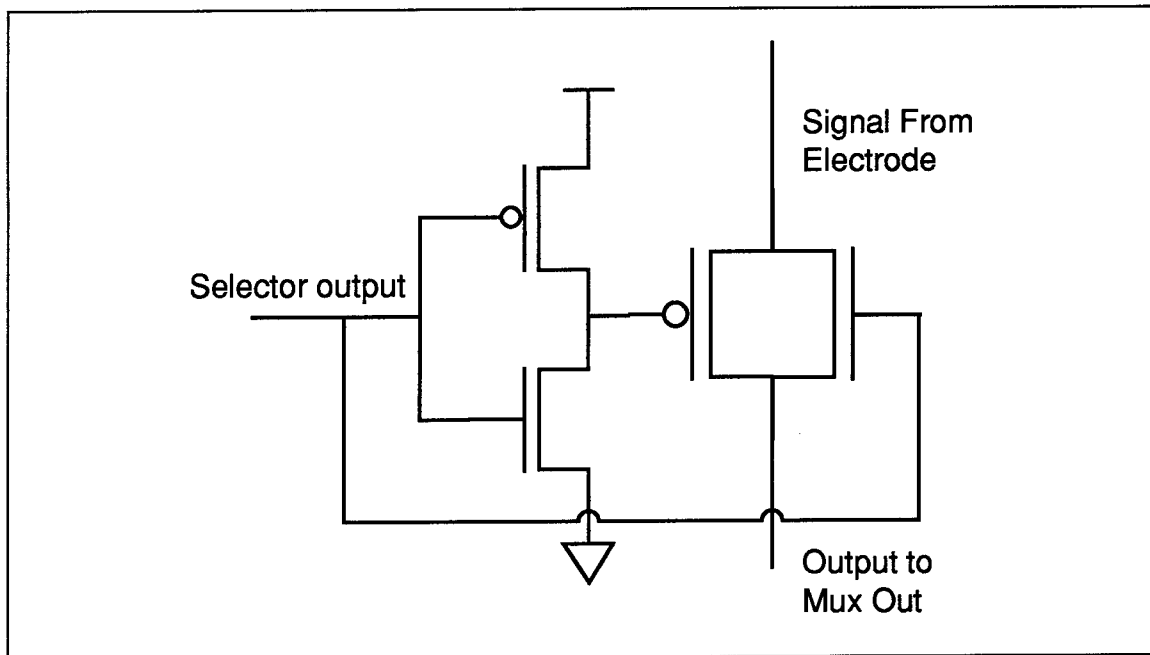
Figure 3-7.   Schematic diagram of gate circuit.

the bottom of the electrode array and perform the final multiplexing. Figure 3-8 shows the

Magic layout of the gate circuit. The gate circuits employ a single inverter and a t-gate.

The "select" line (for the t-gate) is the output of the selector, while the "selectbar" signal

for the t-gate is the output of the inverter. As mentioned earlier, an entire row of electrodes

is active at any given time, so there is always a signal being applied to the gate circuits.

The column selector determines which gate will be on and consequently which signal will

be sent to the multiplexed output. The gate circuit was not tested individually, however it

was tested as part of the signal path that follows.

GND

metal 1
metal 2
n substrate contact
p substrate contact
n diffusion contact
p diffusion contact
polysilicon
metal 2 contact
metal 1 contact
n diffusion
p diffusion

Signal From
Electrode

Vdd

To Mux Out   Select Line
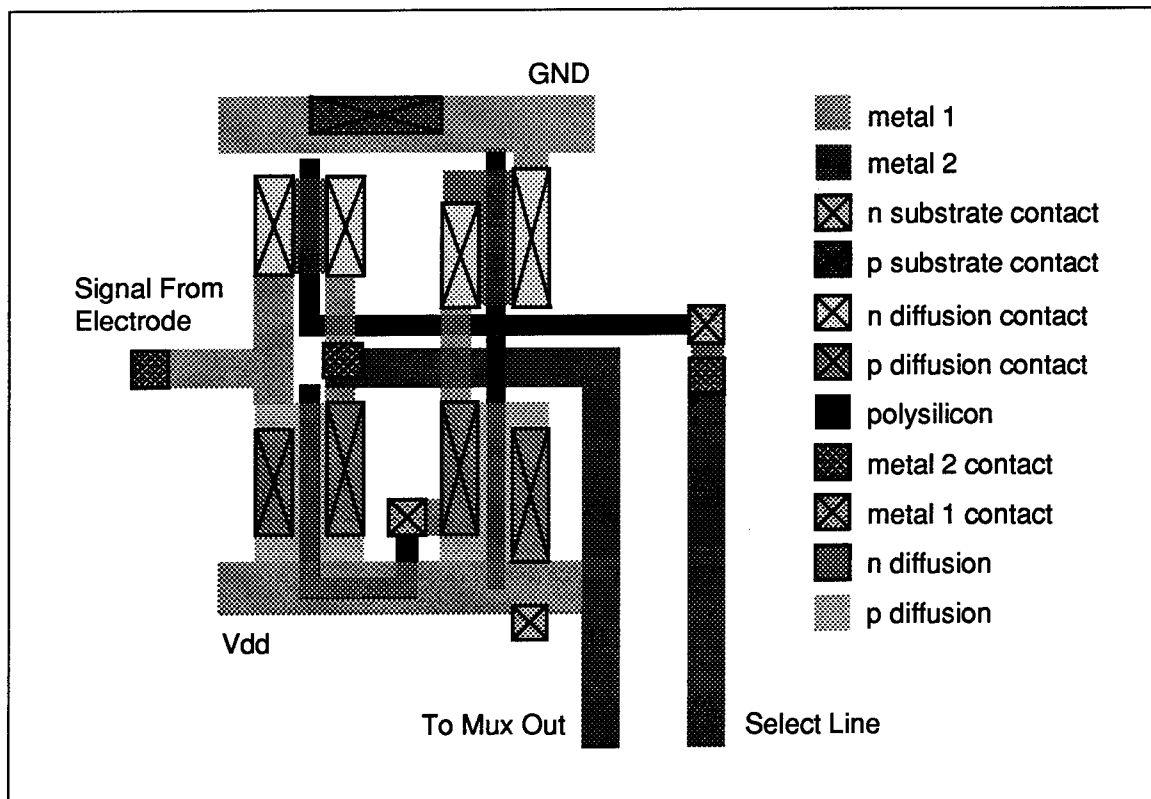
Figure 3-8.   Magic layout of the gate circuit.
               Sixteen of these are located along bottom row of the array.

3.6. Switching circuitry

The entire switching circuitry consisting of the counter, selectors, and rowdriver

was extracted from Magic and tested using Spice. Figure 3-17 shows the current used by

the new design. For a 3.5 VDC power supply, the rms supply current has been reduced

from 4.8 mA to 49.3 μA

3.7. Signal path

The signal path consists of the input electrode, t-gate at the electrode, gate circuit

and multiplexed output pad. Figure 3-9 is a schematic diagram of the input electrode. The

electrode itself is a 180 μm square metal electrode imbedded in a p-well for isolation.
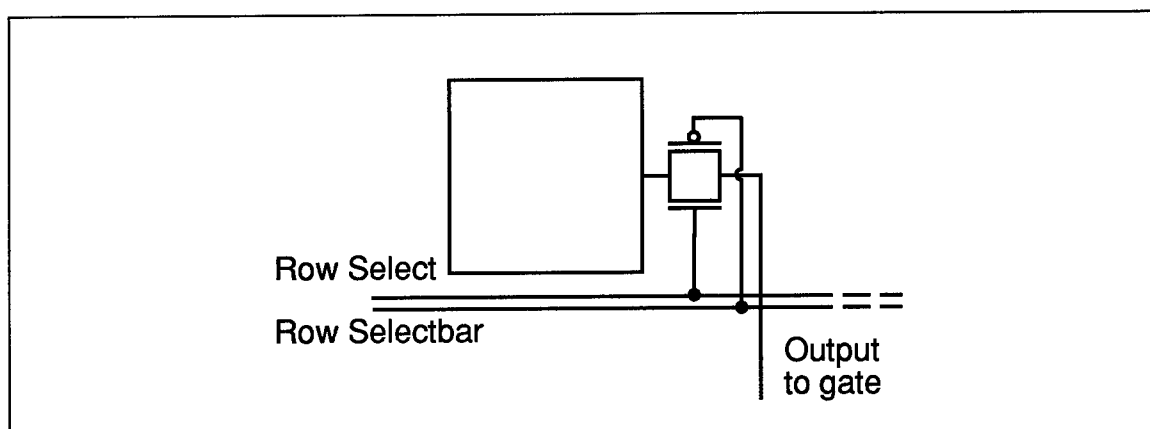
Figure 3-9.   Schematic diagram of input pad and t-gate.

Figure 3-10 is the Magic layout of the input electrode. The actual exposed area is only 160

μm (cross-hatched area in Figure 3-10). Supply power, ground and output lines run verti-

cally between the electrodes, while select and selectbar lines (to turn the t-gates on and

off) run horizontally between rows. Output from the electrode goes to the gate circuit and

finally to the multiplexed input/output (mux out) pad. The mux out pad is a 140 μm square

metal electrode.

Several tests were performed on the signal path to determine the best load imped-

ance for the signal path and the effect of varying the input frequency on the input imped-

ance.

The first test was to find a match load resistor for the signal path. The input signal

was fixed at 200 μV and a frequency of 100 Hz[1]. Shunt load resistances varying from 1

KΩ to 5.5 MΩ were tested to see what effect they would have on the output signal. It was

determined that a load resistance of less than 30 KΩ resulted in a considerable attenuation

in the output voltage (Figure 3-18). Load resistances of between 30–100 KΩ showed no

---

1. 200 μV is the maximum voltage recorded off the surface of a raccoon's brain in DeMott's exper-
   iment [18].
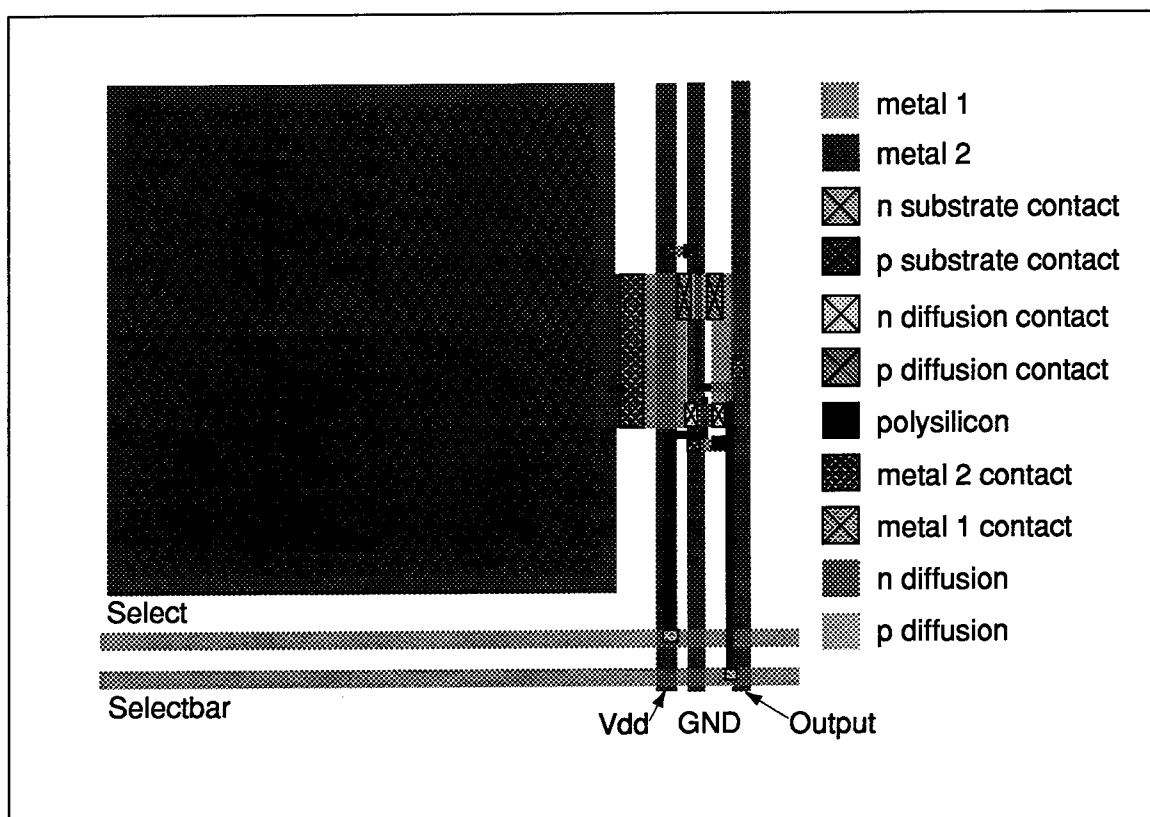
Figure 3-10. Magic layout of the input electrode and t-gate

appreciable drop in the output voltage and very little spiking as the t-gate were switched

off (Figure 3-19). Using a load resistance greater than 100 KΩ caused output spiking as

the t-gate was switched off (Figure 3-20). When the load resistance was greater than 1

MΩ, the row t-gate never fully shut off the signal and output voltage was recorded.

Next the load resistance was fixed at 100 KΩ. With a 200 µV sine wave applied to

the input electrode, the frequency was varied from 100 Hz to 6 KHz and the signal path

current was recorded[1]. From this data the input impedance of the signal path was plotted.

Figure 3-11 shows the results of this test. The impedance reaches a high of 378 Ω at 35 Hz

and then levels off.

---

1. The frequency range of 5 Hz to 50 Hz was based on frequency of theta through gamma rhythms
    of the human brain [28].

3–13
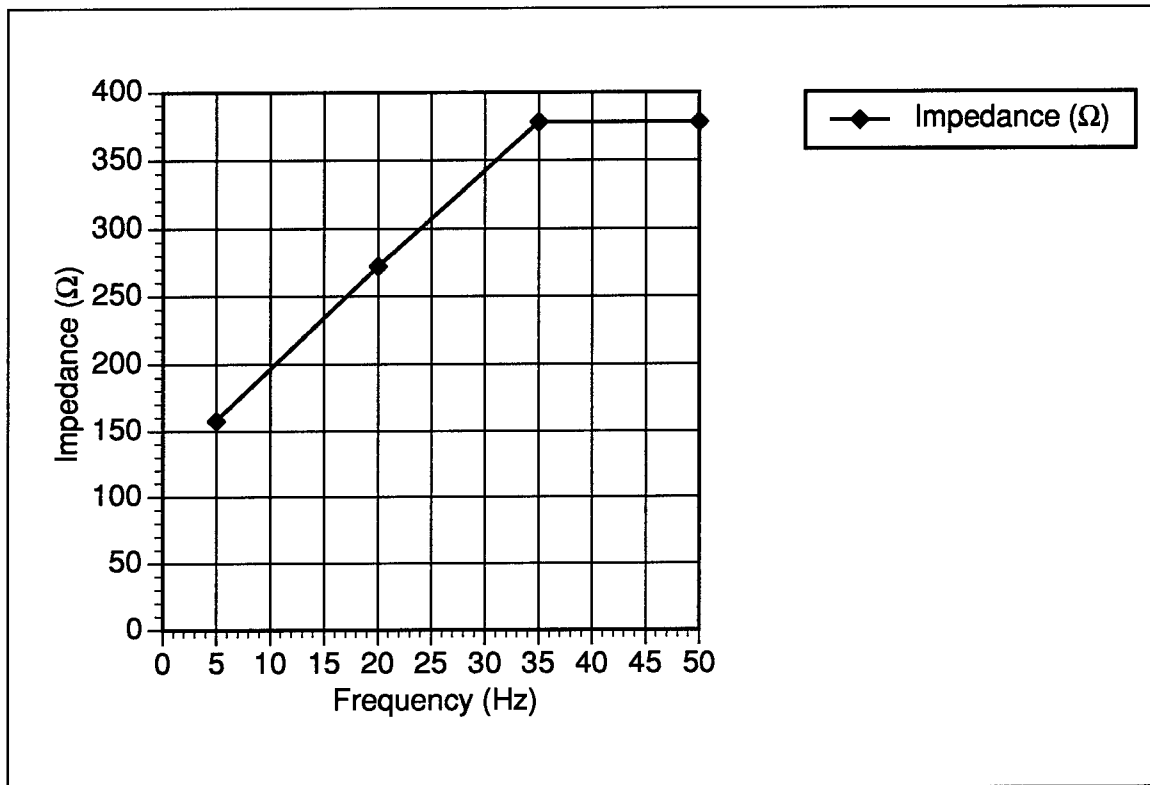
Figure 3-11.　Signal path impedance.

3.8. Synch output

The synch output circuit consists of a NAND gate whose inputs are connected to

the low bit of the the row and column selectors. With this wiring, the NAND gate provides

a negative pulse on the output pad when the top left electrode is selected. During actual

testing, Spenik noted that the synch output signal was not reliable [27]. This is probably

due to the fact that the NAND gate has difficulty driving the synch output pad.

3.9. Miscellaneous

There are also some problems with the general layout of the current device. As

mentioned previously, the column output pads are still on the chip, despite the fact that

they aren't being used. On the left side of the circuit are pads for power, ground, synch
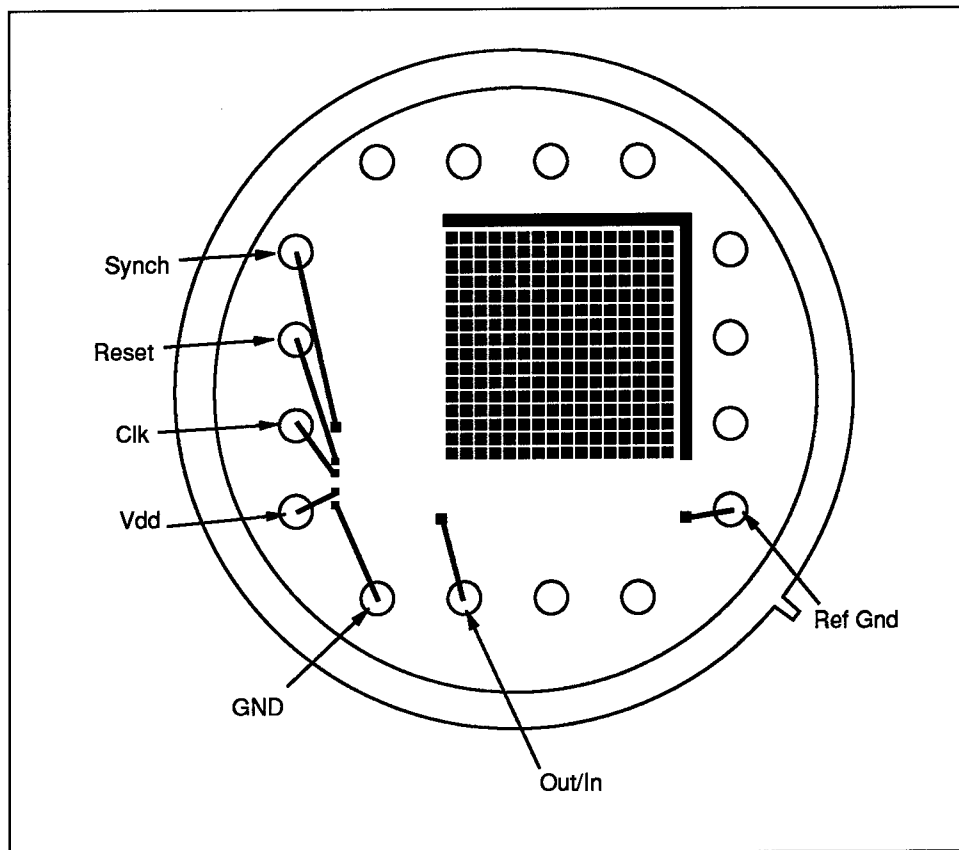
Figure 3-12.   Bonding diagram for the current design.

out, clock input, counter reset, and 8 tests pads to monitor the output of the counter.

Figure 3-12 is the bonding diagram of the current design using the header package

selected for implantation (the scale of this drawing is accurate). Not shown in this diagram

are the test pads for the counter, nor the 16 column output pads. With all the connections

bunched up on the left side of the chip it is possible that some of the bonding wires could

short out other connections.

Finally, during his testing, Spenik, a graduate student also working on this project,

found the "L" shaped reference electrode a poor ground reference [27]. He tried hooking

up a differential amplifier to the output pad, using the reference pad as the ground plane.

In order to get good differential amplification, both inputs should have very similar imped-

ances. The reference electrode has a much greater impedance than the other electrodes. Spenik suggested that it would be better if an electrode adjacent to the electrode being sampled was used as a reference [27].

3.10. Conclusions

The current design has been fully characterized. All components are working as specified, however there are some improvements that should be made.

First, the selector circuits should be redone using a CMOS design. This will cut down the amount of current used tremendously. If for example, each redesigned selector used as much current as the 8 bit counter, the current required for the entire chip would be reduced by 95%.

Next, the reference electrode should be removed and a different source for ground reference should be determined. An adjacent electrode seems to be a good source for such reference.

Finally, the overall layout of the chip should be cleaned up and the power, ground, clock, reset and synch lines be moved to better accommodate the chosen header package.
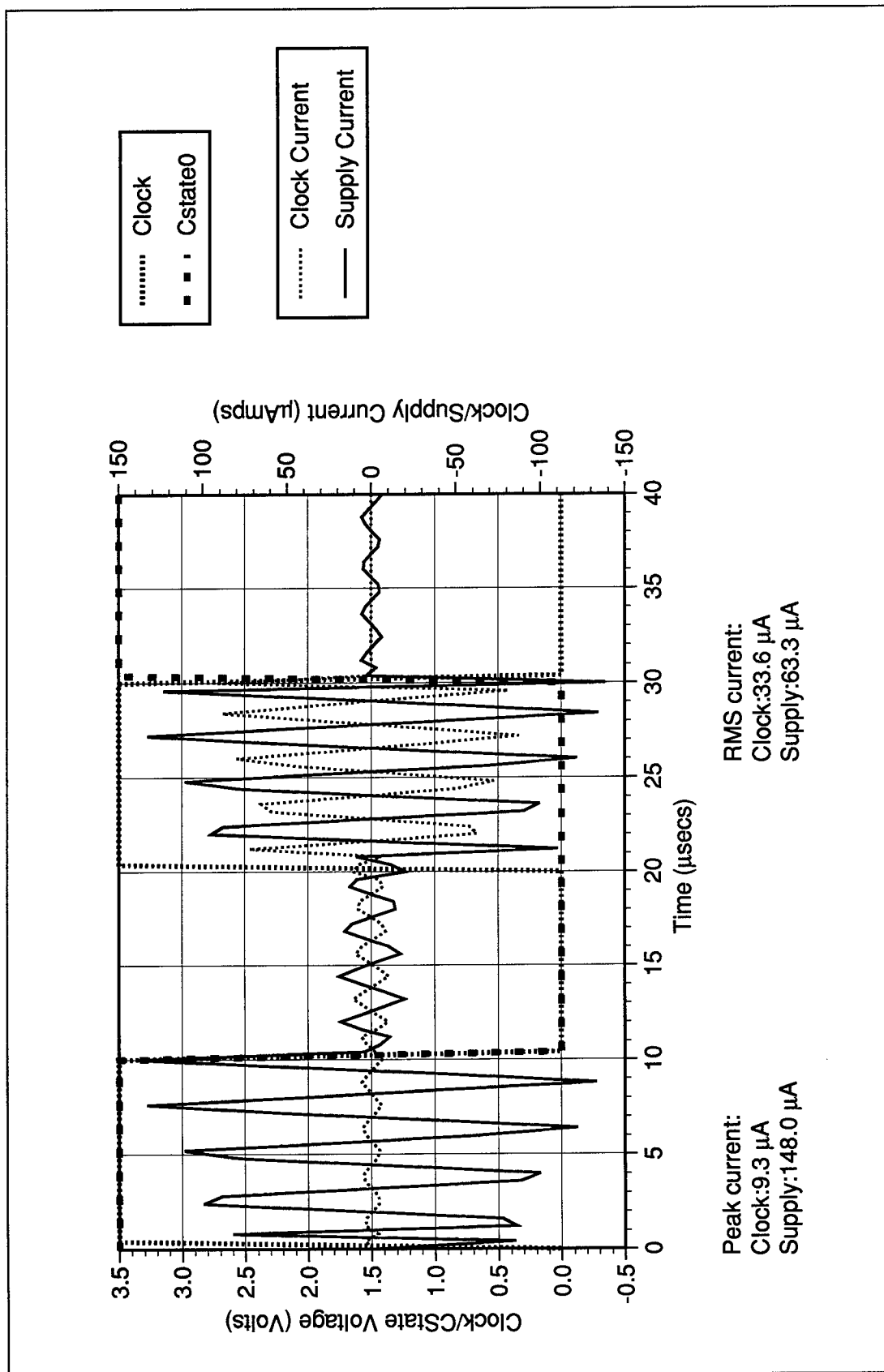
Figure 3-13. 8-bit counter at 50 KHz showing clock signal, Cstate0, supply current, and clock current.
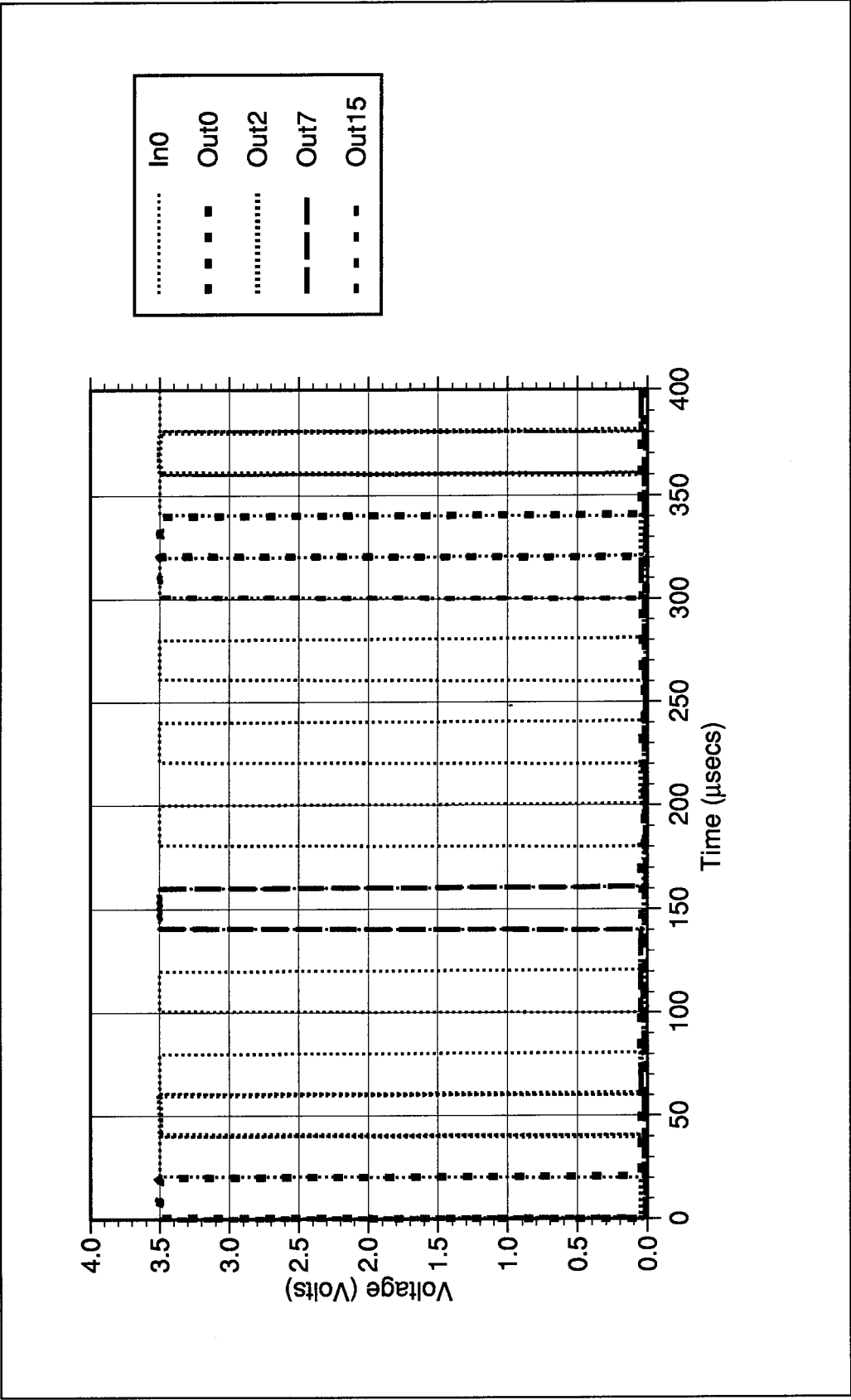
Figure 3-14.   Output from the selector using a 50 KHz clock signal.
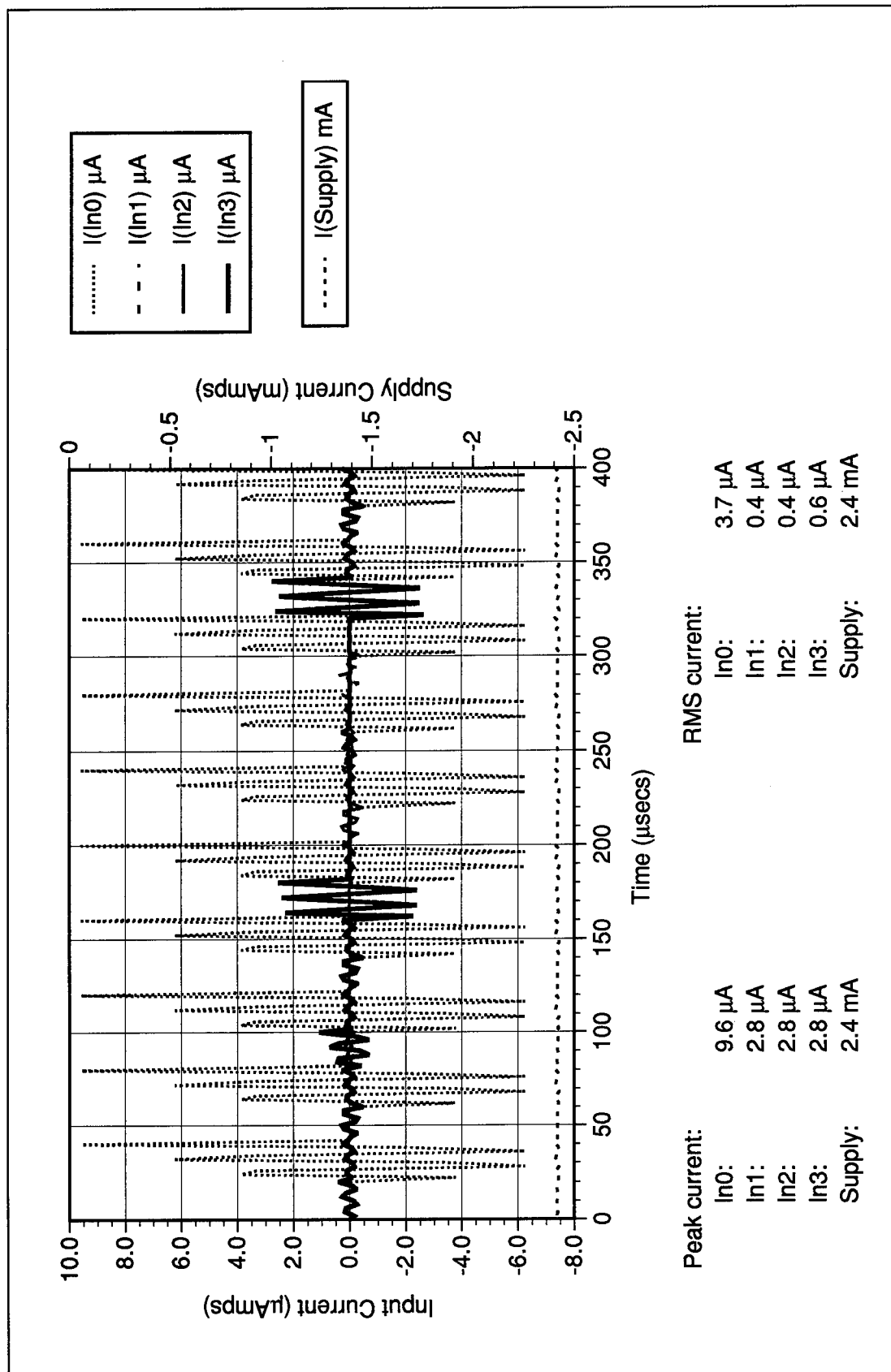
Figure 3-15. Selector current using a 3.5 Volt power supply and a 50 KHz clock signal.
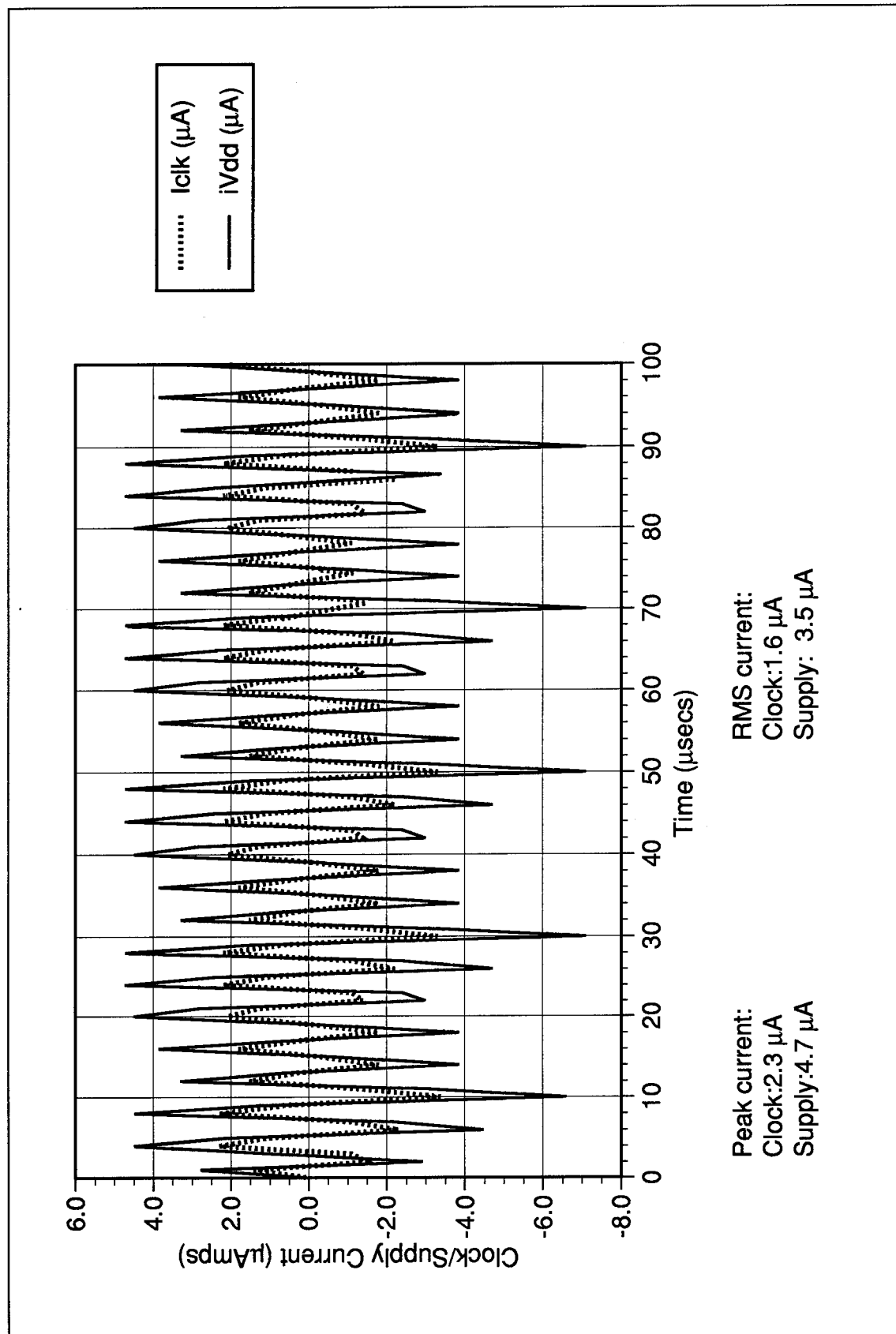
Figure 3-16. Rowdriver current waveforms.
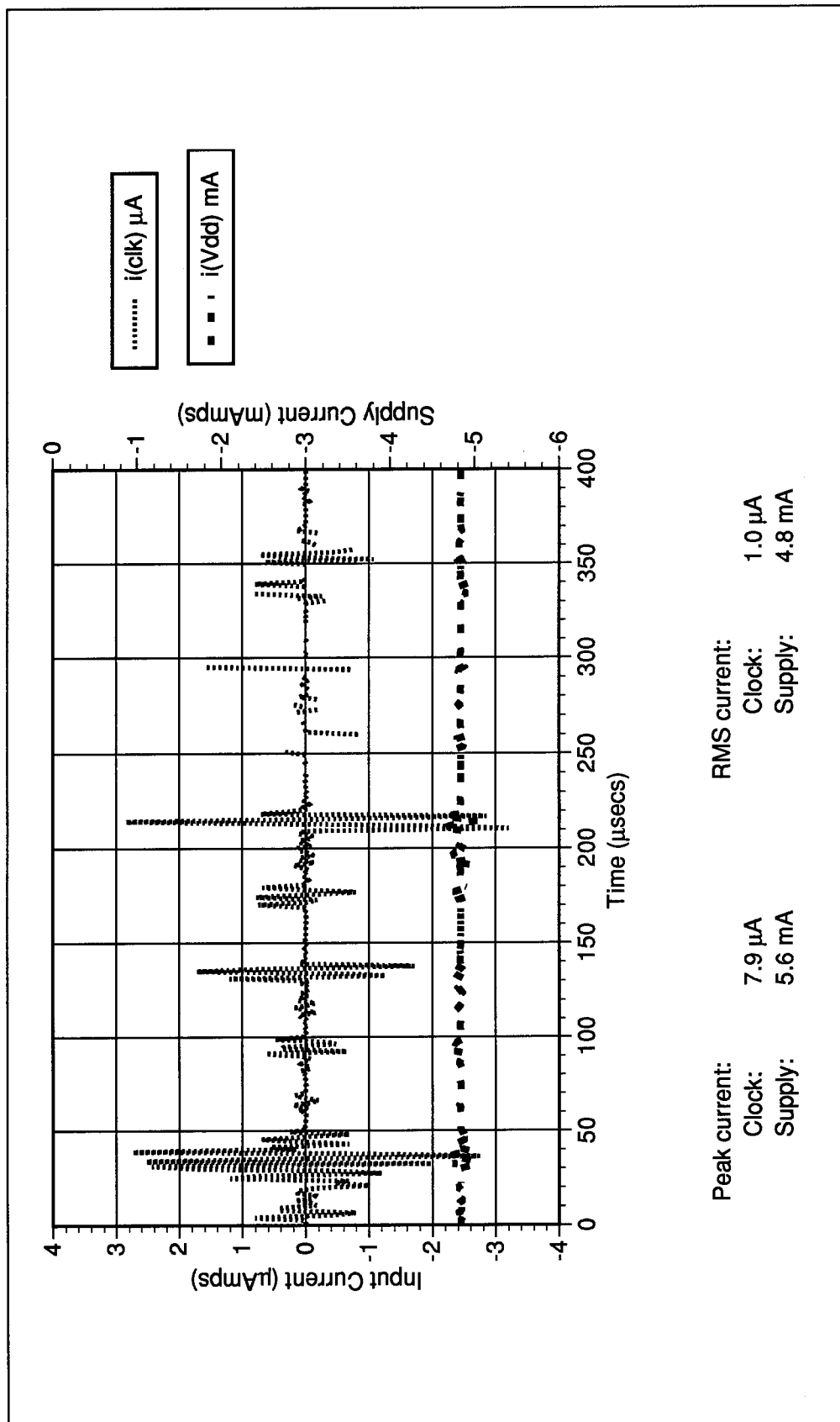Supply voltage is 3.5 V and clock frequency is 50 KHz.

3–20

Figure 3-17. Switching circuit current waveform using a 3.5 V supply voltage. The switching circuit includes: counter, row and column selectors, and row-driver.
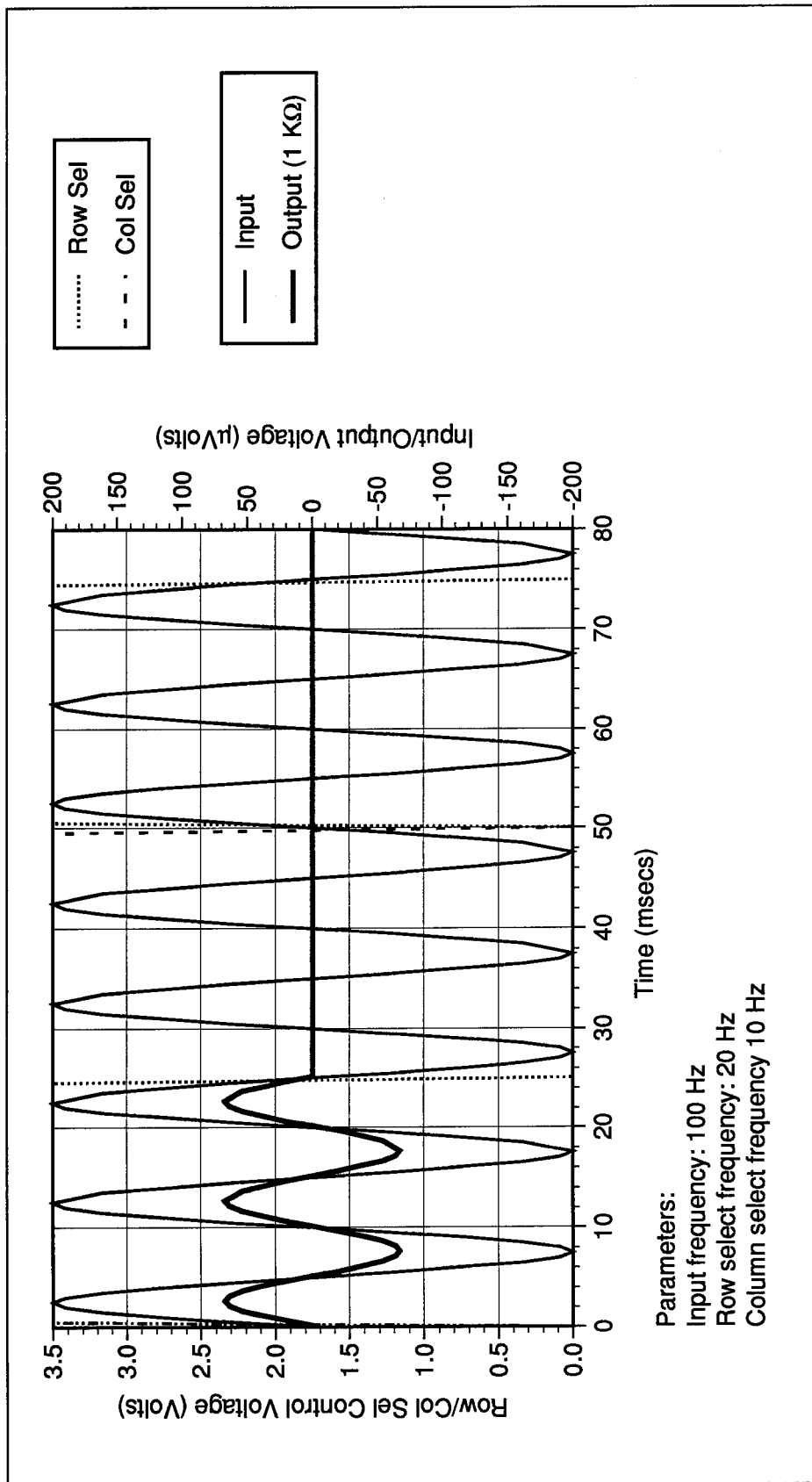
Figure 3-18.   Signal path using 1 KΩ load resistor.
Output voltage is attenuated.
Note: Row select and column select frequency was set low to show effects of
gate switching.
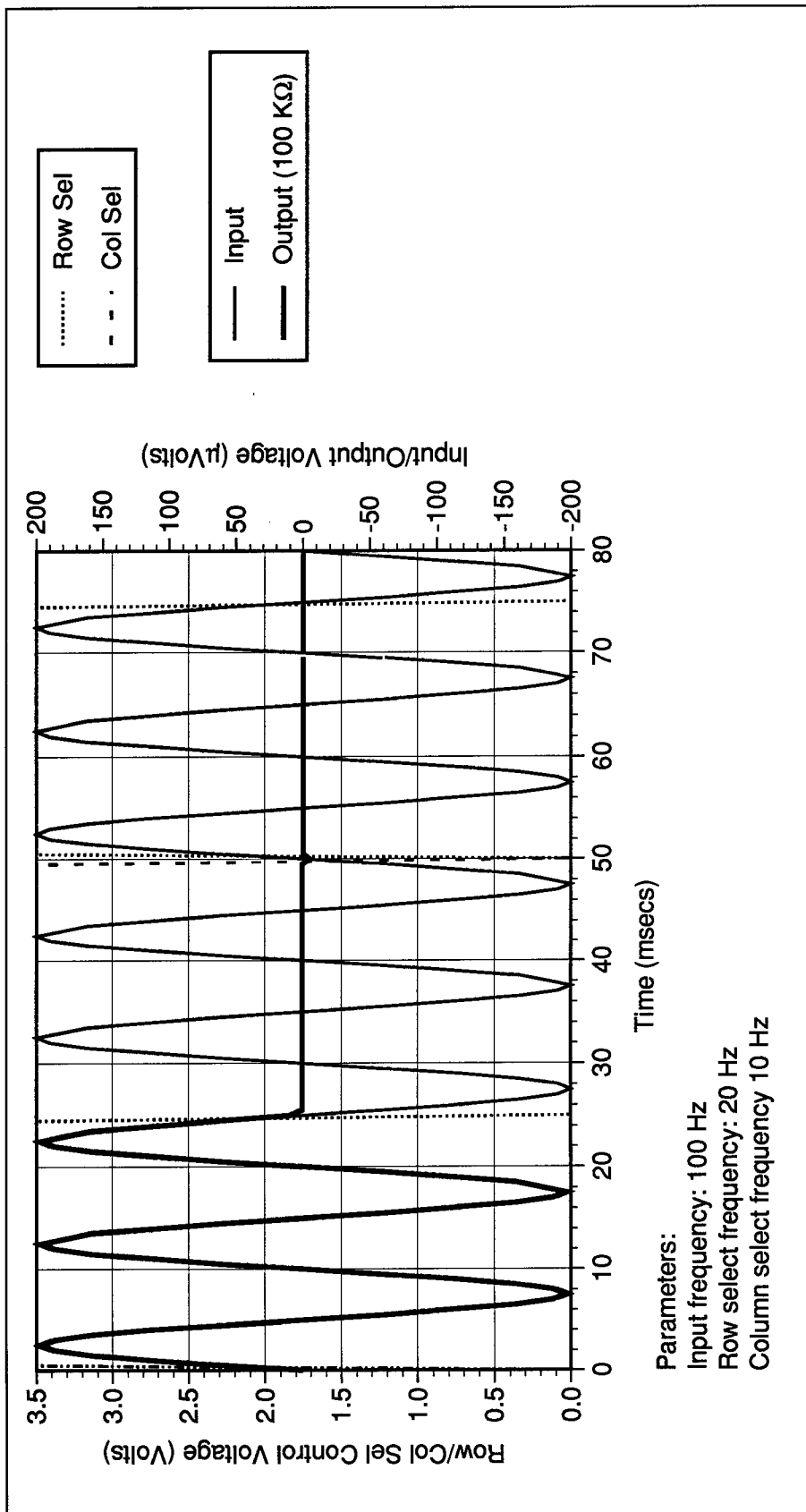
Figure 3-19. Signal path using 100 KΩ load resistor. No appreciable attenuation nor spiking is seen.

Parameters:
Input frequency: 100 Hz
Row select frequency: 20 Hz
Column select frequency 10 Hz
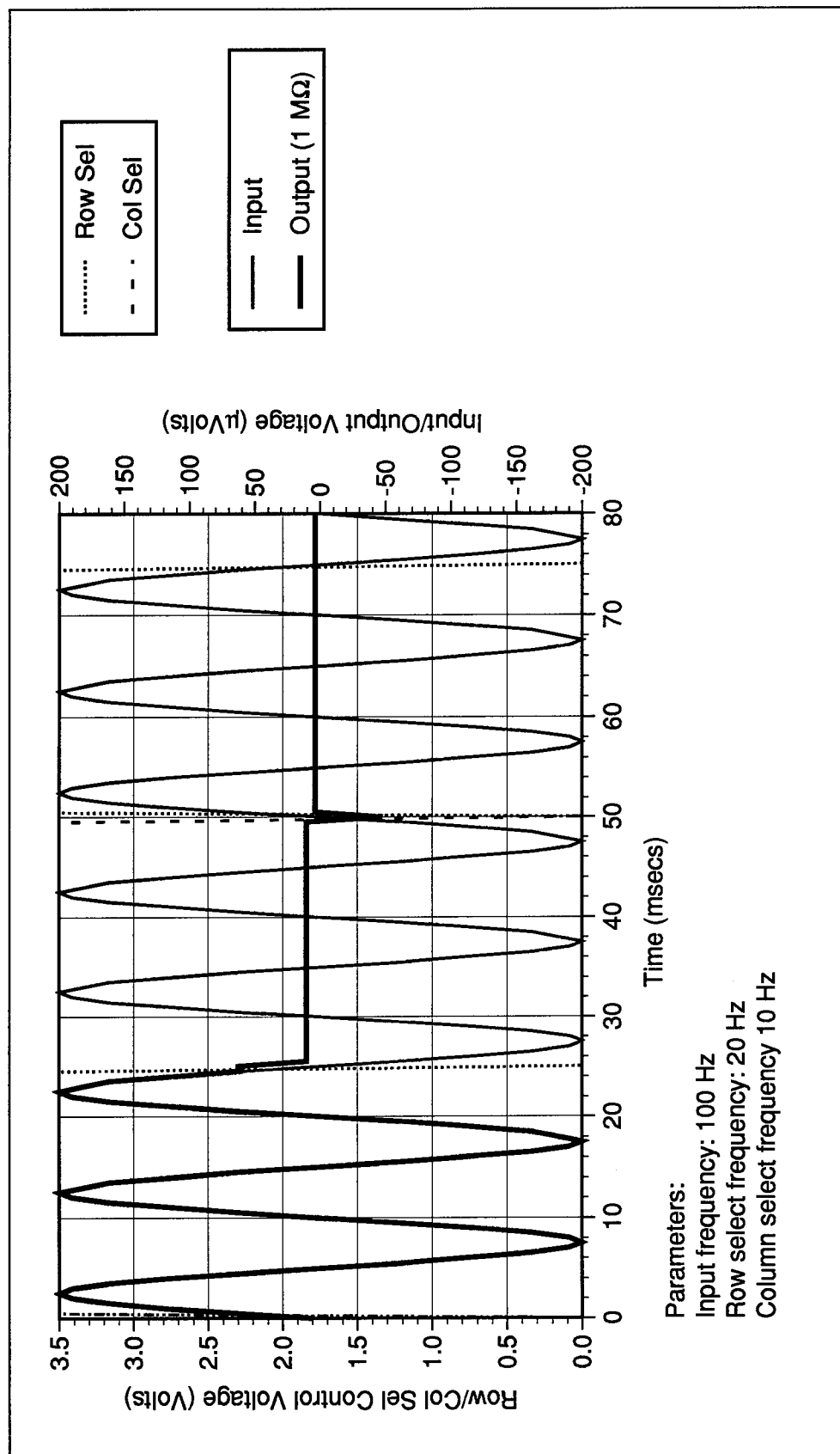
Figure 3-20.   Signal path using 1 MΩ load resistor.
Spiking on the output can be seen at the 50 msec mark.
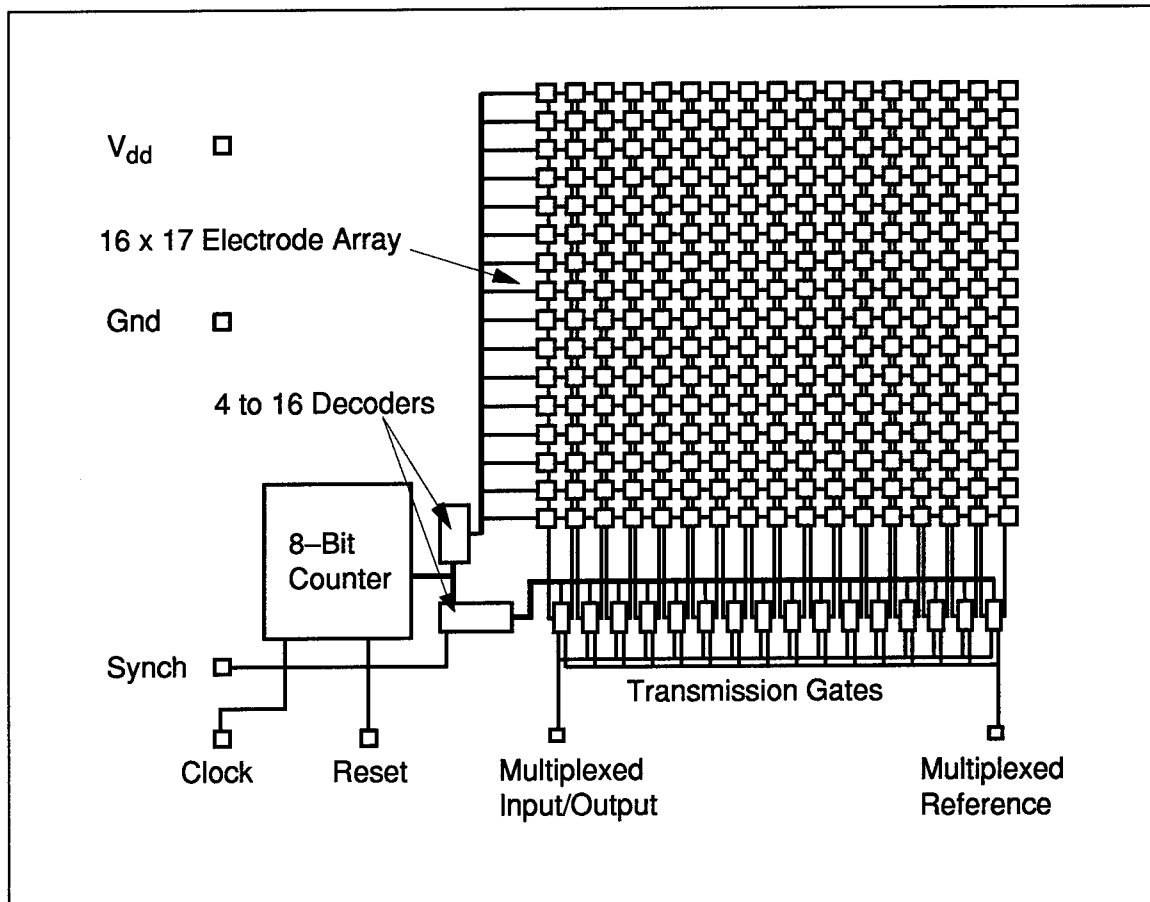
Figure 4-1.   Layout of the new AFIT multielectrode array.

4.1.   Overview

Figure 4-1 shows the layout of the new AFIT multi-electrode array. The goals for

this redesign were to reduce the current draw and noise of the existing circuit. While the

overall signal path and layout are similar to the old design, many changes have been made

(See Appendix C, Figure C-1 for Magic layout of the new design). The selectors/demulti-

plexers have been redesigned using CMOS technology, drivers/buffers have been added to

4–1

the column select lines, the "L" shaped reference pad was removed, all t-gates have been replaced by NMOS gates, the input/output pads have been moved to more closely match the layout of the header package currently being used, and the signal and switching paths have been rerouted to minimize possible noise sources leaking to the signal lines. Each of these changes will be discussed in detail.

4.2. Design

4.2.1. Electrodes/switching circuit.

Few changes were made to the electrode array. The PMOS transistors were removed, while the NMOS gate widths were increased from 16 to 20 μm. Figure 4-2 is the Magic layout of the new electrode. The NMOS transistor was moved farther to the right of the electrode so that it is in the exact center of the columns made between electrodes. This was done to reduce the possibility of ion contamination to the NMOS transistor after the circuit has been encapsulated. These gates are the most susceptible to contamination because they are only 45 μm from the electrodes. By removing the PMOS transistor, the power lines (running vertically through the array) and selectbar lines (running horizontally through the array) were eliminated. An additional output line was routed vertically through each column of the array so two samples from the adjacent electrode in the same row could be taken simultaneously. Finally, the dimensions of the electrode/gate/wiring were changed to be exactly 250 x 250 μm. This was done to make layout of the array much easier. The layout program, Magic, has an "array" command that creates an n x m array from any specified subcell.
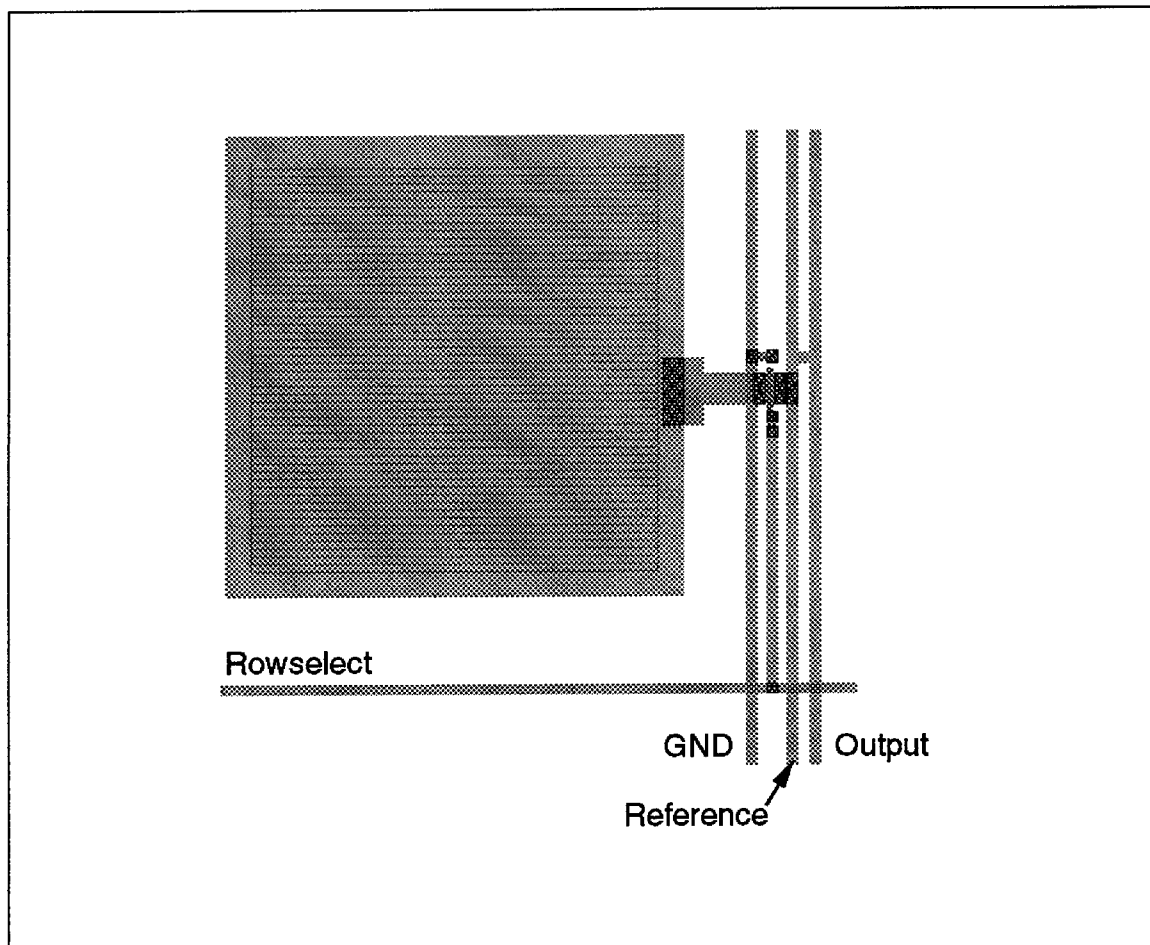
Figure 4-2.   Magic layout of the new electrode.

4.2.2. Selectors/demultiplexers. The selectors were redesigned using behavioral

VHDL. A behavioral description of the circuit was written and tested. Figure 4-3 is the

logic diagram of the new circuit. This design was transformed into logic gates using the

VHDL CAD tools and from this a Magic layout was produced. Figure 4-4 shows the

Magic layout of the new selectors. The old design measured 161 x 465 μm and covers an

area of 0.0748 mm². The new design measures 392 x 296 μm and covers an area of 0.116

mm². One of the disadvantages of using behavioral synthesis in designing circuits is that

the designer has little control over where the input/output lines are placed. For example,

the designer can specify that input lines are on the left and output lines on the right, but the
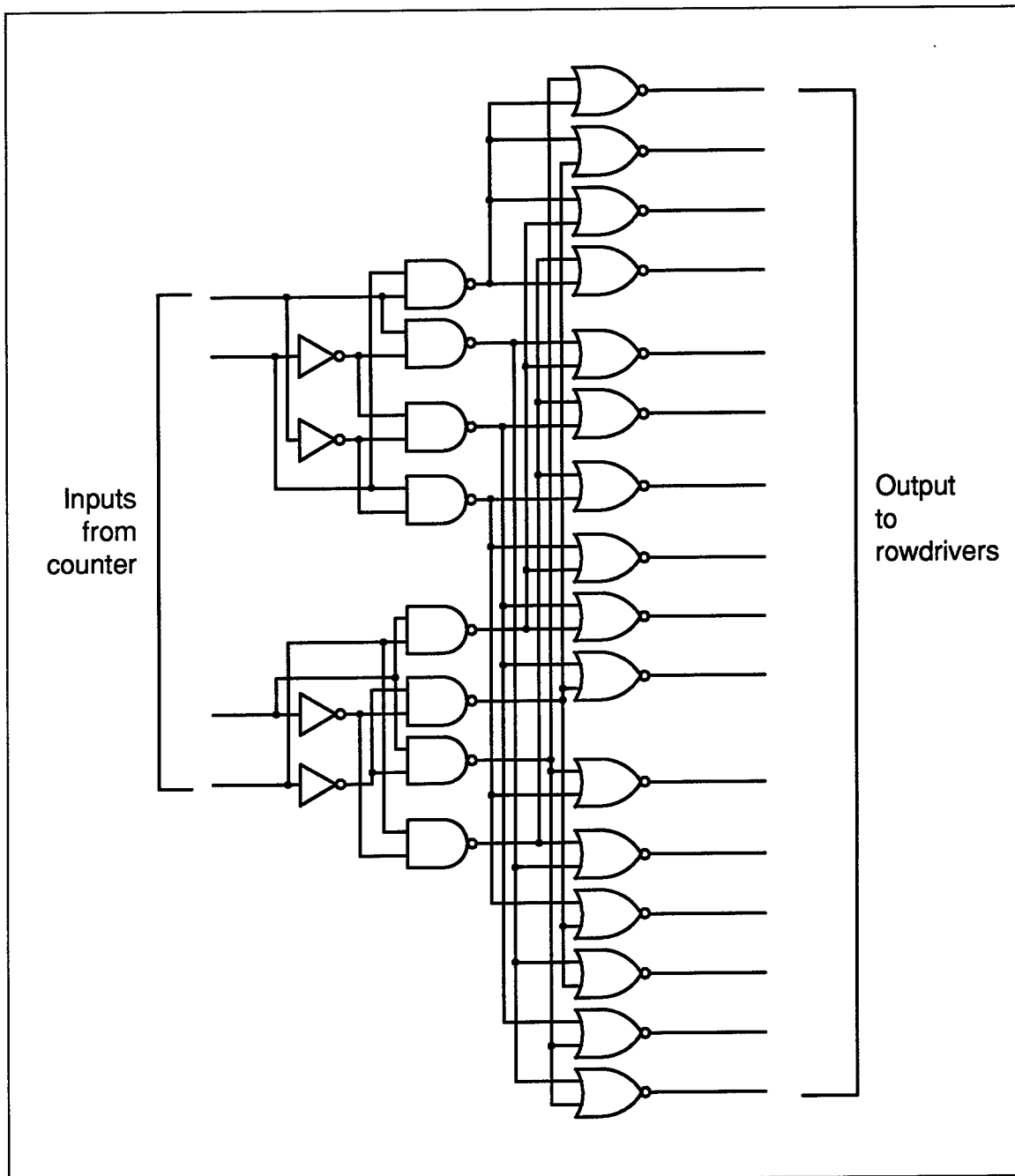
Figure 4-3.   Logic diagram of new selector.

order of placement is not controllable. The automatic routing tools place the input/output

lines on the circuit in order to minimize routing paths. Consequently the input/output lines

are rarely in order which makes routing to other components more difficult. This made

routing of the output lines more difficult and less clean. This design was used for both row
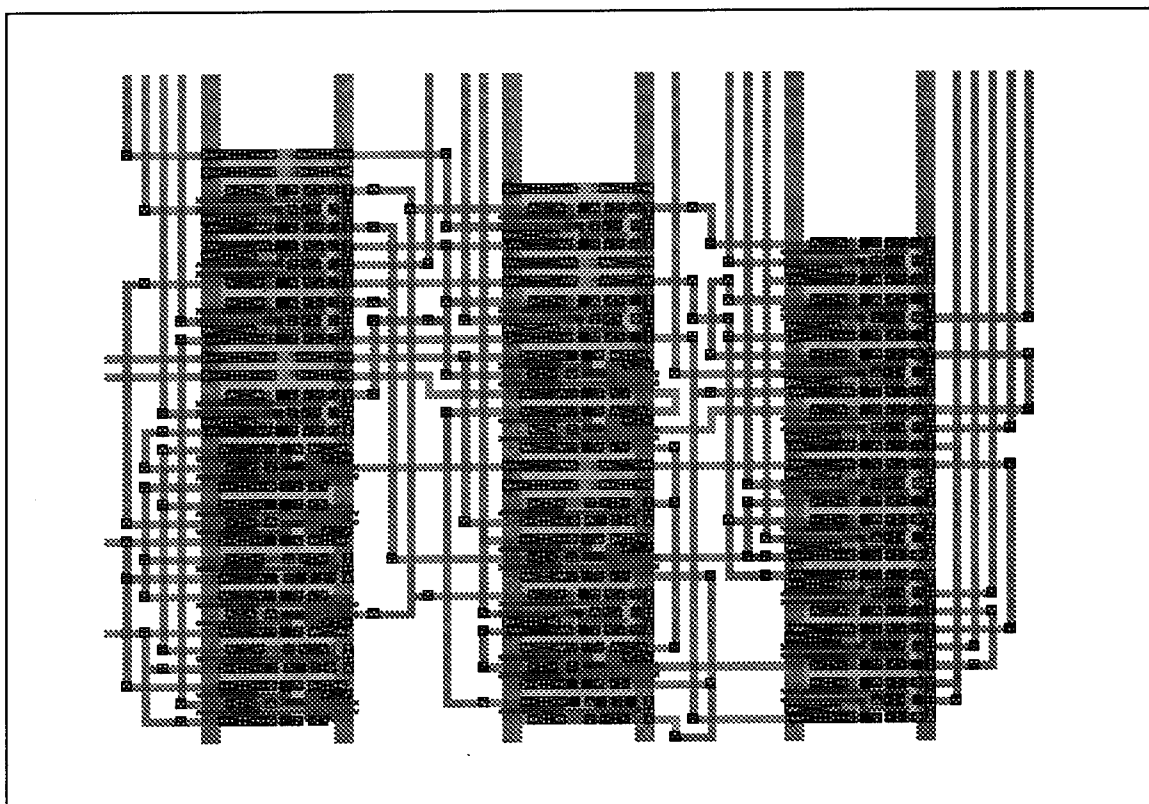
Figure 4-4.   Magic layout of the new selector.
                Note: input lines are on the left side of the circuit and output lines run
                along the top.

and column selectors. The column selector was rotated counterclockwise by 90°. While

not completely eliminated, the voltage spikes on the output of the selectors have been

reduced from about 300 mV to around 150 mV (See Appendix C, Figure C-2).

4.2.3. Rowdrivers. Figure 4-5 is the schematic diagram of the rowdriver. The double

inverting rowdrivers were retained to provide buffering of the selector signal. However,

the gate length of each transistor was reduced from 6 μm to 2 μm. Also, the selectbar was

removed because it was no longer needed. Figure 4-6 is the Magic layout of the new
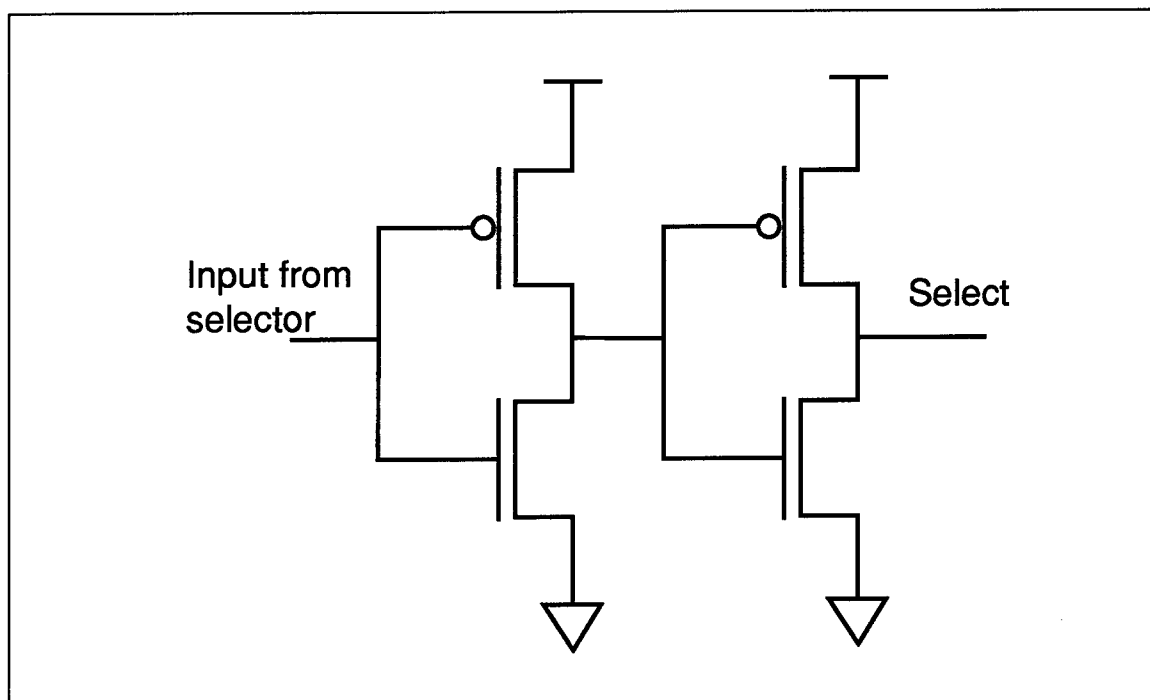
rowdriver.

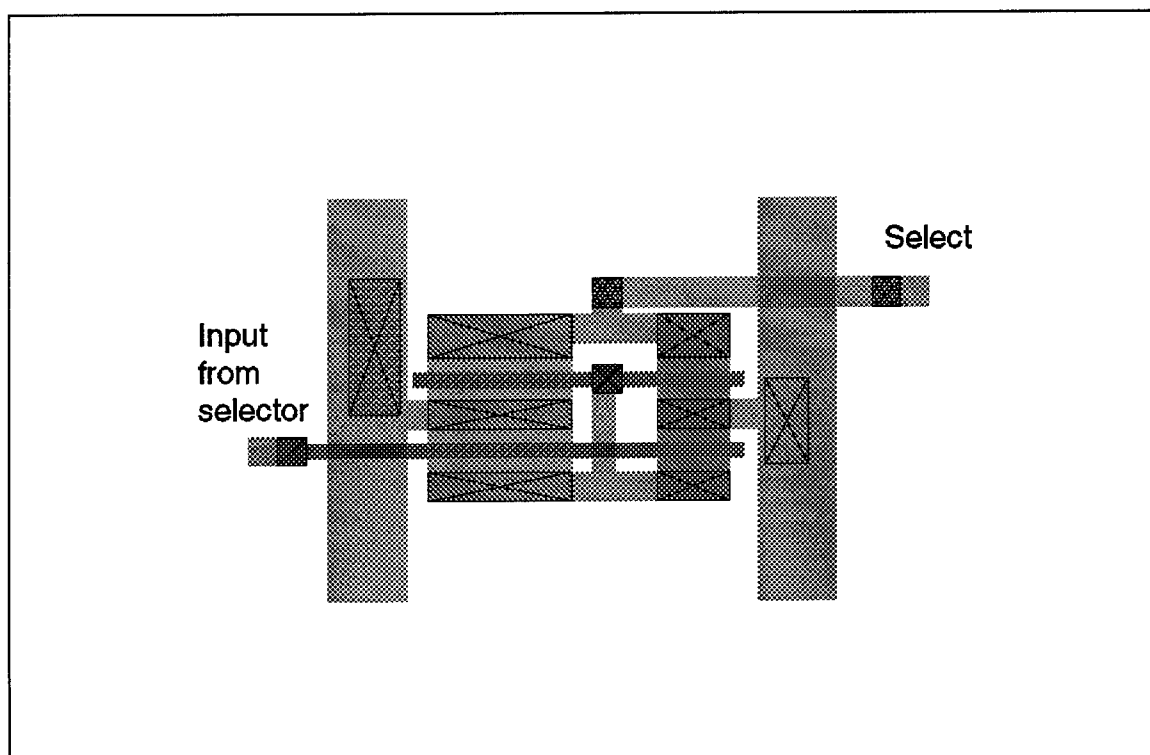Figure 4-5.   Schematic diagram of the new rowdriver.

Figure 4-6.   Magic layout of the new rowdriver.

4.2.4. Reference electrode. The "L" shaped reference pad was removed and another column of electrodes was added to the circuit. Now each electrode and the electrode to it's right are sample simultaneously. The first electrode's output is routed to the "mux out" line and the other electrode's output is routed to the "mux ref" line. On the next clock pulse, the electrode that was used for "mux ref" is now "mux out" and the electrode to its right is "mux ref" (Figure 4-7).
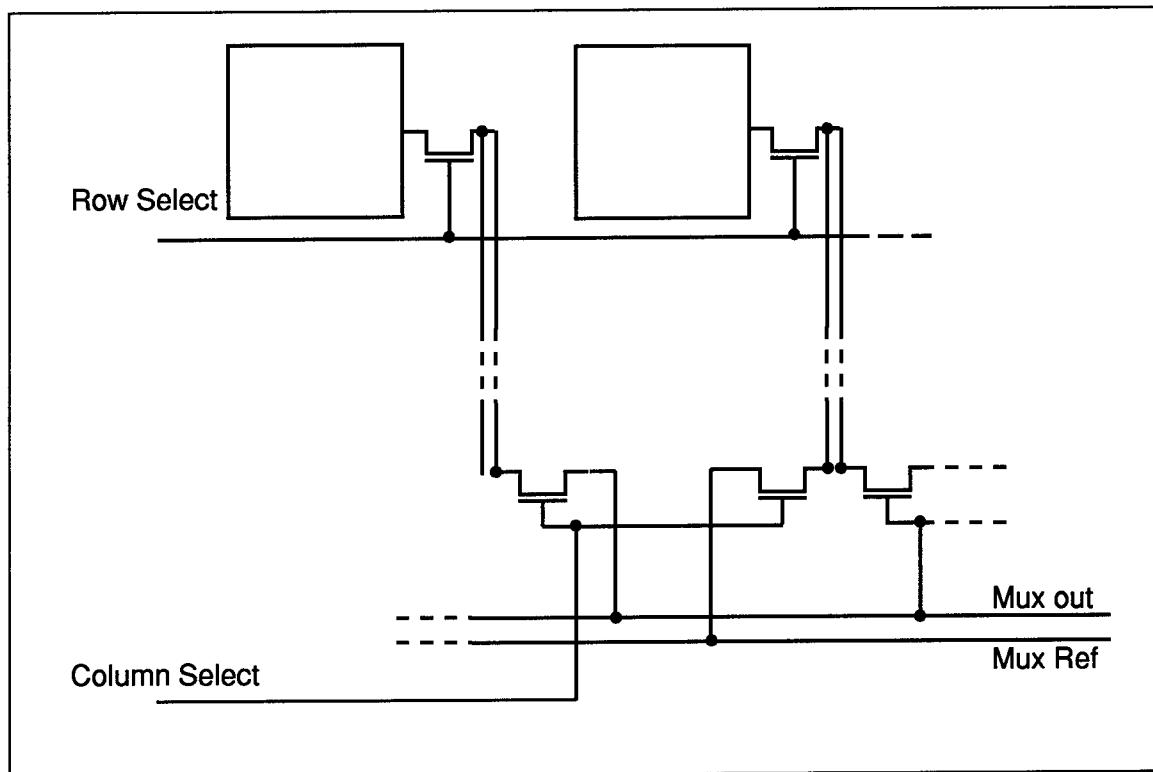

Figure 4-7.   Schematic showing electrode switching

4.2.5. Switching circuitry. The entire switching circuitry consisting of the counter, selectors, and rowdrivers was extracted from Magic and tested using SPICE. Figure 4-10 shows the current used by the new design. For a 3.5 VDC power supply, the rms supply current has been reduced from 4.8 mA to 49.3 μA. The voltage spiking has also been

significantly reduced. Appendix C, Figure C-5 shows a close-up of the voltage spike on the column1 output. The spike has been reduced from 300 mV to less than 15 mV.

4.2.6. Signal path. The signal path has been routed to minimize crossing paths with switching or supply signals. The ground line running between columns was routed along the top of the array and then routed down each column. This was done to avoid having the signal path cross any supply lines. Also, the output signals have been rerouted around the column select lines. The only switching line that now crosses the signal path is the column select line for that particular column. This line crosses the signal line at 90° angles to minimize cross-talk.

4.2.7. Synch Output. Figure 4-8 is a logic diagram of the new synch output circuit.
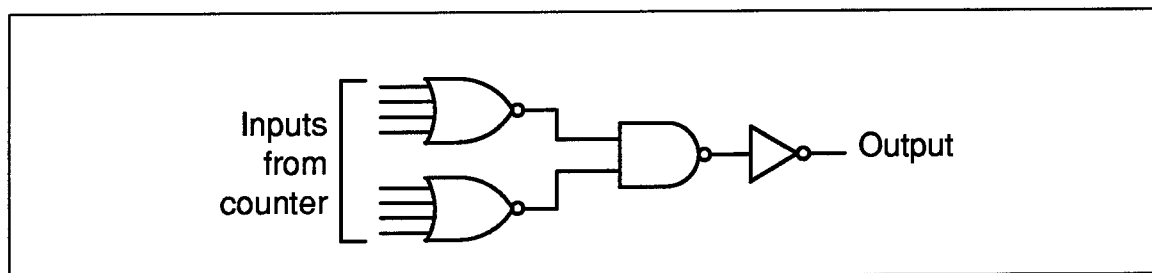

Figure 4-8.   Logic diagram of the new synch output circuit.

Instead of getting input from the row and column selectors, this design receives input from the counter. This change was made because it made the overall layout cleaner. The new design was produced using behavioral synthesis. When the counter's output is '00000000', the new synch circuitry sends a positive pulse to the synch output. Figure 4-9 is the Magic layout of the new synch output. A buffer/driver was added to the output of the
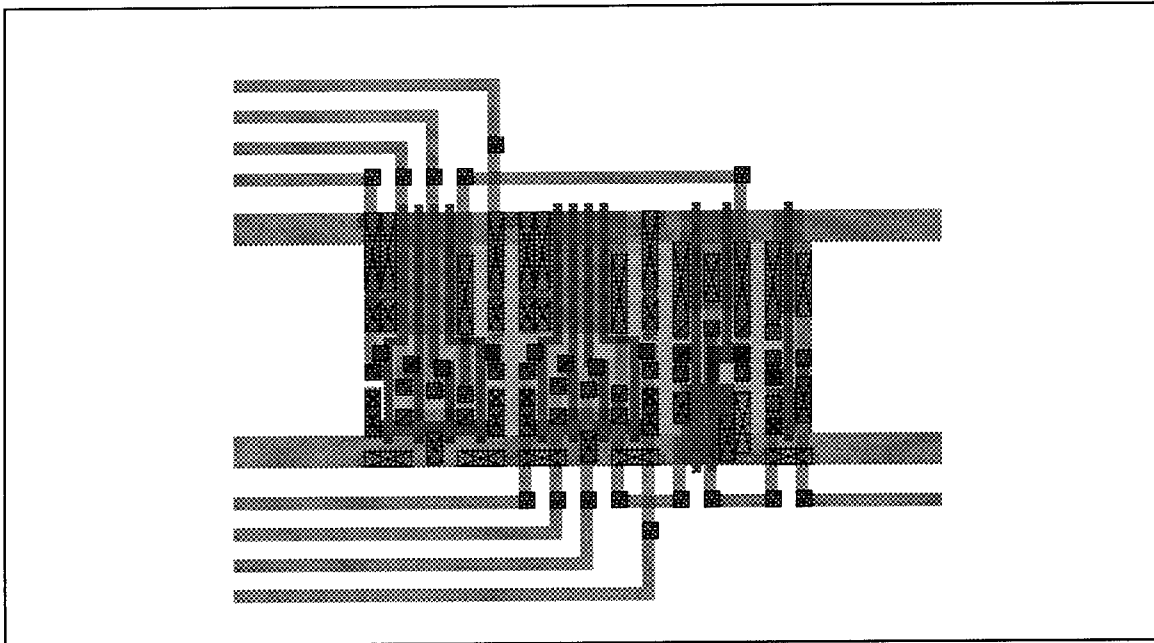
Figure 4-9.   Magic layout of the new synch out circuit.

synch output to help drive the output pad.

4.2.8. Overall layout. Figure 4-1 shows the overall layout of the new design. All

input/output pads have been repositioned so that, at most, only 4 I/O pads are on any one

side of the circuit. This was done for a better alignment with the bonding pads of the

current header package (See Appendix C, Figure C-1 for the Magic layout of the new
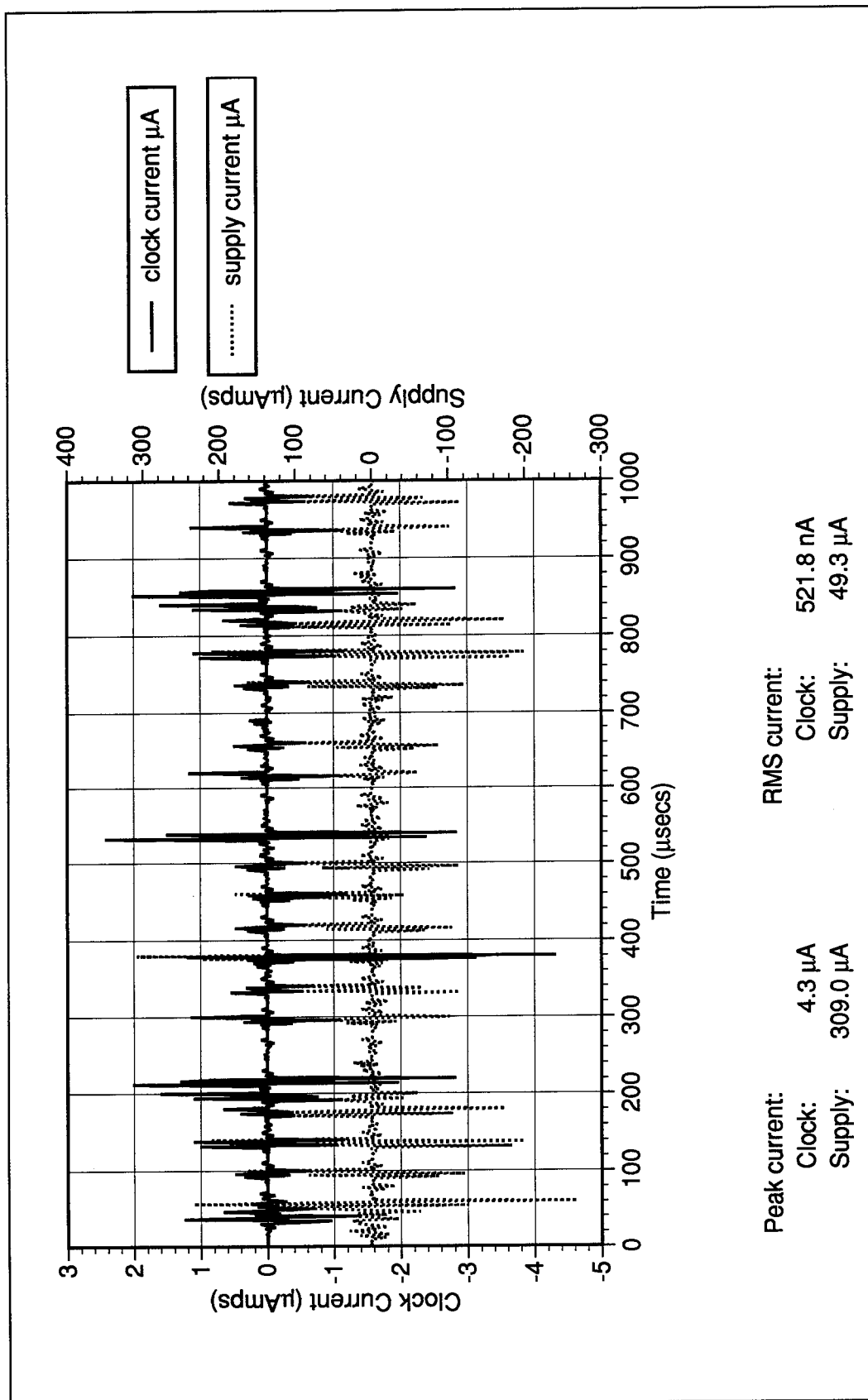
design).

Figure 4-10. Switching circuit current waveform.
The switching circuitry includes: counter, row and column selectors, and row and column drivers.

5. Conclusions and Recommendations

5.1. Conclusions

5.1.1. Characterization of the old design.

The old design was analyzed thoroughly using the SPICE simulation tools and found to be completely functional. However, from this analysis the following weak areas were noted.

5.1.1.1. Selector circuits. These circuits were NMOS devices and were probably from Ballantine's original design [5]. The supply current required to operate each of these circuits was about 2.4 mA, which is too much current for a device intended for implantation into an animal's brain.

5.1.1.2. Layout. There are several problems with the overall layout of current design. First, the column output pads are still on the circuit, even though they aren't being used. The power, ground, synch output, clock input and counter reset, and 8 test pads are all on the left side of the circuit. This makes bonding to the current header package difficult. The "L" shaped reference pad proved to be a poor ground reference. There is no buffering circuitry between the selectors and gate circuits. Consequently, voltage spikes from the selectors fed directly to the gate circuits and showed up on the multiplexed output pad. Finally, the signal path crosses switching lines and supply lines, contributing to the output noise.

5.1.2. Redesign.

5.1.2.1. Selector/demultiplexer. The old selector circuits were replaced using CMOS technology and designed using behavioral synthesis. This new design, when combined with the rest of the switching circuitry accounted for a drop in supply current from 4.8 mA to 49 µA. Additionally, the new design is less noisy, although marginally so. Voltage spikes on the output waveform of the new selector dropped from about 300 mV to 150 mV.

5.1.2.2. Drivers/buffers. To reduce noise further, buffer circuits were place between the column selector and the NMOS switches. This reduced the output voltage spike from 300 mV in the old design to 15 mV.

5.1.2.3. Reference pad. The "L" shaped reference pad was removed. Instead of having a fixed reference, each electrode in the array uses the electrode to its right as a reference. An extra column of electrodes was added to accommodate this new setup.

5.1.2.4. Signal path. The signal path was rerouted to minimize cross talk with supply or switching circuits. The mux output and mux reference lines were routed around the switching circuitry. Although not part of the signal path, the ground wires running vertically between each column of the array were also rerouted to avoid crossing the signal path. As a result, each output signal crosses no supply lines and only crosses on switching line.

5.1.2.5. Switching circuits. All transmission gates have been replaced by NMOS transistors. This simplified the layout without degrading the recording capability of the circuit.

5.2. Recommendations

5.2.1. On chip amplification. Initially, the scope of this research was to design an opamp to be integrated with the old design. Two opamps were built and fabricated. Although they functioned properly using the SPICE simulator, neither chip functioned properly in actual testing. The problem with those designs was that passive resistance was used for the feedback circuit. Unfortunately, the only material available to use as a resistor was polysilicon, which has a resistivity of 20 $\Omega/\square$. This led to extremely long snaking paths of polysilicon along the bottom of the array. The SPICE extraction tools apparently did not correctly account for the capacitance built into this snaking line of polysilicon and the circuit functioned properly in simulation.

With the new design of the AFIT multielectrode array, a differential opamp should be designed, tested and built onto the circuit. The mux ref output should provide a stable enough reference for a differential amplifier.

5.2.2. Input/Output pads. Although the power, ground, clock, reset, and synch pads have protective circuits to guard against static discharge, the mux out and mux ref pads have no such circuitry. This was not added to the new design, because it was not known how much, if any, signal attenuation would be caused by replacing the old pads. The mux

out and mux ref pads are tied directly to the switching transistors on the circuit, which makes the entire circuit extremely susceptible to damage from static discharge. Unfortunately, pad technology is not trivial—therefore it should be investigated to determine if a protected pad can be used for the mux out and mux ref outputs without significant signal attenuation.

5.2.3. Integrate the synch circuit. The new synch circuit should be incorporated into the counter, rather than be external to it. Unfortunately there is no documentation on the design of the counter that can be used to update its design.

Appendix A: *Diagrams of the Human Brain*
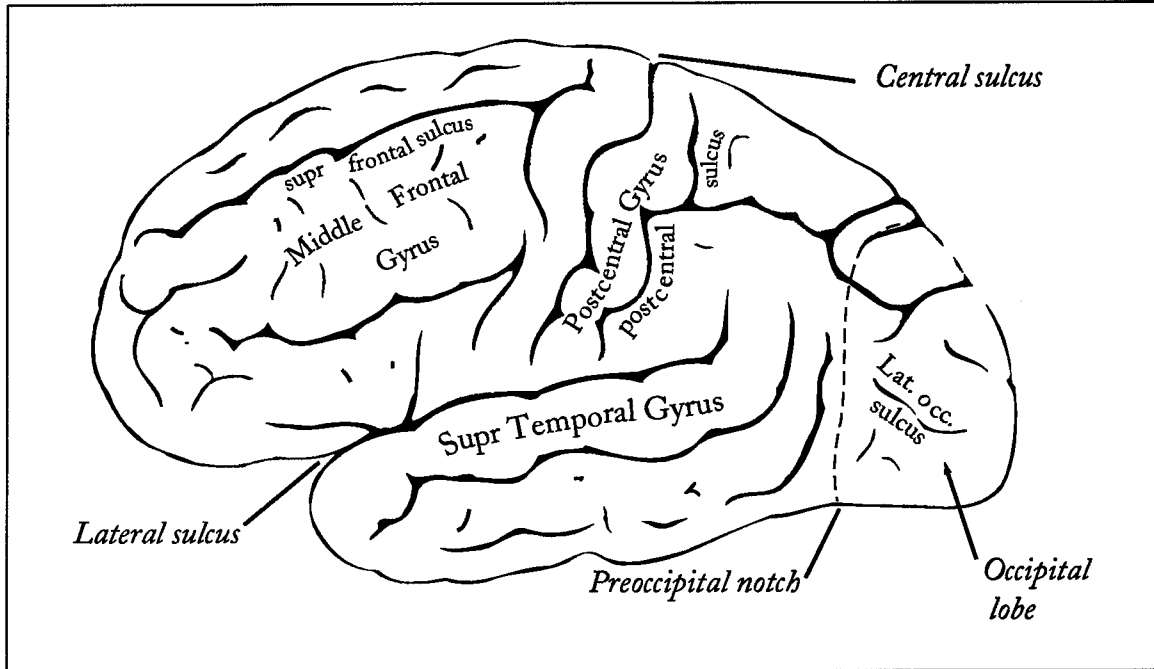
Figure A-1.   Lateral surface of the left cerebral hemisphere, viewed from the side [29].
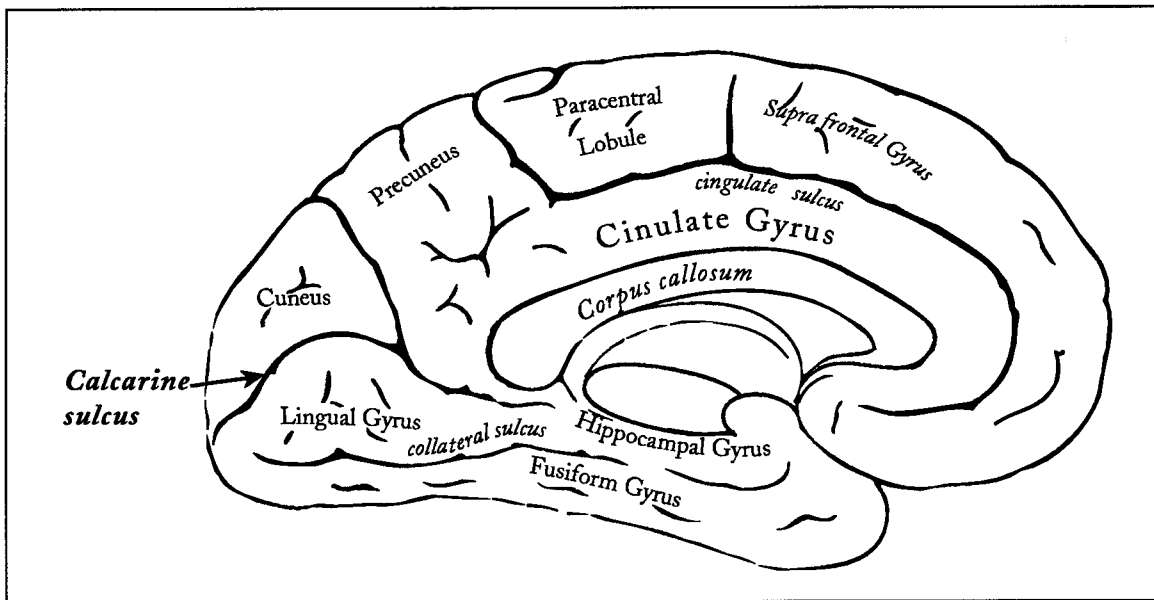

Figure A-2.   Medial surface of the left cerebral hemisphere. Note calcarine fissure (sulcus) on the left [29].
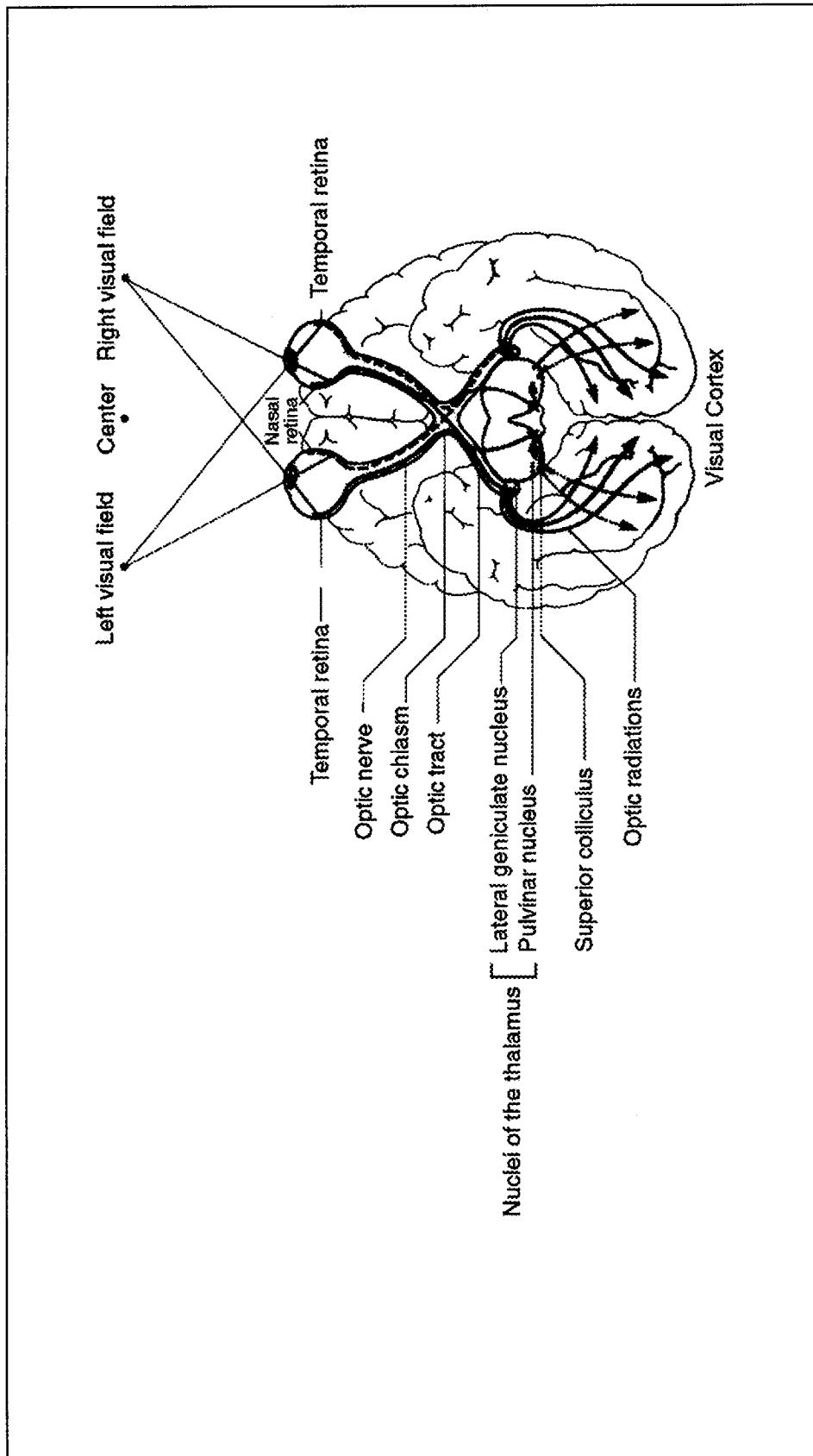
Figure A-3.   Pathways of the human visual system [12].

Appendix B: *Old Design Data*

This appendix contains more data gathered on the old design of the AFIT multi-electrode array. Two of the charts are from the Meta-Software, GSI program. They do a much better job of showing the voltage spikes on the selector.
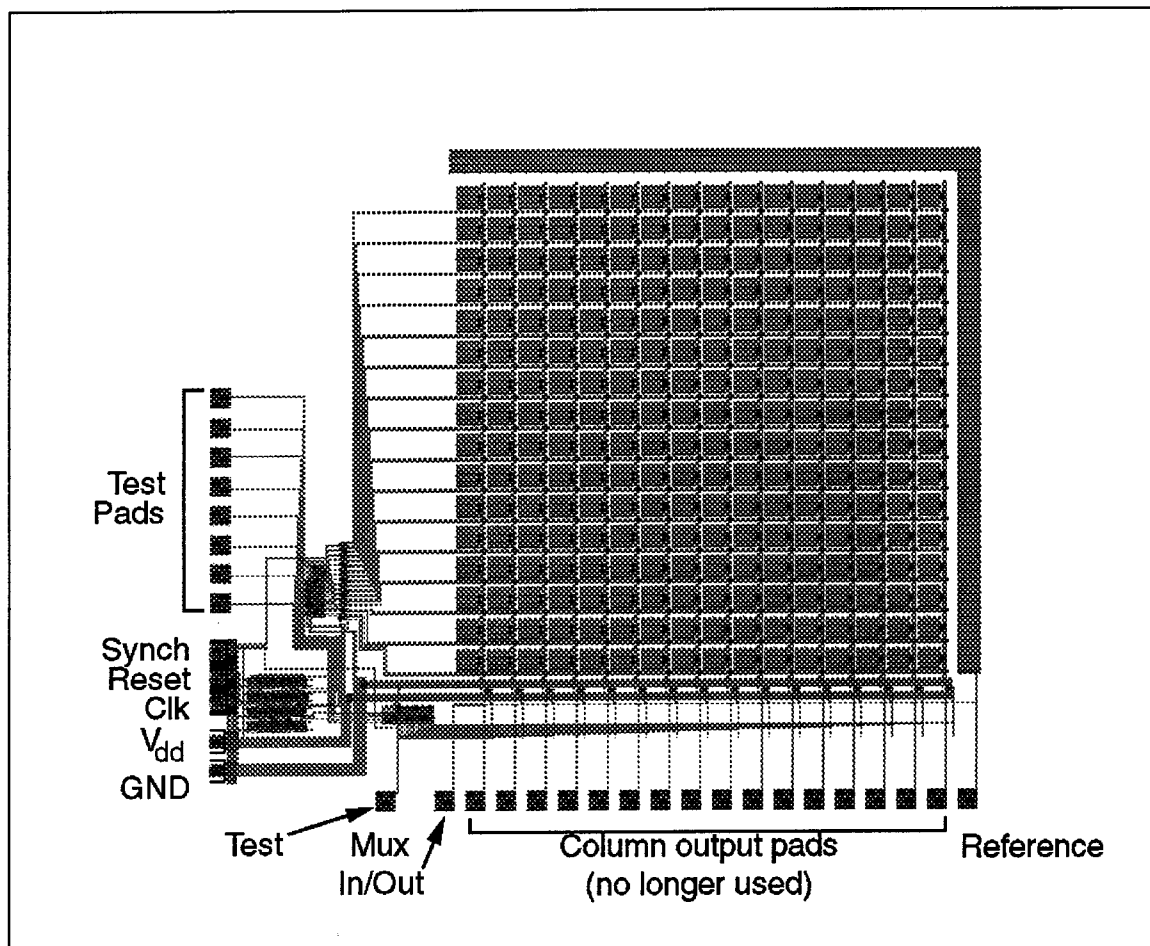
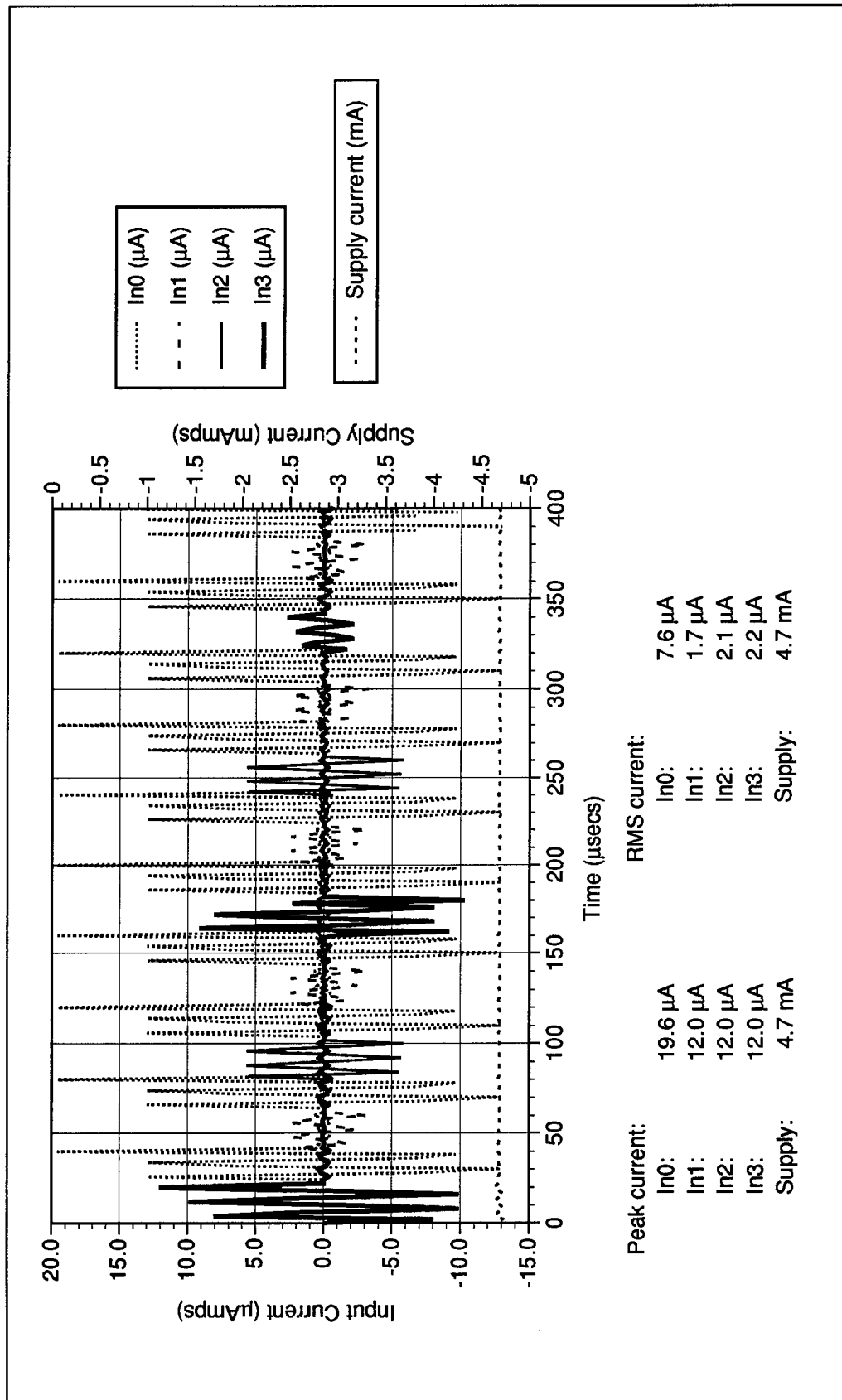Figure B-1.   Magic layout of the current AFIT multielectrode array.

Figure B-2.   Selector current using a 5 Volt power supply and a 50 KHz clock signal
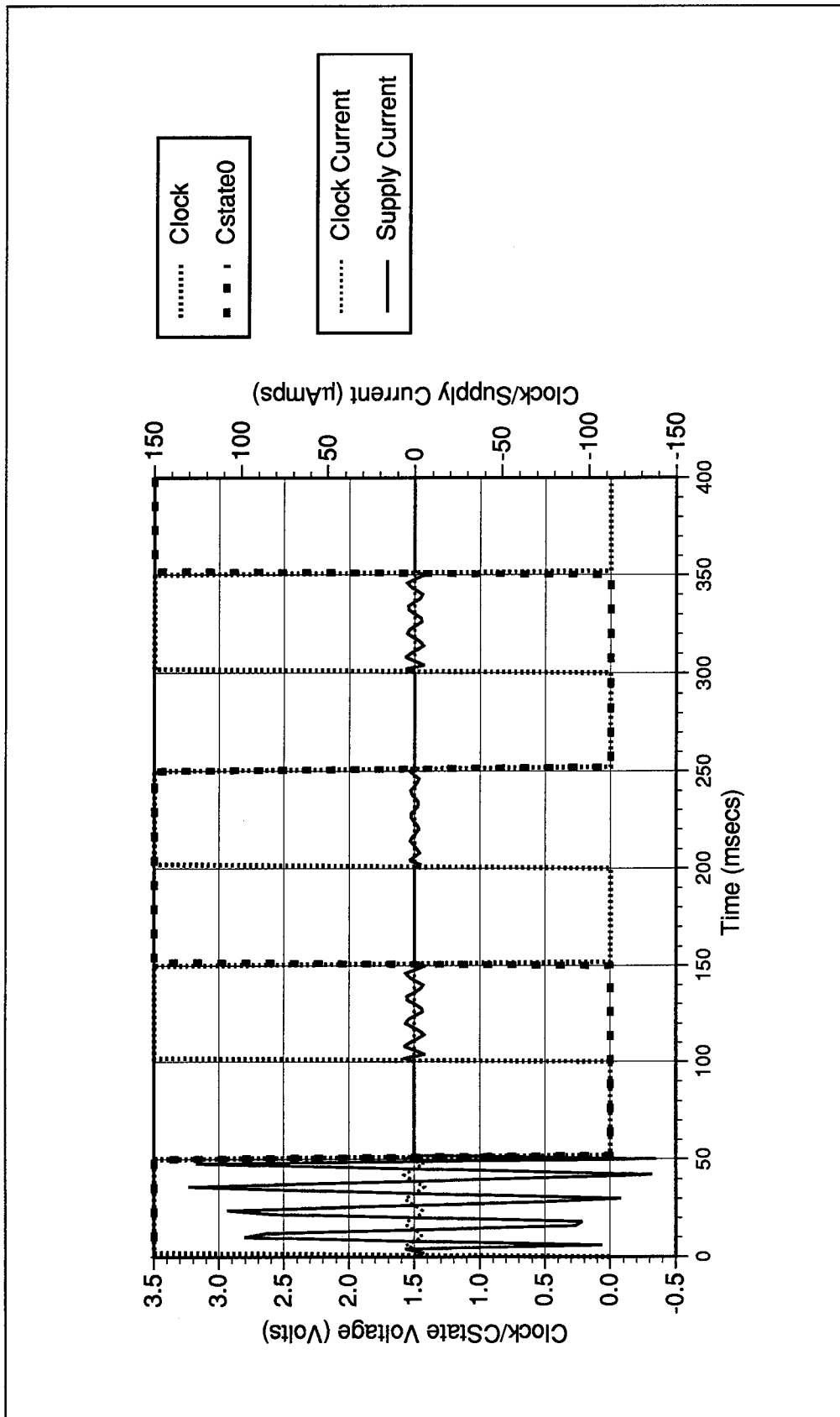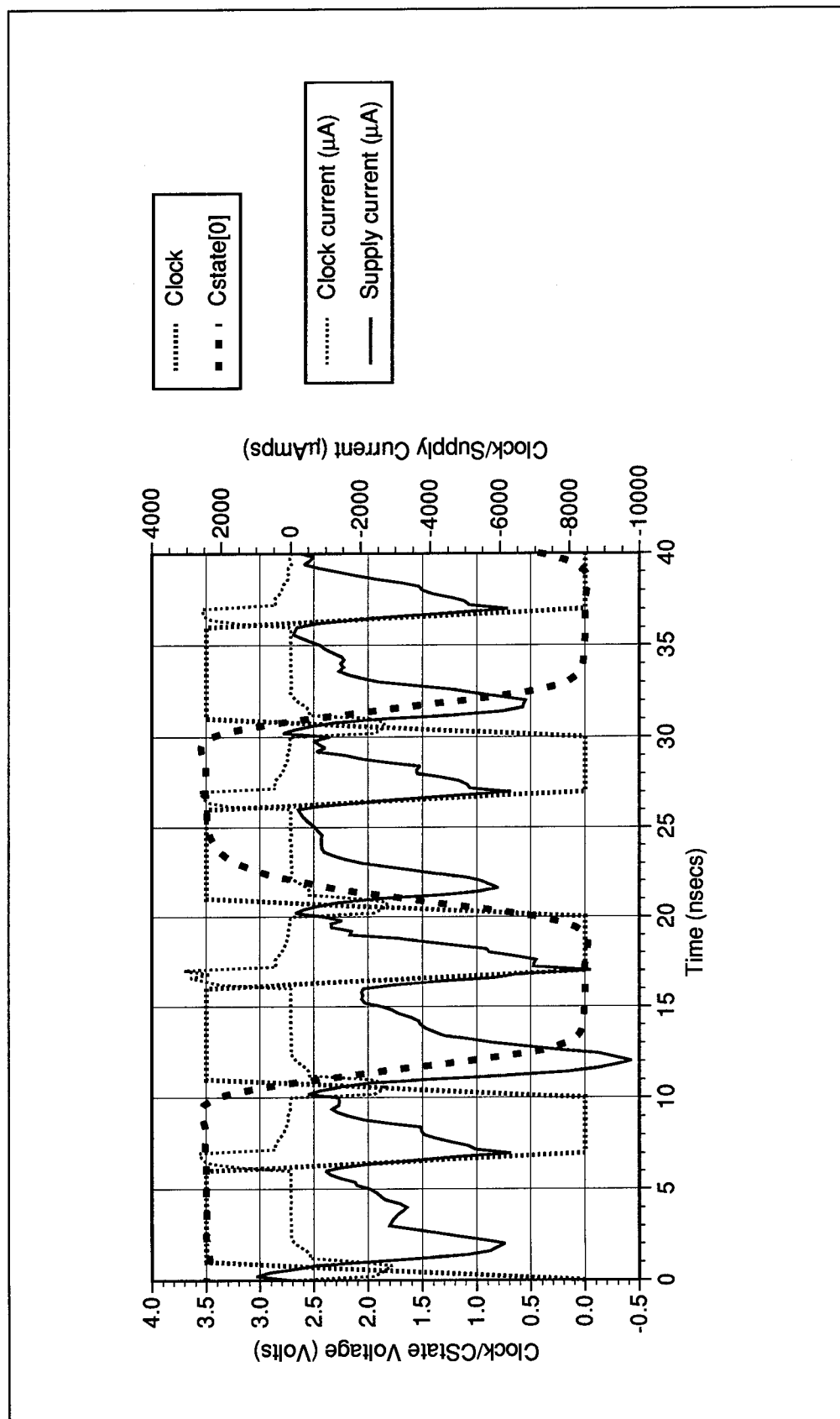
Figure B-3.   Counter output at 10 Hz.

Figure B-4. Counter output at 100 MHz.
Cstate[0] is still a square wave, but it's starting to break down. Supply current is in the mAmp range.
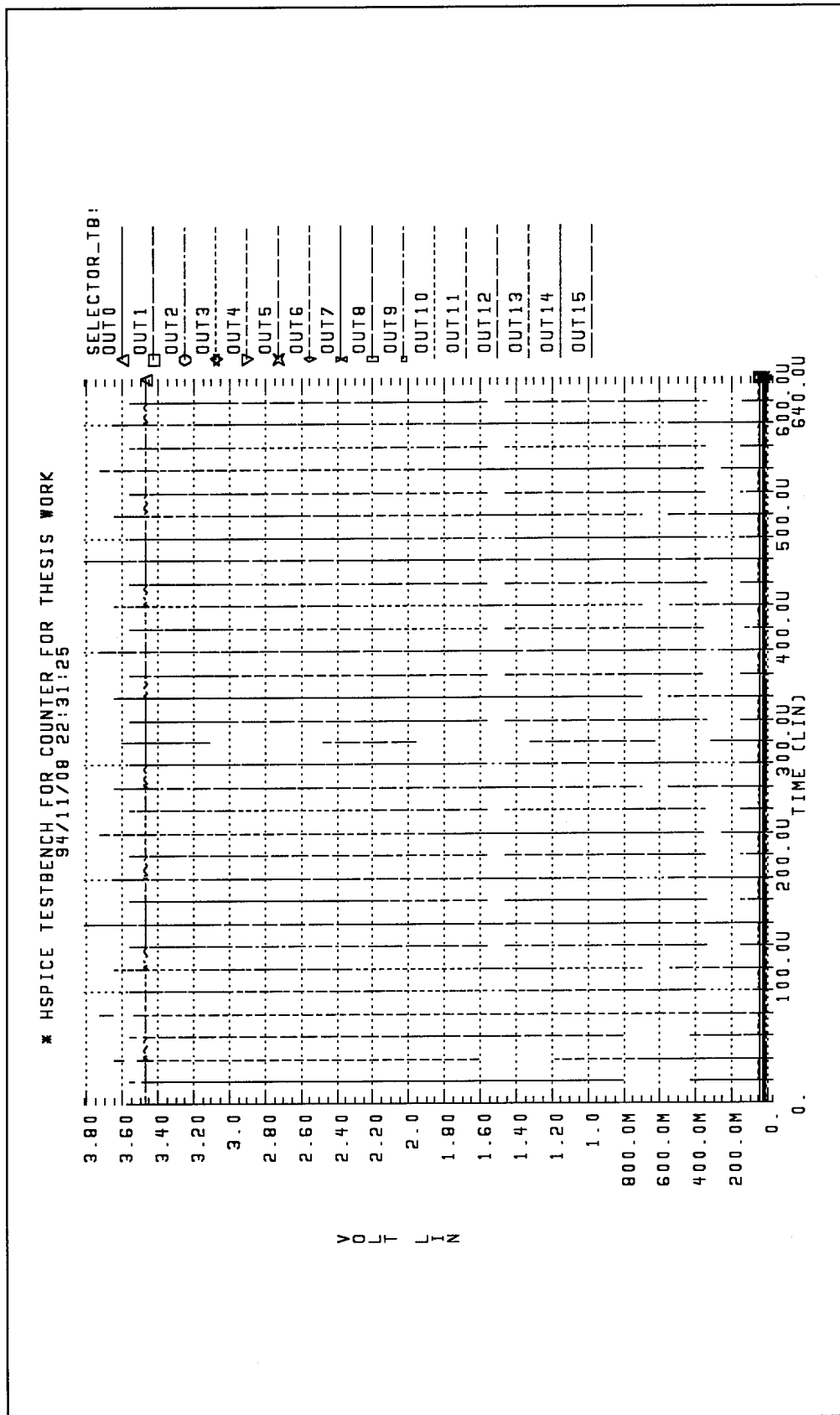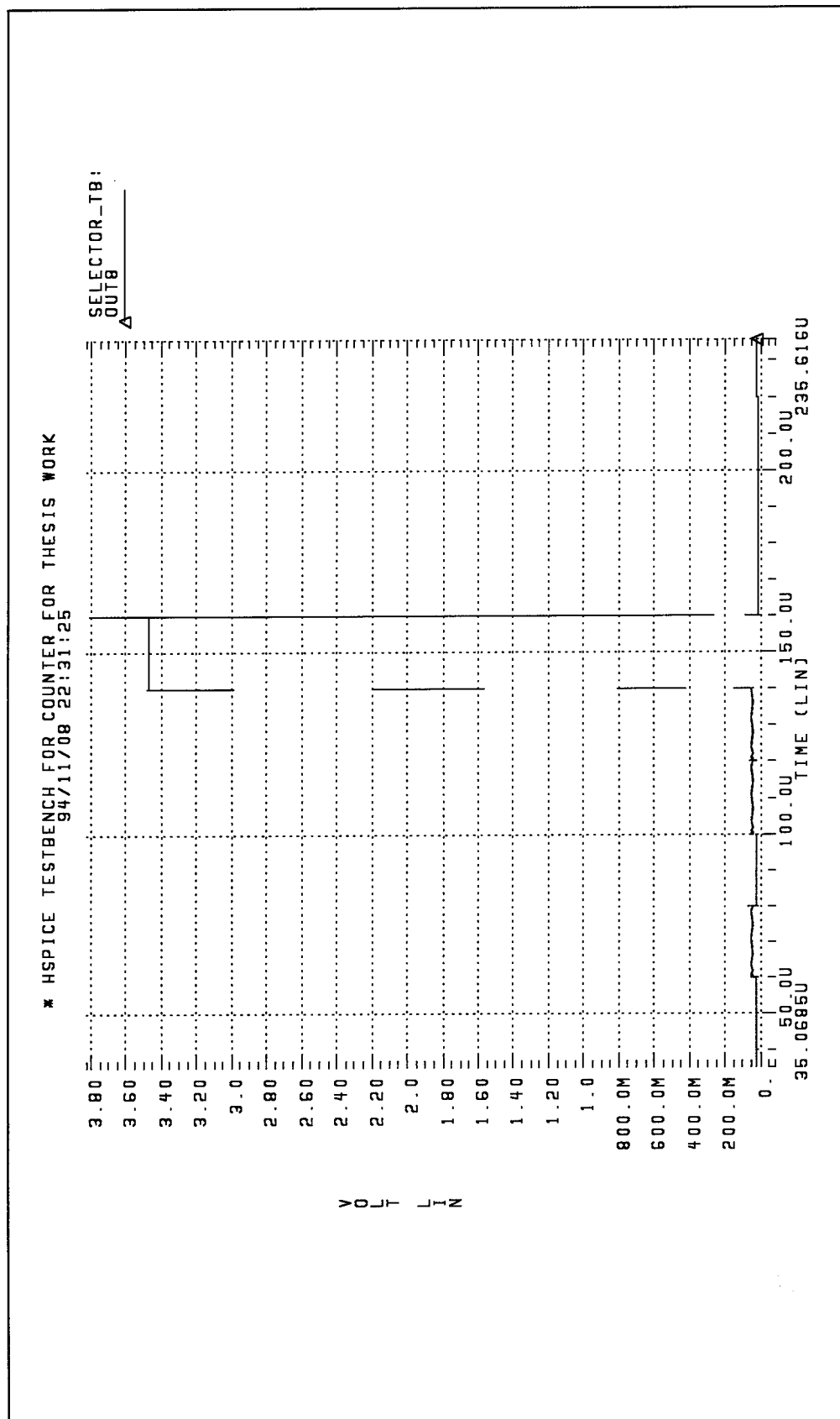
Figure B-5.   Selector output showing voltage spikes.

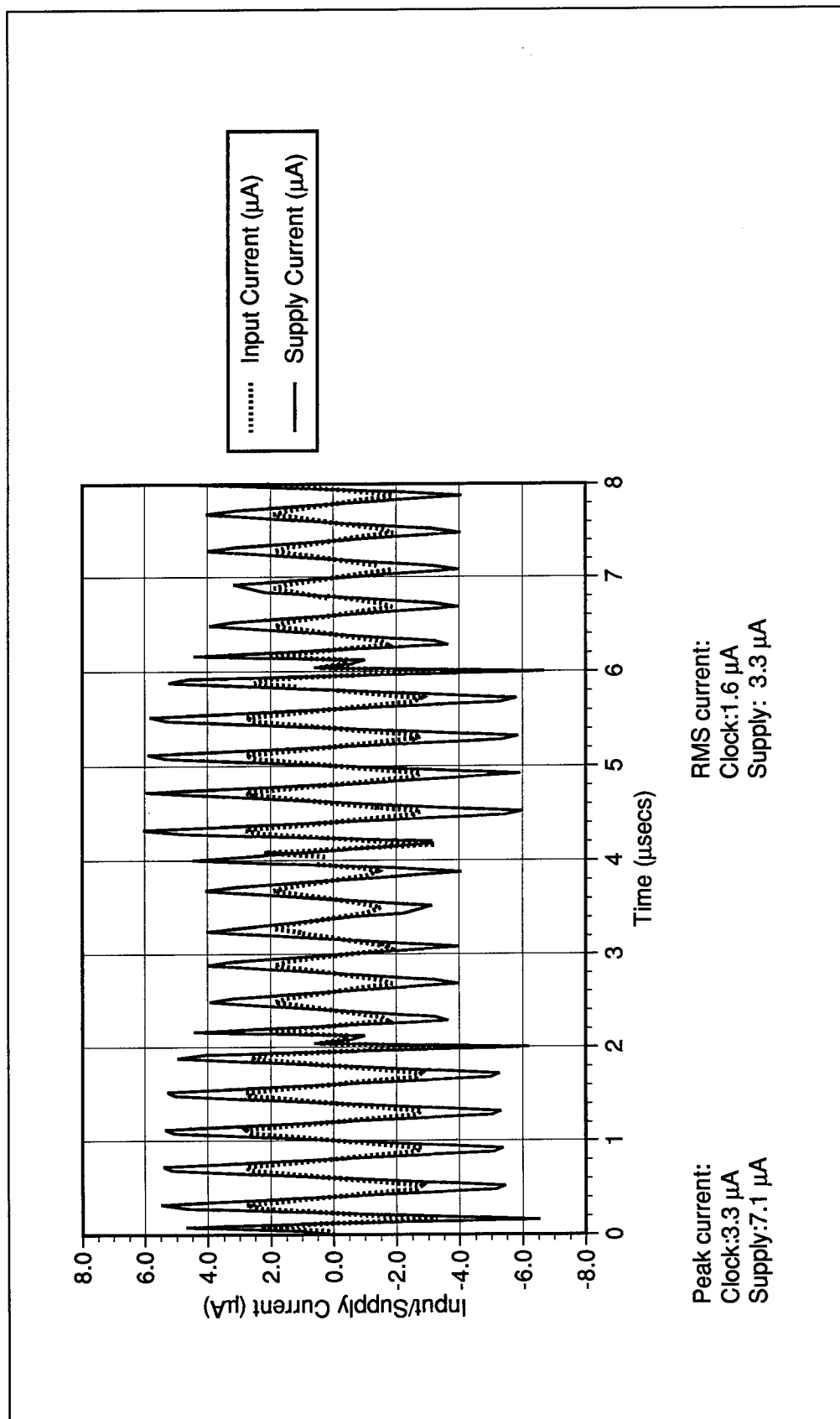Figure B-6.   Selector output close-up of voltage spike on out8 line.

Figure B-7.   Rowdriver current output at 250 KHz.

B-8

Appendix C: *New Design Data*

This appendix contains more data gathered on the new design of the AFIT multi-electrode array. Four of the charts are from the Meta-Software, GSI program. They do a much better job of showing the voltage spikes on the selector.
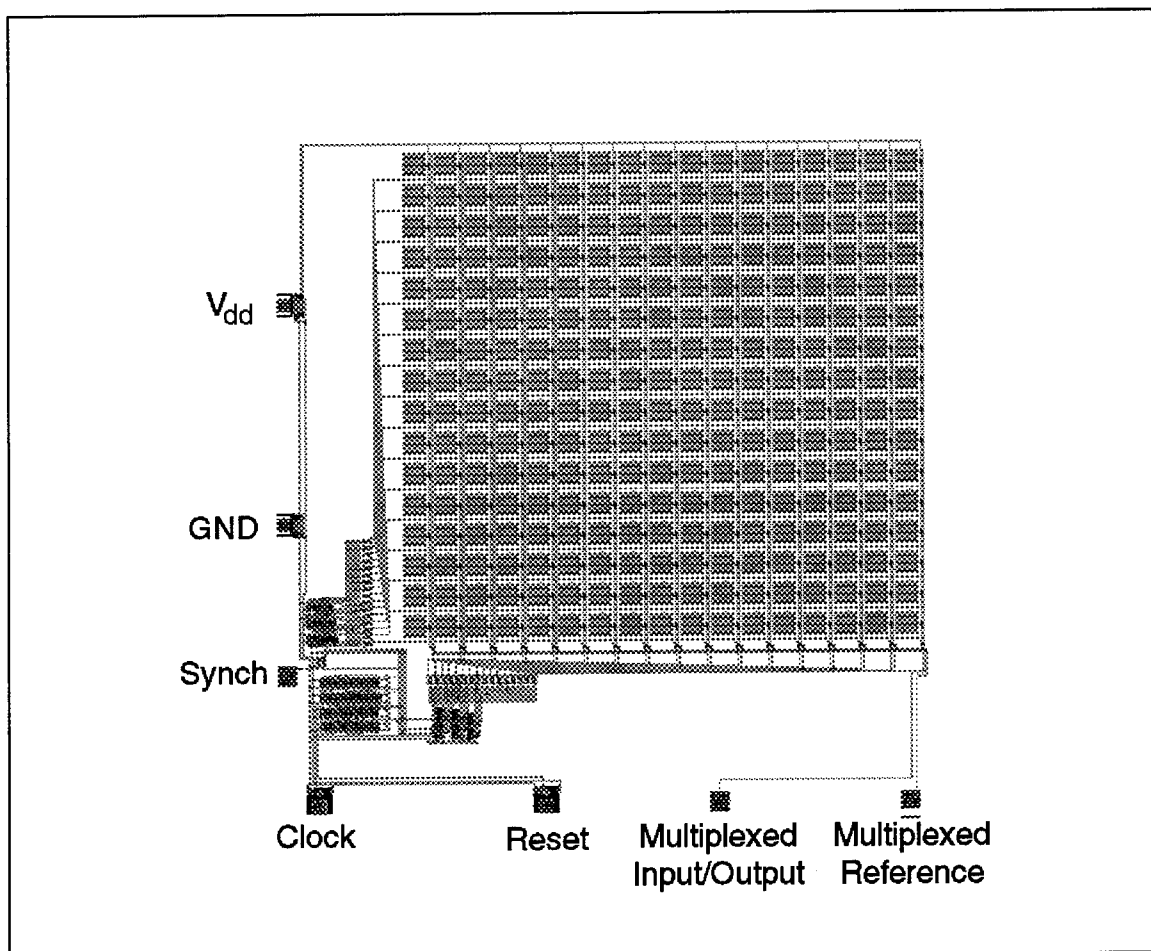
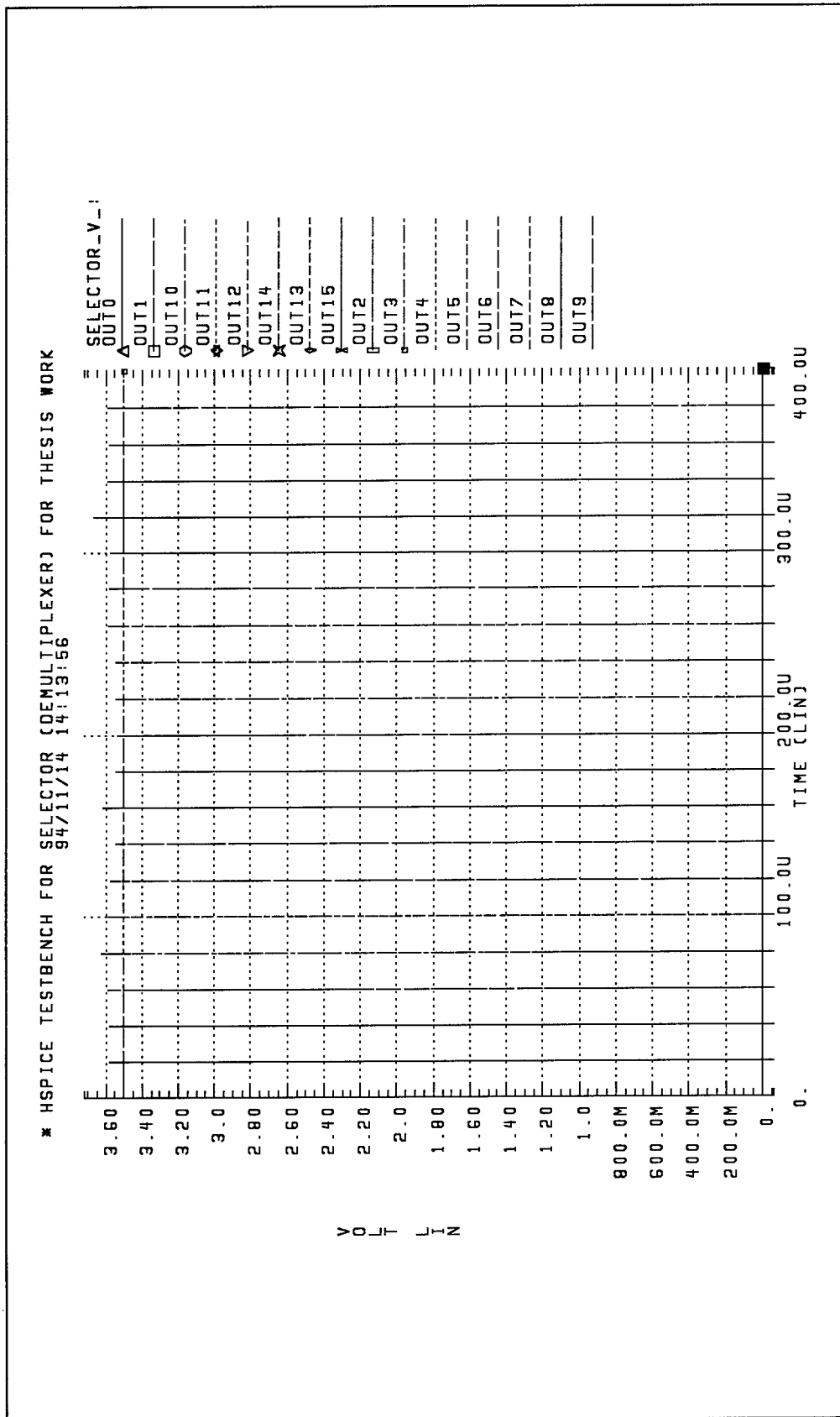Figure C-1.   Magic layout of the new AFIT multielectrode array.

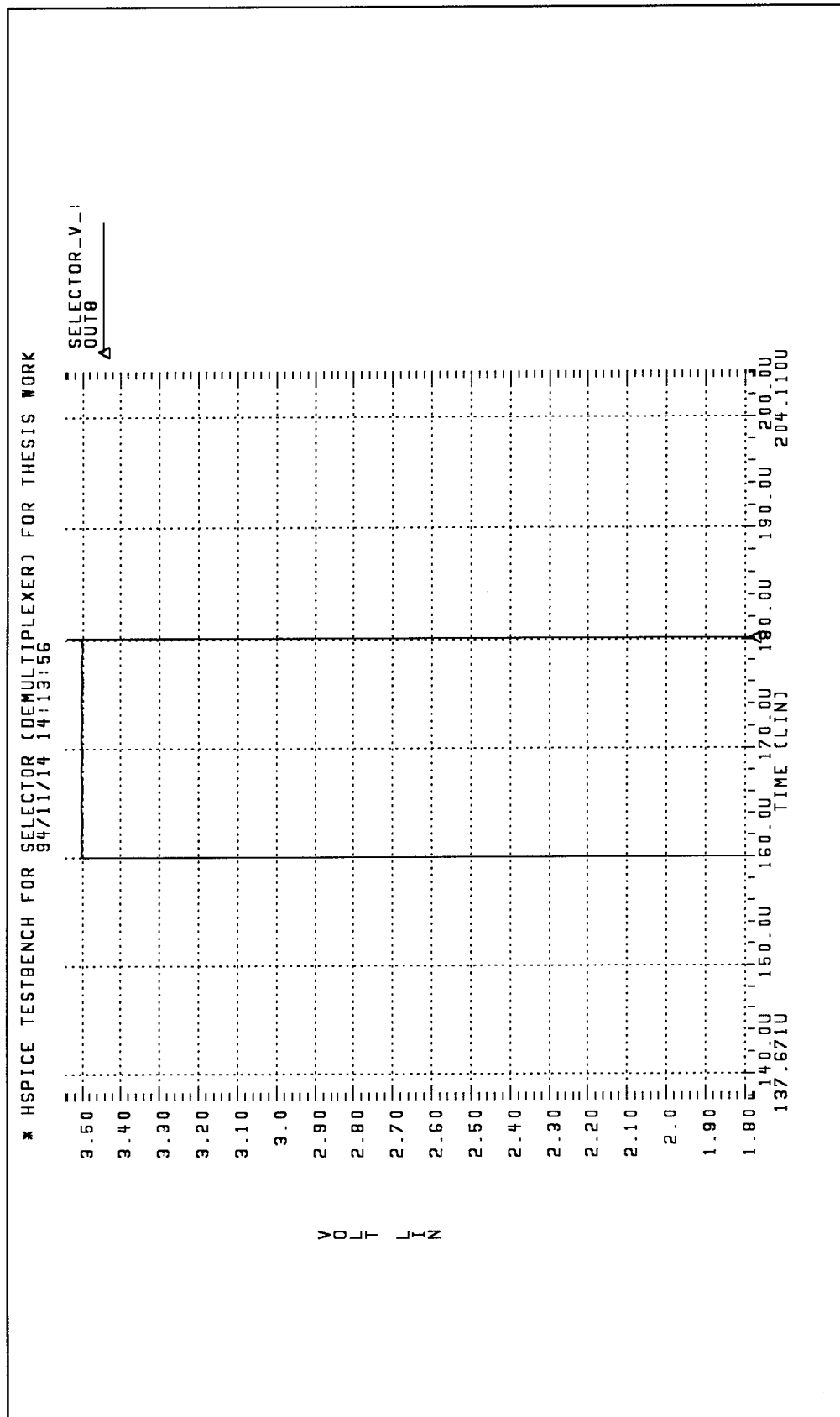Figure C-2.   New selector output.

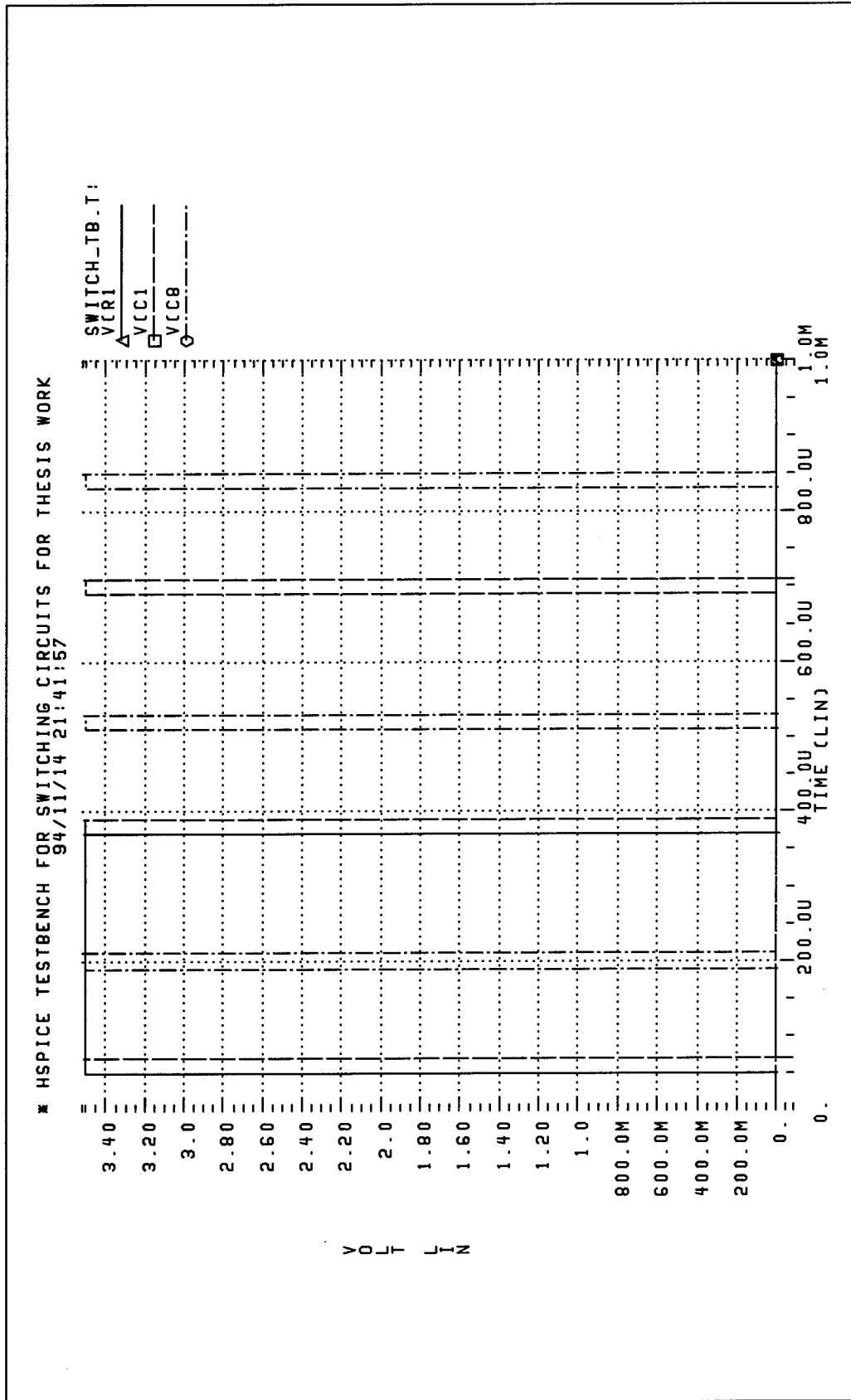Figure C-3.   New selector output. Close-up of voltage spike on out9 line.

Figure C-4.   Row and column outputs from new switching circuitry.
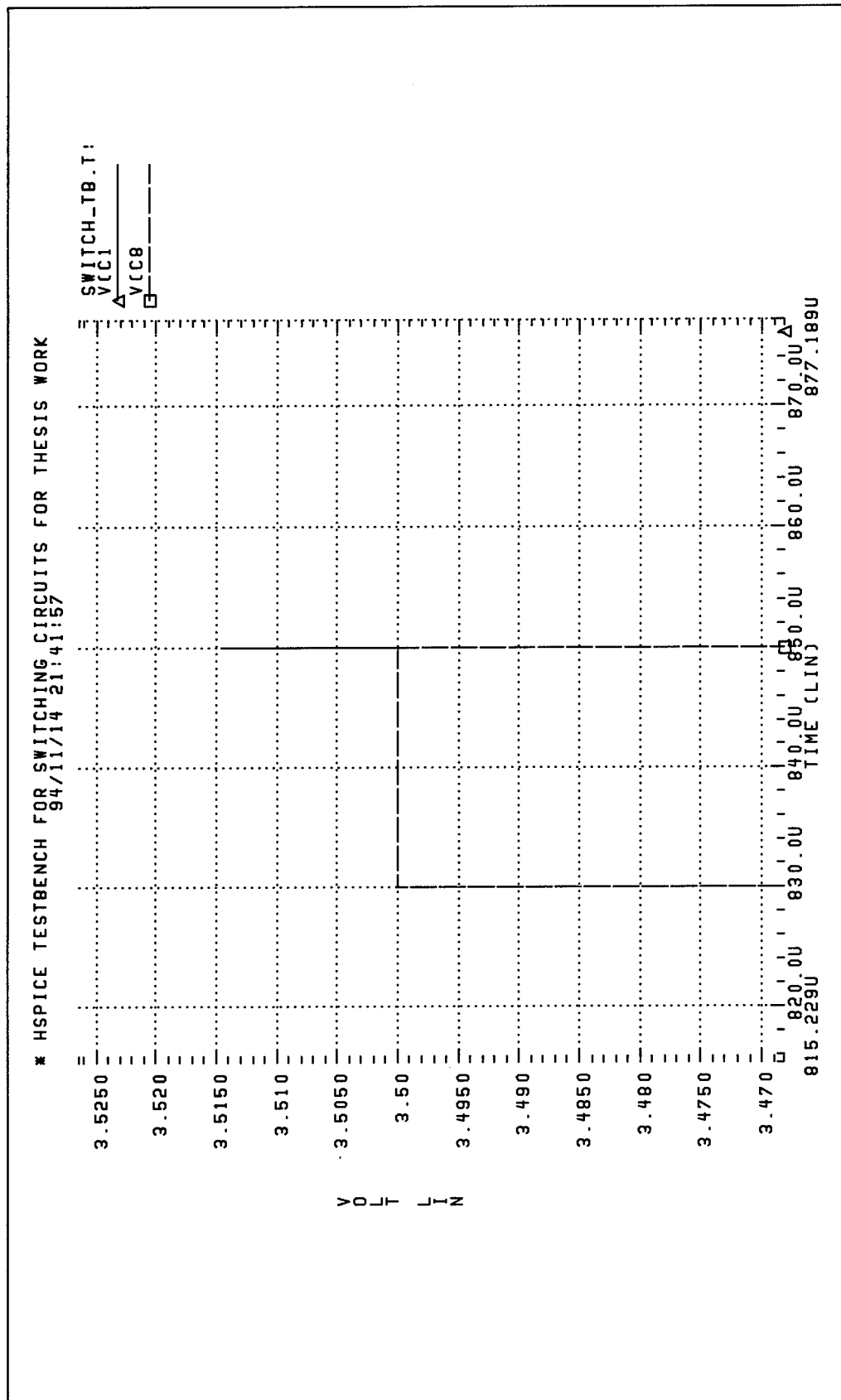Switching circuit includes counter, row and column selectors, and row and column drivers.

Figure C-5.   Switching circuit close-up of voltage spike on column1 line.

Glossary

Area 17 – *See Primary Visual Cortex*

Cerebrospinal Fluid (CSF) – A liquid that is secreted from the blood into the lateral ventricles of the brain and serves to maintain uniform pressure within the brain and spinal cord. CSF contains many ions, the worst of which, from an electronics point of view, is sodium [20].

CIF – Caltech Intermediate Format. This is a computer file format that is generated from Magic layouts of the actual circuit. This file is sent to a circuit manufacturer and is used to specify how the circuit will be built.

CMOS – Complementary Metal Oxide Semiconductor. CMOS uses an equal number of NMOS and PMOS devices.

Contralateral – Affecting the opposite side of the body [20].

Gliosis – Excessive development of neuroglia.[19]

hSpice – hSPICE™ is a commercial version of the freely distributed Berkeley Spice program distributed by Meta-Software, Inc. SPICE is a component level circuit simulator. Release 93a was used in this research.

in vitro – Outside the living body and in an artificial environment [20].

in vivo – In the living body of an animal or plant [20].

Ipsilateral – Affecting the same side of the body [20].

JFET – Junction field-effect transistor. Similar to MOS technology - however the JFET device is normally on. Voltage applied to the gate pinches off the channel and controls current flow.

Magic – Magic is an interactive system for creating and modifying VLSI circuit layouts distributed freely by the University of California, Berkeley. Version 6 is used in this project.

Meningeal – Three membranes (meninx) that envelop the brain and spinal cord [19].

MOSIS® – MOS Implementation System. The MOSIS service, begun in 1980, provides fabrication services to government contractors, agencies, and universities under the sponsorship of the Advanced Research Projects Agency (ARPA) with assistance from the National Science Foundation (NSF). MOSIS® is a registered trademark of the University of Southern California.

Neuroglia – Support tissue that fills the interstices of the brain and spinal cord and supports the essential elements of nervous tissue. It is composed of a network of fine fibrils and of flattened stellate cells with numerous radiating fibrillar processes [19].

NMOS – n-channel Metal-Oxide-Semiconductor. NMOS devices use electrons as the primary carrier. A positive voltage (with respect to the p-type substrate) applied to the gate creates a conducting path (channel) between the drain and source that allows current (electrons) to flow.

Occipital Lobe – The posterior lobe of each cerebral hemishpere that bears the visual areas and has the form of a three sided pyramid [20]. (See Appendix A, Figure A-1).

Pericranium – The external membrane of connective tissue surrounding the skull.

Phosphene – A luminous impression due to excitation. Phosphenes only appear as light spots in the vision.

PMOS – p-channel Metal-Oxide-Semiconductor. PMOS devices use holes as the primary carrier. A negative voltage (with respect to the n-type substrate) applied to the gate creates a conducting path (channel) between the drain and source that allows current (holes) to flow.

Primary Visual Cortex – Located in the back of the brain (occipital lobe). It is directly connected to the retina via the optic nerve and lateral geniculate nucleus (Appendix A, Figure A-3) and effectively contains a map of the entire retinal field [14]. Also called the Striate Cortex, Area 17, and V1.

Ringer's Solution – Named after an English physician, Sidney Ringer - it is a balanced aqueous solution that contains chloride, sodium, potassium, calcium, bicarbonate, and phosphate ions and closely matches the cerebral spinal fluid [20].

Striate Cortex – *See Primary Visual Cortex*

Sulcus – Fissure, Furrow or Groove especially a shallow furrow on the surface of the brain separating adjacent convolutions [20] (See Appendix A, Figure A-1.).

Tantalum – A hard ductile gray-white, acid resistant metallic element of the vanadium family [20].

Tupaia – The principle genus of the family of Tupaiidae - commonly called the squirrel shrew. The squirrel shrew is an insect eating, tree dwelling creature, that, except for a long, narrow, head, closely resembles a common squirrel [19].

V1 – *See Primary Visual Cortex*

VHDL – VHSIC Hardware Description Language. An offshoot of the very high speed integrated circuit (VHSIC) program funded by the Department of Defense in the late 1970's. A new version of the language was proposed in 1981 and called VHDL. In 1987 it was adopted as the IEEE 1076 standard [25].

Bibliography

1. G. H.Fitzgerald. "The development of a two-dimensional multielectrode array for visual perception research in the mammalian brain," MS thesis, Air Force Institute of Technology, 1980.

2. G. W. German III. "A cortically implantable multielectrode array for investigating the mammalian visual system," MS thesis, Air Force Institute of Technology, 1981.

3. J. A. Tatman. "A two–dimensional multielectrode microprobe for the visual cortex," MS thesis, Air Force Institute of Technology, 1981.

4. D. C. Denton and R. W. Hensley. "The first cortical implant of a semiconductor multielectrode array: electrode development and data collection," MS thesis, Air Force Institute of Technology, 1982.

5. R. B. Ballantine. "The development and fabrication of an implantable, multiplexed, semiconductor multielectrode array," MS thesis, Air Force Institute of Technology, 1983.

6. J. E. Lavoie. "Characterization of polyimide for use as an inter–metal insulation," MS thesis, Air Force Institute of Technology, 1983.

7. M. E. Sopko. "Fabrication of a biologically–implantable, multiplexed, multielectrode array of JFETs for cortical implantation," MS thesis, Air Force Institute of Technology, 1984.

8. R. R. Turner. "Encapsulation and packaging of a semiconductor multielectrode array for cortical implantation," MS thesis, Air Force Institute of Technology, 1984.

9. S. P. Ernst. "Surface passivation of an implantable semiconductor multielectrode array," MS thesis, Air Force Institute of Technology, 1986.

10. D. P. Szczublewski. "The redesign of a multielectrode semiconductor array intended for implantation into the brain of a rhesus monkey," MS thesis, Air Force Institute of Technology, 1989.

11. P. K. LeFevre. "Design and fabrication of an implantable cortical semiconductor integrated circuit electrode array," MS thesis, Air Force Institute of Technology, 1990.

12. J. R. Reid Jr. "The AFIT multielectrode for neural recording and stimulation: design, testing and encapsulation," MS thesis, Air Force Institute of Technology, 1993.

13. M. Kabrisky. *A proposed model for visual information processing in the human brain.* University of Illinois, 1966.

14. S. Zeki. "The visual image in mind and brain," *Scientific American,* vol. 267, #3, pp. 69-76, 1992.

15. S. M. Sze. *Semiconductor devices, physics and technology.*New York: John Wiley & Sons, 1985.

16. S. L. BeMent, K. D. Wise, D. J. Anderson, K. Najafi, and K. L. Drake. "Solid-state electrodes for multichannel multiplexed intracortical neuronal recording," *IEEE Transactions on Biomedical Engineering,* vol. BME–33, No. 2, pp. 230-241 February 1986.

17. D. L. Hodges and H. G. Jackson. *Analysis and design of digital integrated circuits.* New York: McGraw–Hill, 1988.

18. D. W. DeMott. "Cortical micro–toposcopy," *Medical Research Engineering,* vol. 5, no. 4, pp. 23-29, 1966.

19. P. B. Gove (ed.), *Merriam–Webster's, 3rd New International Dictionary, Unabridged Edition.* Springfield, MA: Merriam–Webster, Inc., 1965.

20. F. C. Mish (ed.), *Merriam–Webster's collegiate dictionary, tenth edition.* Springfield, MA: Merriam–Webster, Inc., 1993.

21. G. S. Brindley and W. S. Lewin. "The sensations produced by electrical stimulation of the visual cortex," *J. Physiol,* vol. 196, pp. 479-493, 1968.

22. W. H. Dobelle, M. G. Mladejovsky, and J. P. Girvin. "Artificial vision for the blind: Electrical stimulation of visual cortex offers hope for a functional prosthesis," *Science,* 183, pp. 440-443, 1974.

23. W. H. Dobelle and M. G. Mladejovsky. "Phosphenes produced by electrical stimulation of human occipital cortex, and their application to the development of a prosthesis for the blind," *J. Physiol,* vol. 243, pp. 553-576, 1974.

24. D. J. Edell, V. V. Toi, V. M. McNeil, and L. D. Clark. "Factors influencing the biocompatibility of insertable silicon microshafts in cerebral cortex," *IEEE Transactions on Biomedical Engineering,* vol. BME–39, pp. 635-643, June 1992.

25. D. L. Perry. *VHDL.* New York: McGraw–Hill, 1991.

26. N. H. E. Weste and K. Eshraghian. *Principles of CMOS VLSI design, a systems perspective.* Reading, MA: Addison–Wesley, 1993.

27. A. Spenik. "Experimental definition for implantation of the AFIT cortical multielectrode array," MS thesis, Air Force Institute of Technology, 1994.

28. C. E. Macomber. "Implementation of a method to detect the single visual evoked response," MS thesis, Air Force Institute of Technology, 1977.

29. C. M. Boss (ed.), *Anatomy of the human body, twenty-ninth edition.* Philadelphia, PA: Lea & Febiger., 1973.

Vita

Richard George Darenberg Jr. was born on January 3, 1957 in Miami, Florida. He graduated from Bitburg Dependents School, Bitburg, Germany in June of 1975. In May of 1982 he graduated from the University of South Florida, Tampa, Florida with a Bachelor of Science in Electrical Engineering. After Officer Training School, Lt. Darenberg completed Undergraduate Pilot Training at Vance AFB, Oklahoma, in January 1984. Subsequently, he was assigned to Dyess AFB, Clark AB, Republic of the Philippines and Ramstein AB, Germany flying C-130's and C-20's. While stationed at Clark AB, he was also an ALCE (Airlift Control Element) Operations Officer. In 1993, he was assigned to the Air Force Institute of Technology.

Permanent address: 826 Kalli Creek Ln.
St. Augustine, FL 32084

REPORT DOCUMENTATION PAGE

1. AGENCY USE ONLY (Leave blank)	2. REPORT DATE December 1994	3. REPORT TYPE AND DATES COVERED Master's Thesis

4. TITLE AND SUBTITLE

Caracterization And Redesign Of The
Afit Multielectrode Array

5. FUNDING NUMBERS

6. AUTHOR(S)

Richard G. Darenberg, Captain, USAF

7. PERFORMING ORGANIZATION NAME(S) AND ADDRESS(ES)

AFIT/ENG
Wright-Patterson AFB, OH 45433

8. PERFORMING ORGANIZATION REPORT NUMBER

AFIT/GE/ENG/94D-03

9. SPONSORING / MONITORING AGENCY NAME(S) AND ADDRESS(ES)

Mr Ed Zelnio
WL/AARA
Wright-Patterson AFB, OH 45433

10. SPONSORING / MONITORING AGENCY REPORT NUMBER

11. SUPPLEMENTARY NOTES

12a. DISTRIBUTION / AVAILABILITY STATEMENT

Approved for public release; Distribution Unlimited.

12b. DISTRIBUTION CODE

13. ABSTRACT (Maximum 200 words)

Since 1978, faculty and graduate students from the Air Force Institute of Technology (AFIT) have been working on an implantable circuit array that can record visual signals from the brain or stimulate the brain. In the current design the circuit is a 16 x 16 array of pads, each pad being 160 x 160 μm with 250 μm spacing with an "L" shaped reference pad used as a ground reference. The array is multiplexed so that only one I/O line is required to access all 256 pads.

This research was twofold: first to analyze the existing circuit and identify sources for noise and then to redesign the circuit with the intent of reducing noise and power consumption.

As a result of the research, a new 16 x 17 array has been developed. The new design incorporates new demultiplexing and synchronizing circuitry. The new circuitry exhibits lower noise and consumes much less power. The "L" shaped reference pad has been removed—instead each pad and the pad to its right are sampled concurrently—one as the sample and one as a reference.

14. SUBJECT TERMS

Neural electrodes, brain, EEG

15. NUMBER OF PAGES
118

16. PRICE CODE

17. SECURITY CLASSIFICATION OF REPORT Unclassified	18. SECURITY CLASSIFICATION OF THIS PAGE Unclassified	19. SECURITY CLASSIFICATION OF ABSTRACT Unclassified	20. LIMITATION OF ABSTRACT UL

NSN 7540-01-280-5500